# 博　士　論　文

Study on Wireless Ranging and Positioning Methods
Using Active RFID Tags

（アクティブRFIDタグを用いた無線測距および測位の研究）

中村　圭一

## ABSTRACT

Determining position and distance between objects is an important research area of the ubiquitous computing. The purpose of the ubiquitous computing is to provide context aware services to users by deploying small sensory devices to environment and obtaining surrounding contexts of environment using sensory devices. Especially location information is an important contexts in order to provide location based services to the user. This research studies low cost and scalable ranging and positioning methods based on the user-centric communication model using active RFID tags as location sensors.

This research considers three types of location information supported by the location information infrastructure and determines technical challenges associated with each location information type. The proximity detection system needs to satisfy following requirements: ad-hoc communication, real time detection, and scarce computing resource. The proposal for the proximity detection system is made that satisfies these features. For the relative and partial location system, localization methods based on TOF supported active RFID tags are proposed. For the absolute location system, proposals are made considering a large scale deployment, especially the method to capture RF signal characteristics and the one that calculates position of reference tags autonomously. For each proposed method, the effectiveness is evaluated by implementing the proposed method on a real hardware and by conducting field experiments. Lastly, the application of the partial location system is proposed which locates vehicles in indoor parking areas. From discussions on obtained results, proposals made for each location information type are effective, that is, proposals achieve high accurate localization, system's robustness, and scalability on the number of users.

# Acknowledgements

I would like to express my greatest appreciation to my adviser Professor Ken Sakamura for the continuous support of my Ph.D study and research through graduate school and YRP Ubiquitous Networking Laboratory, for his patience, enthusiasm, and most importantly inspiration. Discussions with Professor Sakamura have been insightful all the time and encouraged me to continue my research and write this thesis. Without his guidance and persistent help this thesis would not have been possible.

I would like to also thank Professor Noboru Koshizuka and Dr. Shinsuke Kobayashi for providing continuous advice and guidance since I was a master course student. Weekly meetings with Dr. Kobayashi, Mr. Masato Kamio, and Mr. Tetsushi Watanabe have provided me opportunities to acquire knowledge necessary for exploring my research area of study. My sincere appreciations also goes to Dr. Masahiro Bessho, Dr. Yuki Wakuda, Dr. Kentaro Ishii, Dr. M. Fahim Ferdous Khan, Dr. Lee Fueng Yap, Mr. Takeshi Yashiro, and Mr. Satoshi Asano for their encouragement, insightful discussions, and continuous supports.

Besides staffs from Sakamura-Koshizuka laboratory, I would like to thank co-workers from YRP Ubiquitous Networking Laboratory and Ubiquitous Computing Technology Corporation and staffs I had valuable opportunities to work on projects: Mr. Tatsushi Morokuma, Mr. Tatsuya Izumina, Mr. Shuji Yura, Mr. Hisanori Matsumoto, Mr. Koichi Matsushita, Dr. Masataka Takamura, Mr. Ryusuke Kaneko, Mr. Haruka Kusano, and Mr. Naoki Yoshimura, for their encouragement and greatest support.

I would like to acknowledge the support provided by my parents, my siblings, and my grandparents.

# Contents

# List of Figures

# List of Tables

# Chapter 1

# Introduction

## 1.1 Purpose of the Research

Localization of both static and mobile objects is an important research subject of the ubiquitous computing. The main task of ubiquitous computing systems, as first illustrated in [1] and [2], is to automatically recognize and obtain surrounding contexts of users by exploiting information retrieved from small sensors deployed to everywhere. In the ubiquitous computing, the contexts of a user indicate nearby objects of the user, places where she belongs, and events that are interested by her. Especially the location information of interested objects and the current position of the user are fundamental contexts among others. This research focuses on problems and challenges that arise from realizing the infrastructure that recognizes location information of interested object and provides location information to users in both outdoor and indoor environments.

The location information infrastructure aims to provide three types of location information depending on application requirements.

**Proximity** Proximity information represents nearness to objects and places [3]. Degree of nearness between objects or places and the users depends on applications. Proximity status may be triggered by physical contact or by successful wireless communication.

**Relative** While proximity information merely represents nearness between targets and the users, relative location information includes geometric notions such as

distance and angle to represent position of the users relative to target objects and places. In addition, relative location information includes incomplete or partial position of the users such that only a part of geographical coordinates is obtainable, for example, partial location information contains degrees of latitude but not degrees of longitude. Relative or partial location information is as useful as absolute or complete location information, since the primary purpose of the ubiquitous computing is to detect the relationships of objects and users from sensory devices.

**Absolute** Absolute location information indicates a location of the users represented as geographical coordinate system such as WGS84 a standard geodetic datum utilized in the Global Positioning System (GPS).

The location information infrastructure for the ubiquitous computing systems is expected to be low cost while sensing location information for providing it to the users in outdoor and indoor environments seamlessly. For the location information infrastructure to be low cost, location sensing devices to be deployed to target spaces need to be low cost. In addition, their maintenance cost is expected to be low as well. Thus location sensing devices are expected to operate for years with replaceable batteries.

Furthermore, the location information infrastructure is expected to follow a user-centric approach [4] to maintain its scalability. Figure1.1 shows two types of communication models between infrastructural devices and target devices: user-centric approach and infrastructure-centric approach. With the user-centric approach, each device to be located collects location information retrievable from sensors constituting the location information infrastructure and calculates its position based on location information retrieved from deployed sensory devices using its own computing resources. On the other hand, sensory devices that constitute the location information infrastructure are not required to obtain any information of devices to be located with the user-centric architecture. The GPS is an example of the user-centric location information infrastructure. A GPS receiver captures timing signals transmitted by multiple satellites orbiting the earth and it is responsible for calculating its position from timing signals. As devices of the location information

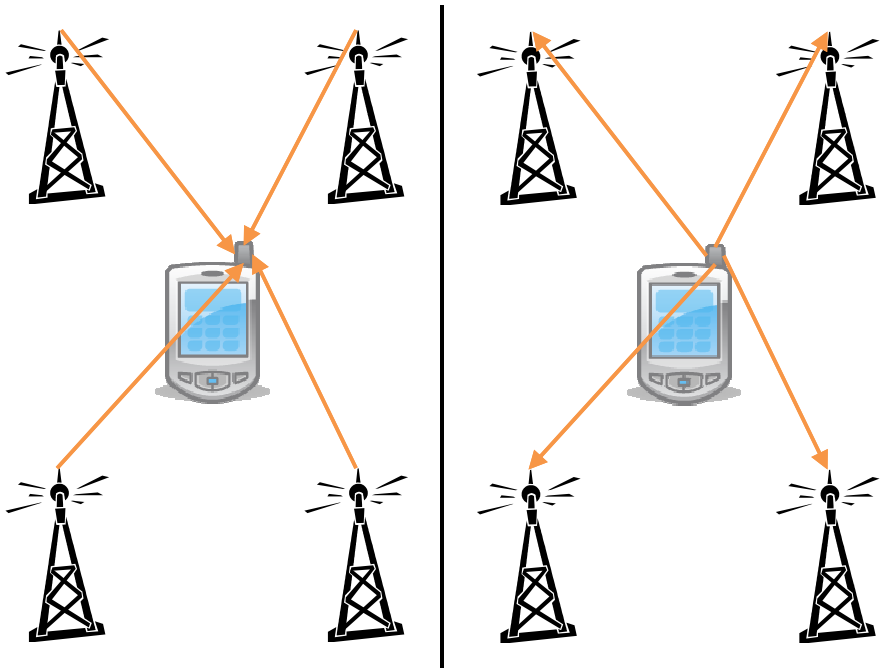

Figure 1.1: Communication models for the location information infrastructure. (Left) User-centric approach. (Right) Infrastructure-centric approach. Directed arrows indicate directions of communications between infrastructural devices and user devices.

infrastructure are expected to be low cost, their computing resources are scarce compared to a high-end desktop PC or a mobile phone, therefore the user-centric approach is suitable for the location information infrastructure. In addition, since smartphones are adopted by users worldwide in recent years, there are rich computing resources available on the user side, which is another evidence that shows advantages of the user-centric approach for the location information infrastructure.

This research considers active Radio Frequency Identification (RFID) tags as devices for constituting the location information infrastructure that follows the user-centric approach while maintaining low cost. RFID tags are devices that store an identifier which can be transmitted to a receiver via a wireless communication. Based on power source, RFID tags are classified into two classes: active and passive. An active RFID tag contains a battery for transmitting its identifier,

while a passive RFID tag requires radio signals sent by a RFID reader device to generate its operating power. With the location information infrastructure based on active RFID tags, active RFID tags are deployed to target spaces and each tag transmits its unique identifier periodically. Devices to be localized estimates its proximity status with respect to deployed active RFID tags by measuring a strength or a time of flight of received signals. A relative location of the located device is obtainable by collecting signal characteristics from multiple RFID tags. Moreover, by exploiting a database system that associates geographical coordinates and identifiers transmitted by active RFID tags, devices to be localized are able to obtain its absolute coordinates from estimated position relative to multiple RFID tags. Although the cost of active RFID tag products are around a few thousand yens in recent years, it is expected to be lower than the current cost as demands of active RFID tags increase and the mass production of active RFID tags is achieved.

The location information infrastructure based on active RFID tags has several advantages over existing location systems. GPS provides a robust and scalable location service to users in outdoor environments. However the location service provided by GPS is not available in urban areas where multistory buildings and skyscrapers are concentrated and in indoor environments where GPS receivers cannot receive signals from satellites. In contrast, since active RFID tags are deployable to both outdoor and indoor environments, the location service that seamlessly available anywhere is achievable.

Alternatively, in recent years, location services based on WiFi access points are available on commercial mobile devices as the number of WiFi access points in urban areas increases at an accelerated pace. By associating an identifier of access points, such as its SSIDs, with location information, devices to be located can estimate their location by accessing the location information database of access points when devices received signals from an access point. Since most of WiFi access points are not placed for the location service, the location information database needs a frequent update to deal with newly added or removed access points from a installation location. In addition, WiFi access points require a power supply for their operation, thus they need to be placed where power supplies are available. On the other hand, active RFID tags operate with a battery and they can provide the

location information infrastructure to places where power supplies are difficult to obtain, and frequent update of the location information database is not necessary since they are dedicated devices installed for the location service.

## 1.2 Problem Statements

There are three measures that can be utilized either directly or indirectly to estimate the distance between two wireless communication devices, namely received signal strength (RSS), time of flight (TOF), and angle of arrival (AOA). Among these measures, obtaining AOA requires antenna arrays on communication devices, which increases size and cost of devices, thus it is not considered in the location information infrastructure based on active RFID tags.

**RSS** Received signal strength (RSS) is a measure obtainable by a wireless device when it receives a signal emitted from an other wireless device. In addition to commercially available wireless devices such as WiFi, Bluetooth, and ZigBee, active RFID tags are capable to measure RSS at its physical layer. To estimate the distance between two wireless devices, the log distance path loss model [5] is often exploited, which models the relationship between distance and the attenuation of a signal propagated in space. A path loss of a signal is retrieved from observed RSS samples by assuming that a transmission power of a signal transmitter is known or constant.

**TOF** Time of flight (TOF) is a direct measure related to distance between two wireless devices with the distance, speed, and time equation. In order to accurately estimate distance using time of flight information of a captured radio signal, a transceiver is required to have a good time resolution, for example, 3 ns time resolution is required for achieving one meter accuracy. Although it is difficult to realize a fine time resolution on narrowband radio devices such as WiFi or ZigBee, ultra-wideband impulse radio (UWB-IR) devices are capable of capturing signals at nanosecond order time resolution which achieves a sub-meter ranging accuracy using the TOF method. With a recent advancement of a wireless device technology, UWB-IR devices are

available as an active RFID tag as presented in [6].

In practice, however, RF signal propagation is affected by environment of target domains of the location information infrastructure, which includes buildings, obstacles, walls, and people. Thus there are many previous studies that try to solve or mitigate ranging and localization issues that arise when RSS and TOF are exploited as distance measures.

Distance measurement systems that exploit RSS need to deal with variations of sampled RSS in order to accurately measure distance between two wireless devices. Variations of sampled RSS are caused by channel fading effects [7], which can be further classified as small-scale and large-scale fading effects. Small-scale fading occurs as a result of multipath interference of a RF signal, which generates quick variations on observed RSS samples. Large-scale fading, as known as shadowing effect, occurs due to changes in environmental features such as buildings, vehicles, and people, which obscure direct path signal propagation, and it produces variations on mean value of signal strength observed over long time period.

On the other hand, TOF based location systems are required to satisfy two conditions in order to execute distance measurement. First requirement is to maintain the line-of-sight (LOS) condition between wireless devices. The LOS condition is essential for a target device to properly measure the time of flight of a direct path signal transmitted by a source device. If the LOS condition is not maintained, a transmitted signal reaches the target device via several paths, which makes the target device impossible to measure the source-to-target distance since the exact path of the transmitted signal is not retrievable without the layout of the target environment. Obtaining the layout of the target environment for evaluating and determining causes for multipath propagation is usually difficult and costly, since deployed devices for the location information infrastructure need to have a capability similar to a sonar system for analyzing the RF propagation characteristics of the target environment. In addition, a time synchronization mechanism between the source and the target devices is necessary in order to obtain the time of flight. To measure the time of flight at the target device, the target device needs to know the time that the source device transmitted a signal, in addition to the received

time of the signal from the source device.

Instead of directly measure distance between two wireless devices using RSS and TOF, previous studies have attempted to solve more difficult problem than the proximity detection or the distance measurement, which is to locate the target device from elaborated location information obtainable from multiple location sensors. In order to measure the position of a target device using signal strength, RF map surveying method [8] [9] [10] [11] [12] [13] [14] and RF model estimation method [15] [16] [17] [18] [19] [20] [21] [22] are rigorously studied in the literature. As for the time based location systems, cooperative localization techniques [23] [24] are adopted. For example, measuring the time difference of arrival (TDOA) [25] of signals transmitted by multiple sensory devices is a well known cooperative localization technique.

A large body of research on localization focuses on improving localization accuracy and precision, since these are the key aspects of the localization system in order to provide reliable location information to the users. However, a practical localization system needs to consider an applicability of localization algorithms on real hardware devices and scalability of the total system, in addition to localization accuracy and precision. This research focuses on practical issues that arise from realization of three types of location information systems: proximity, relative, and absolute location information systems, using active RFID tags as primary devices constituting the user-centric location information infrastructure.

## 1.3 Overview of Research Contributions

This research explores issues and solutions for the proximity detection system, relative and partial location systems, and absolute location systems based on active RFID tags. Proposed methods are empirically evaluated through extensive real-world experiments using various types of active RFID tags that have a capability to measure RSS or TOF. Contributions of the research are summarized for three types of location information as follows.

### 1.3.1 Proximity Detection System

A Media Access Protocol (MAC) specialized for RSS measurements and on-line filtering methods for improving distance estimation accuracy using RSS are proposed for the proximity detection system. For the proximity detection system, communication between involved wireless devices is necessarily ad-hoc and the proximity status needs to be estimated as quickly as possible in case such that the target device is mobile and moving through the location information infrastructure. From real-world experiments, the variation of proximity detection distance is suppressed to 3 meters in a busy shopping district while 10 meter variations have been observed for a naive approach.

### 1.3.2 Relative and Partial Location System

A relative positioning system that measures the lateral distance between two mobile objects is proposed using TOF enabled active RFID tags. The proposed method exploits TOF based bilateration to localize relative positions of two mobile objects. With TOF based location system, geometric dilution of precision (GDOP) [26] degrades depending on the geometric layout of active RFID tags [27]. An error mitigation technique for the lateral distance measurement system is proposed and thoroughly evaluated by both simulations and real-world evaluations. The results have shown that the estimation error of the lateral distance between two mobile objects is reduced from 8 m to 3 m.

In addition, a partial positioning system that locates target objects is proposed using TOF enabled active RFID tags. In order to minimize error due to geometric layout of infrastructural devices, a common TDOA based location system requires infrastructural devices to surround the target areas. However, this layout condition imposed on TDOA based location systems demands a target device to maintain LOS conditions on all directions in order to successfully measure TDOA for the localization, which is not satisfiable on applications targeted for areas filled with objects that obstruct RF signals. Thus the proposed positioning system relaxes the LOS condition required for the target localization to only one direction, which gives more availability to the location system than ordinary surround-based location

systems. The proposed positioning system achieves a user-centric architecture for scalability and asynchronous mechanism among TOF enabled active RFID tags for reducing deployment cost. The results have shown that the target localization accuracy of 50 cm is achieved in the direction parallel to infrastructural devices. The proposed system have achieved a successful localization rate of 70 % while the ordinary TDOA location system have completely lost the localization capability due to obstacles in the target areas.

### 1.3.3 Absolute Location System

For the absolute location system, systematic procedures to generate RF models for each deployed active RFID tag are proposed for RSS enabled active RFID tags. As discussed above, most previous studies on localization systems focus on accuracy and precision and there are two general approaches toward increasing accuracy and precision of localization. Building RF signal map is one of approaches for RSS based location systems, but it requires extensive pre-survey efforts to increase localization accuracy. Another approach is to exploit a signal propagation model such as the log distance path loss model. This approach is adopted in many studies, but previous studies often assume a fixed propagation constant for each infrastructural device. The proposed approach has developed systematic procedures to estimate a propagation constant for each active RFID tag and for each transmission power. The experimental results have shown that the proposed method has successfully reduced localization error from 10 meters to 2 meters.

Another problem for the absolute location system is to reduce the cost of deployment of infrastructural devices in user-centric localization systems. The deployment cost can be reduced if deployed positions of active RFID tags are estimated automatically. In addition, if positions of infrastructural devices can be obtained automatically, the localization system can be installed to areas where an exact map does not exist, for example, a disaster site. The proposed system exploits TOF enabled active RFID tags to execute a self-calibration algorithm. The experimental results have shown that the proposed algorithm can locate positions of infrastructural devices with a sub-meter accuracy.

## 1.4 Thesis Structure

The rest of chapters are organized as follows. Chapter 2 summarizes related work on RF location systems and provides previous approaches for issues that arise from RSS and TOF as distance measures. Chapter 3 provides the proximity detection system targeted for ad-hoc communication between scarce computing resource devices. Chapter 4 introduces the relative location system and the partial location system based on TOF enabled active RFID tags. The efficient RF modeling method for large scale RSS based positioning systems and the self-calibration method for obtaining deployed positions of infrastructural devices are introduced in Chapter 5. Chapter 6 discusses applications of the location information infrastructure. Finally conclusions are provided in Chapter 7.

# Chapter 2

# Related Work

In this chapter, related work on proximity detection and localization systems is presented. Various localization systems, both commercial and experimental, are introduced with a classification based on hardware technologies employed. Then for each location information scheme, previous approaches and issues are discussed by focusing on deployment cost and scalability.

## 2.1 Localization Infrastructure for Ubiquitous Computing

The concept of ubiquitous computing provided by Sakamura [1] and Weiser [2] has brought a new computing paradigm to the computer science. They have shown that computers are embedded to everywhere to silently execute tasks to obtain contexts from surrounding environments and obtained contexts are provided to the users via network. As briefly discussed in Chapter 1, the most important contexts is the location of objects in the ubiquitous computing. This section explores means for obtaining location information contexts of objects and the users, and shows advantages of active RFID tag based localization systems over existing and other localization technologies.

### 2.1.1 Global Localization Infrastructure

Global Positioning System (GPS) is a globally available location system. A target device receives timing signals transmitted from multiple satellites orbiting

the earth to locate its absolute position represented as geographical coordinate system. Each satellite knows its ephemeris and the almanac of other satellites, which represent the calculated position of the satellite on its orbit and estimated positions of other satellites respectively, and it equips accurate and precious atomic clocks usually based on cesium and rubidium that achieves a precision of one part in $10^{14}$ and $10^{13}$ respectively [28]. A satellites delivers the ephemeris, the almanac, and the signal transmission time to GPS receivers on the ground, to allow receivers to calculates the time difference of arrival (TDOA) of GPS signals from multiple satellites. TDOA information of GPS signals along with positions of satellites allows the receiver to execute multilateration to locate its geographical coordinate in 3-dimension.

The main advantage of the GPS localization is that it is a scalable system that can support any number of users in worldwide, as the GPS receivers calculate its position by using its available computing resources, while GPS satellites are ignorant about the number of GPS receivers on the ground. As GPS shows, the user-centric approach is a key concept for achieving a scalable localization system.

The main disadvantage of GPS localization is that the target device cannot receive GPS signals transmitted from satellites when the target device resides within a building since signals are blocked by concretes and metals constituting buildings. The target device in outdoor environment suffers from the line-of-sight problem when there are many buildings surrounding the target device so that the line-of-sight between the target device and satellites is obstructed. In addition, a GPS receiver in a reset state, so-called cold start, requires to receive the ephemeris and the almanac from a satellite in order to start localization. This procedure usually takes about 30 seconds to 60 seconds since the receiver needs to download the whole GPS frame.

### 2.1.2 Exploiting Existing Communication Infrastructures

As stated in previous subsection, GPS requires the LOS condition with multiple satellites orbiting the earth for the localization procedures, thus it is not a suitable solution for the indoor usage. Therefore there are many studies that attempt to

exploit existing communication infrastructures for realizing the location services seamlessly available in both indoor and outdoor environment.

The proliferation of mobile computing devices, such as smartphones, mobile PCs, and electronic book readers, have resulted the deployment of cellular network towers and wireless access points in almost everywhere. This subsection introduces research and commercial location systems that exploits existing communication infrastructures.

### Cellular Networks

Mobile phones are very popular from children to seniors and cellphone service providers are demanded to deploy cellular towers everywhere including both indoor and outdoor environment for providing cellphone connectivity. There are studies to exploit the mobile infrastructure for estimating the position of the target device [12] [29] [30] [31]. Statistical approach such that profiles of signal attributes are pre-measured in target areas, so called war-driving, is a commonly accepted method for the localization system that exploits cellular networks [12] [29] [31], since it is difficult to collect deployment plan of cellular towers and to measure a direct path distance between a cellphone tower and a mobile device in indoor environment. In [30], the authors have shown a dead reckoning approach such that sensory devices mounted on a mobile phone are exploited for the location estimation of mobile phone users. Although collecting patterns for pedestrian walking paths in off-line phase is required, the amount of work for the off-line phase is reduced compared to the RF signal collection technique.

The advantage of the localization scheme that exploits cellular networks is that it can utilize cellular towers to locate target objects, thus the localization system does not require any cost on anchor node deployment. In addition, the network architecture that utilizes the RF fingerprinting is user-centric, that is the localization is conducted by user's devices, which provides a scalability to the location system. Furthermore, the location information is obtainable by mobile phones which increases the chance of system's availability since mobile phones are popular among people in the worldwide.

The major drawback of these approaches is that the off-line phase for developing the localization system requires large efforts in order to achieve sub-decimeter localization accuracy. Also, the achievable accuracy is in the order of few meters with RF fingerprinting approach [31] and few decimeters without war-driving [30], thus applications of the localization system based on mobile networks are limited to room or area recognition.

**Wireless LAN**

In addition to cellular towers, the dissemination of mobile devices has brought a large scale deployment of Wireless LAN access points available both in indoor and outdoor environments. Academic and industrial research communities have vigorously worked on developing a location information system based on Wireless LAN access points, because WLAN access points can be deployed freely to target areas compared to mobile towers. Also the communication range of WLAN signals is typically longer than other solutions; a range of 50 to 100 meters is achievable in free space.

Localization approaches adopted for the WLAN based systems are similar to the one adopted by mobile network based localization systems. Instead of directly measuring distances between WLAN access points and the users using signal strength, RF fingerprinting approach is a common solution among WLAN based location systems. RADAR [8] [32] is an early example that exploited a RF map of a target area to determine a position of the users. The authors have proposed a location algorithm similar to $k$-nearest neighbors ($kNN$) search algorithm with the RF map obtained from the pre-surveying. With $kNN$, a measured RSS at a target device is compared with recorded RSS profiles of known locations to obtain $k$ location candidates, then the position of the target device is estimated by averaging positions of $k$ location candidates. Horus system [11] [33] exploited a pre-surveyed RF map and a statistical approach that classifies candidate location coordinates into a cluster to reduce the computational requirements. It is a notable work which has shown that the fingerprinting technique can achieve a localization accuracy less than 1 meter using RSS as distance measure. To reduce the pre-measurement

efforts for building a RF map of the target areas, some work have shown to exploit crowd-sourced calibration in order to improve and update the RF map [34] [35] [36]. Other work have shown a reduced amount of RF measurement to achieve a room level accuracy [13] or adding more access points to a small area to increase the localization accuracy [10]. However, since RF map approach requires an extensive pre-survey of the target areas before the usage, its applicability to large area localization system is difficult while maintaining a localization accuracy.

Another approach for localization based on RSS samples of WLAN access points is to develop a RF propagation model. By using a pre-obtained location information of all WLAN access points, the authors of [17] have proposed to use a linear interpolation to generate a RF map. Each access point were modified to sample RSS from other access points, so that RSS values at target areas are estimated by the interpolation. Other approaches exploit packet sniffers at known locations to measure RSS and build the log distance path loss model for access points in order to generate the RF map of the target space [20] [21]. Yet another approach tries to simultaneously locate a set of clients by aggregating a collection of RSS samples from multiple clients using Bayesian probabilistic models [19]. EZ [22] utilizes location information obtainable with a GPS receiver when the client mobile devices are near windows of the indoor environment, to enhance the localization accuracy. Although the localization accuracy obtainable with the RF model based approach is approximately a few meter, the approach dramatically reduces pre-survey efforts compared to the RF map based approach.

The main disadvantage of using WLAN access points is that the signals are easily disturbed since the frequency band utilized for WLAN is shared among many wireless devices. In addition, in recent years, there are many personal devices which enable the user to execute WiFi tethering on her personal mobile device. These nomad devices produce extra noises to the pre-surveyed RSS maps prepared for WLAN access points.

### 2.1.3 Location Sensors

Another approach to building a location information infrastructure for ubiquitous computing is to exploit various location sensors. This subsection introduces location sensors that can be utilized for obtaining location contexts.

#### Near Field Communications

In recent years, many commercial smartphones support Near Field Communications (NFC), which is a set of radio-frequency identification (RFID) standards including ISO 14443 and FeliCa. Smartphones can read out a data stored to NFC compatible passive RFID tags by passing RFIDs over the internal RFID reader of the mobile device. Since many smartphones support NFC standards, there are attempts to localize the user with a NFC enabled smartphone when the user have read the NFC RFID tag [37]. Previous studies attempt to incorporate other location sensors exploited together with passive RFID tags [38] [39].

The advantage of utilizing passive RFID tags comes from the spread of mobile devices among the users, so that the location service can easily be started using passive RFID tags by deploying RFID tags to points of interest or by attaching it to objects. In addition, the cost of passive RFID tags is low compared to any other technologies, thus the large area deployment is possible. The disadvantage of using passive RFID tags is that the users who want to receive a location based service need to actively read tags by enabling RFID readers and scanning tags. Since the action needs to be taken by the users, it reduces a motivation of users to enjoy the location based service built from passive RFID tags.

#### Optical Communication/Sensory Devices

Among early studies of localization systems, Active Badge location system [40] utilized infrared sensors to build an indoor location system. A dedicated infrastructure prepared for a target room consists of infrared receivers and an infrared transmitter is prepared for the user to be tracked by the system. The location system locates users with the transmitter by receiving infrared signals from the transmitter and the system identifiers users by processing identifiers emitted by

the transmitter.

An optical information is often combined with RF transceivers to supplement the location information obtainable with RSS or TOF. In [41], a RF device with a light reflector is proposed for the agent based localization system. The unmanned aerial vehicle (UAV) emits lights to the target area where RF devices are deployed, and the visual image of reflected light is captured by the UAV to process the location of devices. In [14], visual features of the target area are recorded along with RSS samples to build an extended RF map. In addition, optical information can be utilized to measure the distance by observing a time of flight of lights. An optical radar is proposed in [42], to measure the lateral distance between vehicles or distance to crash barriers on the road using infrared light.

As for the ranging and positioning system based on visual or infrared lights, the performance is greatly affected by the surrounding environment, for example, direct sunlight can be an error source for the infrared light location systems. Thus infrared light approach is often limited to the use in indoor environment.

#### Ultrasound Devices

Since ultrasound propagates much slower than light, there are positioning systems based on time of flight of ultrasound. Bat [43] is a notable study such that a grid of ultrasound receivers is deployed to the ceiling of the target room to receive ultrasound emitted by the transmitter device of the target user. The transmitter device of the user emits RF signals as well when it emits an ultrasound signal so that receivers on the room can synchronize to obtain time difference of arrival of the emitted signal. Also, Cricket [44] takes a similar approach but it supports an user-centric communication architecture by implementing an ultrasound receiver to the sensor device.

The range of ultrasound pulse is relatively short compared to RF based system and thus the number of infrastructural devices required for performing a localization becomes large. Therefore the overall cost and the lack of scalability are disadvantages of the ultrasound based localization system.

### Active RFID Tags

Active RFID tags are small wireless transceivers such that their main purpose is to transmit an identification stored to their memory. SpotON [45] exploits active RFID tags and their receivers to build a location system. RSS measurements are conducted to estimate distance between active tags. Estimated distance information is aggregated to conduct ad-hoc lateration to locate devices. Another example of active RFID tag based localization system is LANDMARC [46]. In LANDMARC, some active tags are deployed to the target area as reference nodes to increase the accuracy of the localization based on RSS measurements. The LANDMARC employs $kNN$ method to calculate the location of target devices.

In addition to RSS based tags, there are TOF enabled tags available in recent years. There are several vendors that provide TOF enabled tags, which utilize ultra-wideband communication. Ubisense [1] provides UWB products that utilize high-band frequency between 6 GHz to 8 GHz allocated for the UWB usage. It has a communication range up to 50 meters line-of-sight, and provides positioning accuracy of 30 centimeters in 3-dimensions. It supports time-difference-of-arrival and angle-of-arrival for the positioning measurement by implementing an antenna array to the device. Time Domain [2] also produces UWB products that utilize low-band frequency between 3.1 GHz to 5.3 GHz allocated for the UWB usage. It supports 354 meters line-of-sight communication range and time-of-flight measurement achieving an accuracy less than 3 centimeters. The main advantage of UWB based positioning systems is the achievable accuracy and precision with relatively long communication range compared to ultrasound sensors. The disadvantage is that the time-based localization always requires a line-of-sight between transmitters to measure distance. In addition, most packaged system requires a wired synchronization among anchor nodes which measure timing information of transmitted signals. This brings an additional cost on the system deployment.

The advantage of active RFID tags as location sensors is that they are freely deployable to both outdoor and indoor environments since active RFID tags can

[1] Ubisense http://www.ubisense.net
[2] Time Domain http://www.timedomain.com

operate without electric power source. In addition, it is not necessary to update the location information database for the RF mapping technique for the RSS enabled active RFID tags since active tags are deployed specifically for the location retrieval purpose.

## 2.2 Localization Schemes and Problems

### 2.2.1 Proximity Detection

Active RFID tags are attached to points of interest with the location information infrastructure based on active RFID tags. To determine a proximity status with deployed devices, the users receive periodic signals transmitted from active tags in order to estimate the relative distance to tags using RSS or TOF obtained from received signals.

The proximity detection system for the active RFID tags is expected to execute an ad-hoc communication as the proximity status is determined between active tags and mobile users. Proximity detection is expected to detect the proximity status as fast as possible in order to provide contextual information to the users. In addition, a distance approximation method is expected to be light weight and simple to store on a limited memory of the device since the computing resource available on active RFID tags are scarce.

RSS based tags are suitable for the application since the proximity status between tags may occur when they are not in line-of-sight condition. With RSS based tags, reducing the effect of the small scale fading is the main challenge to overcome as discussed in Chapter 1. Simple statistical methods proposed for estimating quality of communication links between low-power wireless devices [47] are evaluated for this research, especially the applicability of filtering methods are evaluated in outdoor environment.

### 2.2.2 Relative and Partial Localization

#### Relative Location System

For the relative location system, geometric notions are added to the proximity status. TOF enabled tags are suitable in order to accurately measure distance and angle between two objects. A triangle is formed placing two TOF enabled tags to the target object and one TOF tag to the receiver. Similar approach is proposed by Richardson et al. [48]. They propose a novel time synchronization technique to increase ranging accuracy of the UWB device and have shown that a relative position of a target node is accurately estimated in an urban area using simulations by adjusting suitable synchronization parameters. This research extends their work by evaluating real-time filtering method which is targeted for a low power embedded system to reduce positioning error caused by the layout of active tags. The estimation technique utilized for the relative location system is called the bilateration. This research studies and evaluates a data filtering method for increasing accuracy of estimated lateral distance for TOA-based bilateration.

#### Partial Location System

With TOF based location system, maintaining LOS condition between devices is the most important requirement to build a robust location system. In addition, TOF based location system requires a synchronization mechanism to measure timing information of transmitted signals. Furthermore, the user-centric communication is preferable to provide location services to a large number of users.

To maintain LOS condition, one approach is to reduce the number of anchor node required for the localization procedure. In terms of the number of anchor nodes required for the positioning, the most simplest algorithm among others is to find an intersection of two circles to find two candidate positions of a target node, so-called the bilateration method [49] [48]. With the bilateration method, two anchor nodes are required to determine the position of the target node in a 2-dimensional area by limiting the area of the possible position, so that both anchor nodes are allowed to be placed in front of the target vehicle for calculating the position of the target. To reduce the network overhead of obtaining TOA between the target

node and anchor nodes, the authors of [50] and [51] have proposed the cooperating positioning algorithm, which finds intersections of a circle and an ellipse obtained from TOA and TDOA information respectively. The algorithm can be initiated by the target device by measuring the distance to one of anchor node pairs from the target, but the target device must retrieve TDOA information measured by other half of anchor node pairs to calculate self-position of the target device. In addition, both bilateration and the circle-ellipse intersection method require the target node to send a reply or initiation signal for the TOA measurement, so that the network traffic is busy compared to the passive location system.

The passive location system [25] takes the infrastructure-centric approach to locate the target object using aggregated TDOA information. The main advantage of the passive location system is that the approach allows the target node to implement a transmitter function only, which greatly reduces the hardware cost. The UWB products of Ubisense [3] also support the passive location. However, this approach requires a roaming system to expand the target area. In addition, a radio congestion management mechanism among target nodes is necessary. Thus the positioning system on the infrastructural side becomes complex.

This research proposes an active sonar system based on anchor node triples aligned in a line. Although the core of the positioning method is TDOA, an anchor node triple cooperates each other to provide TDOA information to the target device and the task of the target objects for the positioning procedure is to receive signals from anchor nodes. Thus the scalability of the system is maintained even when the number of target node increases. In addition the proposed method does not require an anchor node triple to be synchronized, which reduces the deployment cost. The synchronization is maintained by building an anchor node triple from one initiator and two reflectors, which allows a service provider to easily expand the location system by adding an anchor node triple to the target site.

[3] Ubisense http://www.ubisense.net

### 2.2.3 Absolute Localization

#### RF Map Survey

There are many previous studies on RF localization and one of popular approaches in the literature is to utilize an existing wireless local area network (WLAN) infrastructure to realize localization systems based on wireless communication. Since RSS is not a reliable measure to directly estimate the distance between wireless nodes, a popular approach with WLAN infrastructure is to build a RF map of the target area as explored in this chapter.

The advantage of this approach is that one can capture RF characteristics in target areas *as is*. Estimating RSS behaviors with a RF propagation models produces undesirable results in localization accuracy and precision, since it is difficult to accurately model the propagation paths of RF signals and methods adopted take heuristics approaches. The main disadvantage of the RF map surveying method is that it requires a detailed survey of the target area, requiring to sample RSS in 1 meter mesh and in all directions and all possible postures if the sampler is held by a person.

For the location information infrastructure based on active RFID tags, locations of deployed tags are managed since tags are newly attached to the places of interest by a service provider. Thus, instead of taking approaches based on zero-calibration or RF map, the proposed method tries to construct RF models for each deployed tag from training data collected by conducting a pre-survey.

#### Obtaining Anchor Node Position

Another issue related to the deployment of location sensor devices to large areas is the localization of sensor devices themselves that operate as anchor nodes. The important condition necessary for the anchor node localization is to check if the graph is globally rigid [52]. This research utilizes TOF enabled active RFID tags to develop an algorithm to find a globally rigid quadrilaterals.

## 2.3 Summary

This chapter explored global localization infrastructure, localization approaches taken for exploiting existing communication infrastructures, and various location sensors that can be utilized to build the location information infrastructure for the ubiquitous computing. The advantage of active RFID tags are discussed compared to other approaches. Then for each localization scheme, technical problems are stated for the realization of the location system, and the proposal made within this research is briefly explained.

# Chapter 3

# Proximity Detection System

In this chapter, a proximity detection system supported by the location information infrastructure is introduced. An overview of the proximity detection system is provided first, then approaches and designs of the system are presented. A real-world field experiments have been conducted by using light-weight active RFID devices. Results and discussions are provided in the end of the chapter.

## 3.1 System Requirements

A proximity detection system provides information on nearness to a known set of points of interest [3]. Points of interest may include objects, places, or even human beings. With the location information infrastructure based on active RFID tags, active RFID tags are attached to points of interest and the users determines the proximity status based on the relative distance estimated by RSS or TOF obtained from received signals.

The proposed proximity detection system solves following technical challenges: ad-hoc communication, real-time detection, and scarce computing resources. The proximity detection is executed between an active RFID tag deployed to target areas and a mobile user, so communication between the tag and the user must be executed in an ad-hoc manner. In addition, proximity detection is expected to detect the proximity status as fast as possible in order to provide correct contextual information to the users without a delay in proximity notification. Furthermore,

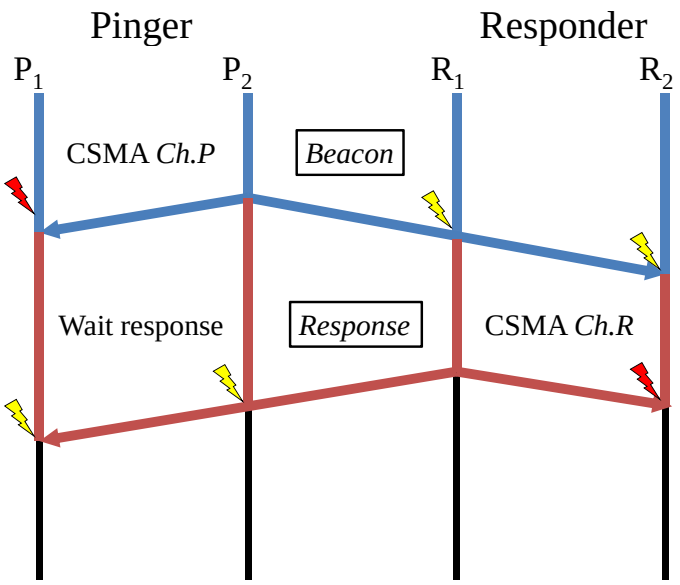


Figure 3.1: Packet flow diagram of the communication protocol for the proximity detection.

since the computing resource available on active RFID tags are scarce, a distance approximation method is expected to be light weight and simple to store on a limited memory of the device.

## 3.2 Communication Protocol for the Proximity Detection

The communication protocol for the proximity detection system is based on broadcast exchange between active RFID tags. Since RF frequency is a limited resource and expected to be shared among devices, a media access control (MAC) is necessary for the proposed protocol. To simplify a description of a communication protocol for the proximity detection, the protocol is divided into protocols for a pinger and a responder. Figure3.1 shows a packet flow diagram between pingers and responders. Details of protocols are given in following subsections.

### 3.2.1 Pinger's Protocol

A pinger continuously broadcasts a beacon to search for a nearby responder. A beacon is sent out via a specific communication channel prepared for pinger's beacons. The communication channel for the beacon is called the probe channel, $Ch.P$. The pinger sends a beacon when the probe channel is available. For each sending procedure, the pinger executes carrier sense to check if the channel is not occupied by another pinger participant in close proximity. The pinger enters a listening mode after it successfully sent a probe beacon or it detected another device sending a probe beacon. Using the response channel, $Ch.R$, different from the probe channel, the pinger listens for a response packet from responders. If there is a responder that sends a response packet via the response channel within a predefined timeout period, probe nodes samples RSS of the response packet to evaluate the proximity status between the pinger. Figure3.2 shows the state diagram of the pinger's protocol.

### 3.2.2 Responder's Protocol

A responder listens for the communication channel, $Ch.P$ to wait for a beacon from a pinger. When the responder receives a beacon, it samples RSS of the beacon to evaluate the proximity status. By analyzing sampled RSS, the responder determines if the pinger is in proximity or not. The responder prepares to send a response if the pinger is in proximity, otherwise it waits for another beacon from a pinger. The responder also execute carrier sense before sending a response packet. If the response channel $Ch.R$ is clear, then the responder broadcasts a response packet. Figure3.3 shows the state diagram of the responder's protocol.

## 3.3 Statistical RSSI filtering methods

A pinger and a responder determine the proximity status by sampling RSS of broadcast beacons. Usually a single sample RSS cannot give an accurate estimation of the proximity status since RF signals are affected by fading effects caused by surrounding environments. Especially for an ad-hoc communication case as

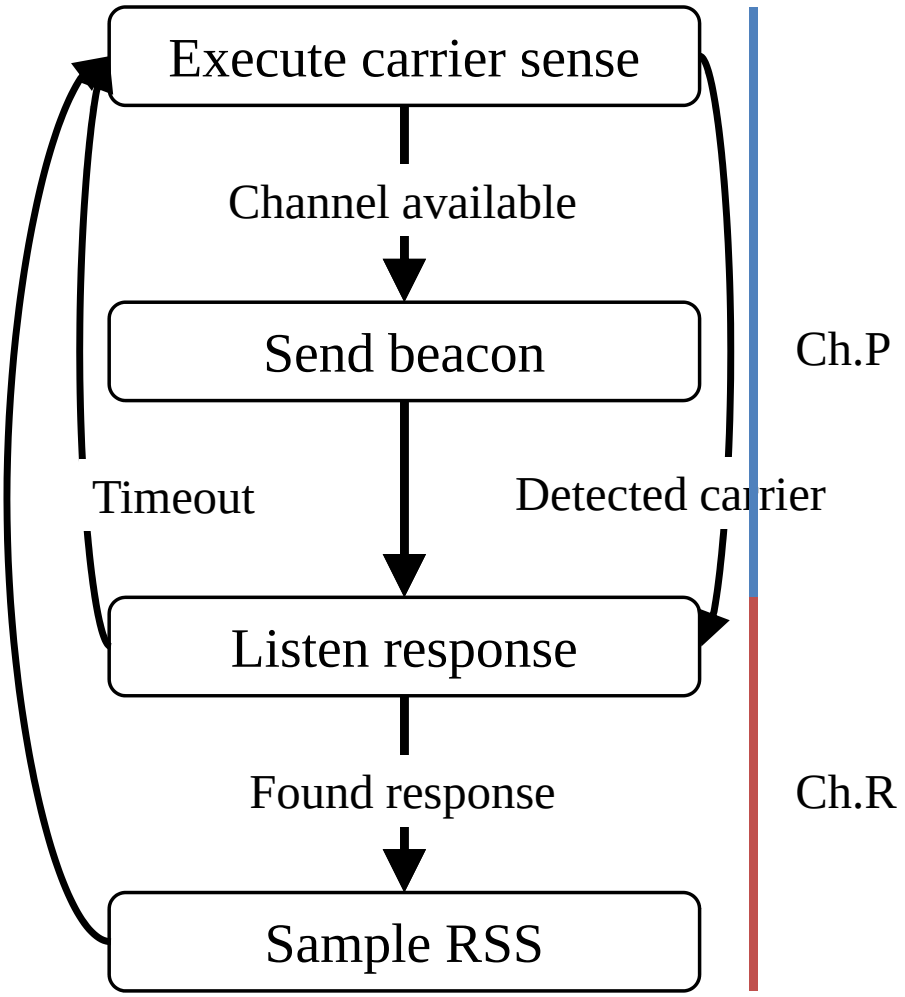


Figure 3.2: State diagram of the communication protocol for pinger devices.

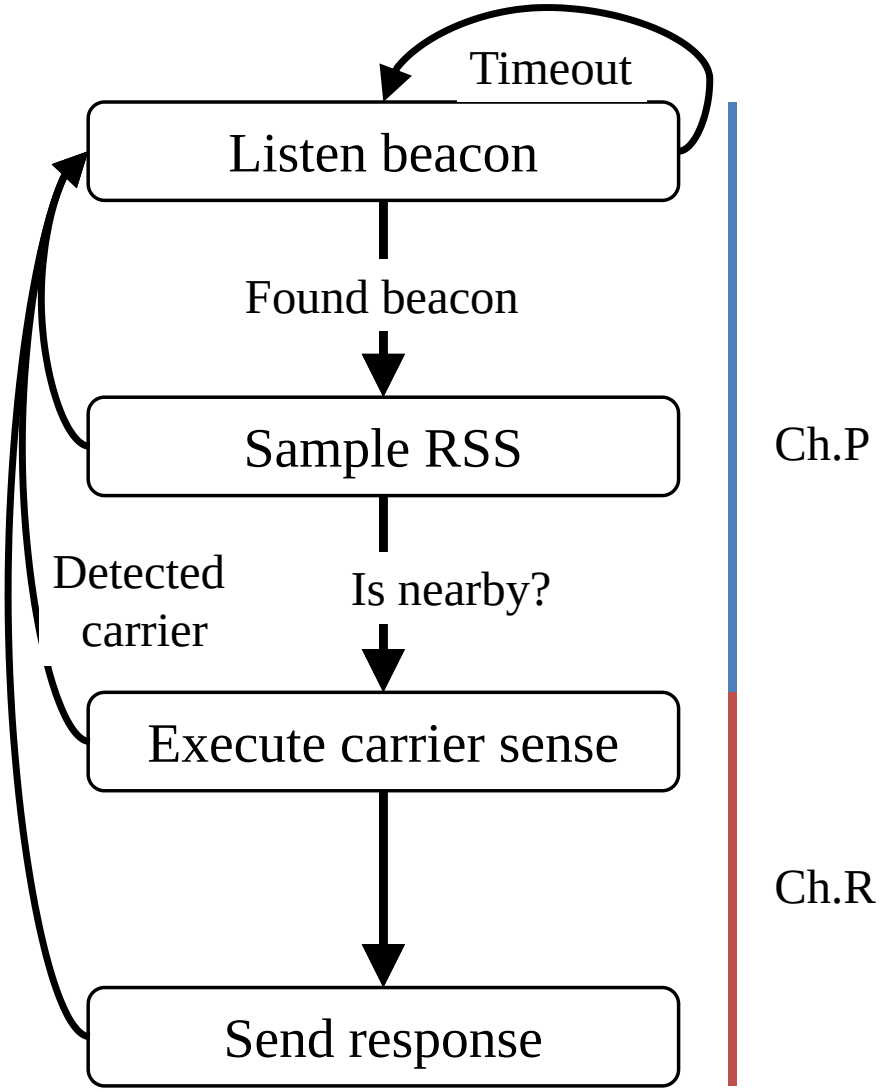


Figure 3.3: State diagram of the communication protocol for responder devices.

discussed in this chapter, the small-scale fading effect is the evident factor that affects the proximity status detection based on RSS measurements. Thus a RSS sampling procedure needs to be incorporated to the communication protocol in order to accurately detect nearby devices. In following subsections, descriptions of 4 sampling procedures which are suitable for resource scarce devices to process RSS sampling in real-time.

### 3.3.1 Consecutive comparison (CC)

RSS samples are obtained for $n$ times from an observed RF channel. The observed RF channel indicates the probe channel, $Ch.P$, and the response channel, $Ch.R$, for pingers and responders respectively. Each sampled RSS values are compared with a predefined threshold value determined from a log-distance path loss model and a distance that the system requires for detecting nearby devices. A device assumes that there is a nearby device, when all RSS samples are greater than or equal to the predetermined threshold for $n$ times in a consecutive manner. The number of times that a RSS sample exceeded the threshold value is recorded for each device sent a broadcast.

The advantage of this algorithm is that a device does not need to store RSS samples to its memory, which is a critical factor when there is limited RAM resource to a device running the proximity detection protocol. Since the algorithm stores record for each device that has sent a broadcast, it requires $O(N)$ memory where $N$ represents the number of nearby devices.

On the other hand, since the algorithm relies on the fact that all sampled RSS exceeds the threshold value, it is possible that the proximity detection accuracy degrades when a distance to a nearby device is close to the threshold value. As stated above, RSS values varies due to the small-scale fading effect, thus sampled RSS does not always represent the true distance between devices. In addition, since the distance is estimated by a log-distance path loss model, the rate of change of RSS due to distance is greater when the distance between devices is small, compared to when the distance between devices is large as shown in Figure3.4. This fact indicates that the large variation of RSS samples are not acceptable in

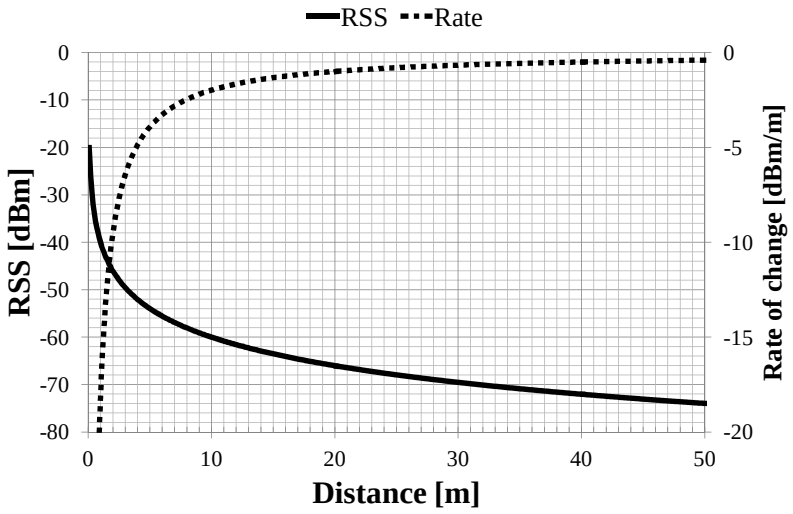


Figure 3.4: RSS and its change rate State diagram of the communication protocol for responder devices.

order to accurately measure the distance between devices is small.

### 3.3.2 Window mean (WM)

Instead of consecutively comparing RSS samples with a threshold value directly, it is preferable to compare the statistics of RSS samples with the threshold value for the proximity detection system based on RSS as a distance measure. One of the simple statistical approach is to calculate a moving average of recent samples of RSS values. A following equation shows the calculation procedure for the window mean algorithm:

$$WM_t = (RSSI_{t-(n-1)} + \cdots + RSSI_t)/n$$

at time $t$. A device recognizes a nearby device when the calculated average is greater than or equal to the threshold value.

This algorithm requires a memory space to record recently sampled RSS values

for each nearby device. Thus the memory space required for the window mean procedure is $O(MN)$, where $M$ represents the length of the window and the $N$ represents the number of nearby devices.

### 3.3.3 Exponentially weighted moving average (EM)

An exponentially weighted moving average of sampled RSS values reduces the number of memory space while providing a statistical threshold comparison. The exponentially weight moving average is calculated as follows:

$$EM_t = (1 - \alpha)EM_{t-1} + \alpha RSSI_t$$

at time $t$, where $\alpha$ is a smoothing coefficient which takes a value between 0 to 1. A device recognizes a nearby device when this value is greater than or equal to the threshold. The initial value, $EM_0$, is set to zero or a RSS value that is observable from an unused RF channel. By assuming a common smoothing coefficient among all devices, the memory space required for the algorithm is $O(N)$ where $N$ represents the number of nearby devices.

### 3.3.4 Window mean of exponentially weighted moving average (WE)

In addition to *WM* and *EM*, the third statistical filter is composed of the combination of them, which is to calculate the window mean of exponentially weight moving average. An *EM* is calculated from the sampled RSS values, then a moving average *WE* of the most recent $n$ *EM* is calculated and compared with the threshold value.

$$WE_t = (EM_{t-(n-1)} + \cdots + EM_t)/n$$

at time $t$.

## 3.4 Exchanging More Packets in Communication Protocols

Because of the small-scale fading effect, there is a chance that the sampled RSS values at a fixed distance is greater or smaller than the ideal value estimated from the log-distance path loss model. This is one of factors that cause a great variation

of the detection distance. It is also known from previous studies that observed RSS values are centered around the ideal value at a fixed distance estimated from the log-distance path loss model, that is, the distribution of observed RSS values follows the normal distribution [53] [54]. To exploit this fact and increase the ranging accuracy, the communication protocol described above is modified so that packets are exchanged between tags after a beacon is sent by a pinger and received by a responder. It is expected that reliable ranging between tags based on RSS is achievable by estimating distance from multiple RSS samples.

After a responder node detects a beacon from a pinger, it initiates a packet exchange by sending an acknowledge packet to the pinger using a communication channel, $Ch.A$, different from $Ch.P$ and $Ch.R$. As a response to the acknowledge packet, the pinger sends a reply packet to the responder using $Ch.A$. Pingers again execute carrier sensing before sending a reply packet, and if it detects another pinger sending a reply packet, if quits sending a reply packet. The modified protocol is called an $N$ exchange protocol if the sequence of exchanging packets is repeated for $N$ times. For the $N$ exchange protocol, a node perceives an approaching node when RSSI values obtained from exchanged packets are greater than or equal to the threshold, in addition to the condition that is required by a filtering method employed together with the packet exchange. A communication sequence between nodes for the 1 exchange protocol is illustrated in Figure3.5.

## 3.5 Evaluations

### 3.5.1 Implementation Details

An active radio tag developed by Yokosuka Telecom Research Park Ubiquitous Networking Laboratory [1] is utilized for the evaluation of two communication protocols and four filtering methods. Its picture is shown in Figure3.6, and its specification and configuration used for experiments described below is briefly shown in Table 3.1. Although the device's maximum transmission power is 10 dBm, the transmission power is set to 9 dBm to avoid a loss of an actual output power trans-

[1] YRP Ubiquitous Networking Laboratory http://www.ubin.jp

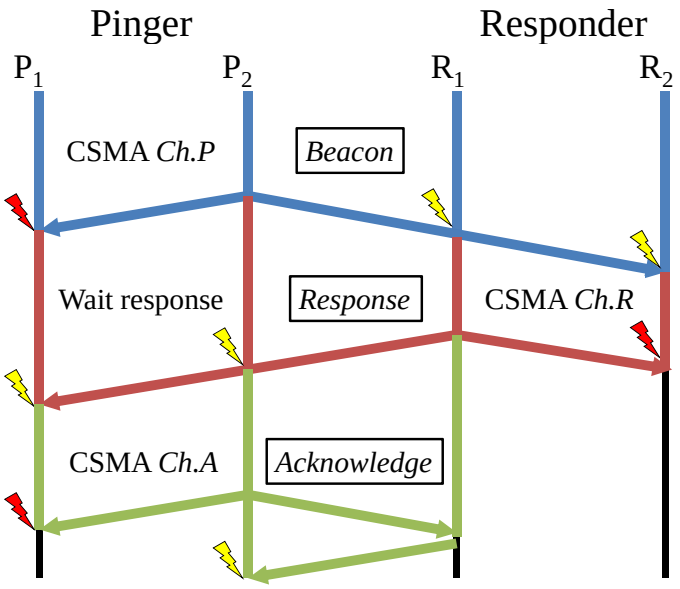


Figure 3.5: Packet flow diagram of the communication protocol for the proximity detection with more packet exchanges.

mitted as reported in [55]. For the purpose of notifying a proximity detection to users, a buzzer box is prepared, which is attachable to the active radio tag and controllable using a general purpose input/output (GPIO) pin of the tag.

A size of a packet sent for the $N$ exchange protocol is 10 bytes total. The packet consists of a physical layer header and fields for specifying a packet type and a radio channel utilized for sending the packet. A duration that each beacon is sent is 44 ms, which is equal to the sending time of the 10 byte packet at the communication rate of 1800 bps. Timeouts for waiting a warning beacon, a verification packet, and a reply packet are all set to 100 ms. It is calculated from the sum of the carrier sensing time and twice the beacon sending time. The carrier sensing time is 4 ms, which is determined from the RSSI attach-time of the radio chip implemented on the active radio tag [56].


Figure 3.6: *Dice* a low power active RFID tag.

Table 3.1: A specification and a configuration of *Dice*

| | | |
|---|---|---|
| Dimensions | 72.4 mm x 32.8 mm x 16.5 mm | |
| CPU | Type | Renesas H8S/2212 |
| | Clock | 6.144 MHz |
| | ROM / RAM | 128 KB / 12 KB |
| Radio | IC | Chipcon CC1020 |
| | Antenna | Built-in spiral dielectric antenna |
| | Frequency band | 429 MHz |
| | Selected output power | 9 dBm |
| | Communication rate | 1800 bps with Manchester |

### 3.5.2 Experiment Setup and Procedures

Throughout the experiment, a user who is interested with a proximity information of place of interests is assumed to be mobile at a relatively high speed. Assuming that a user rides on a bicycle and wishes to stop in front of the place of interest where an active RFID tag is attached, a distance $d_{thd}$ that the proximity detection procedure starts can be calculated as follows:

$$d_{thd} = (t_{dly} + t_{pr}) * v + d_{stop} - dif_{det} + var_{det}$$

where $t_{dly}$ is a time required for the proximity detection, $t_{pr}$ is a perception-reaction time of the user, $v$ is a velocity of the user, $d_{stop}$ is a stopping distance of the user, $dif_{det}$ is a difference between detection distance and $d_{thd}$, and $var_{det}$ is a variation of detection distance. Setting $d_{thd}$ arbitrary long is not a solution for a successful proximity detection, because a resolution of estimating a distance between active RF tags gets coarse at the long distance. From the preliminary experiment that investigates a relationship between RSS and distance with the YRP UNL's active radio tag, the median of observed RSS is -104 dBm when the distance between tags is 40 meters, and it is -105.5 dBm when the distance is 50 meters, which indicates that it is indistinguishable between 40 meters and 50 meters with observed RSS samples. Therefore, it is necessary to make $d_{thd}$ as small as possible, and that is achievable by minimizing $t_{dly}$, $dif_{det}$, and $var_{det}$.

The purpose of a following experiment is to evaluate $var_{det}$ and $dif_{det}$ of proposed methods in a real-world environment such that there exists a line of sight communication between RF tags. In the experiment, 20 combinations of filtering methods and MAC protocols have been evaluated, which consist of 10 variations of filtering methods and 2 types of protocols. Variations of filtering methods are generated by preparing 2 configurations for 2 parameters used in filtering methods. The configuration is called *Short* when the window size $n$ is 3, and *Long* when $n$ is 6. It is called *Agile* when the smoothing coefficient $\alpha$ is 0.6, and *Stable* when $\alpha$ is 0.3. As for protocols, there are two variations: the one that does not exchange packets, which is called *0-exchange protocol*, and the one that exchanges packet once, which is called *1-exchange protocol*. In addition, $d_{thd}$ is set to 20 meters, which is calculated from the equation shown above when $t_{pr}$ is 2.5 seconds, $v$ is

20 km per hour, and $d_{stop}$ is computed using a friction coefficient of icy road [57] assuming the worst case friction coefficient. $t_{dly}$, $dif_{det}$, and $var_{det}$ are ignored for the calculation. A corresponding RSSI value of $d_{thd}$ is empirically determined by the preliminary experiment that investigated the relationship between RSSI and distance.

The experiment is conducted as follows.

1. Ambient noise levels over 429 MHz, 858 MHz, 1257 MHz, 214.5 MHz, and 143 MHz frequency bands are obtained using a spectrum analyzer. This is done to quantitatively measure an experiment field and to determine radio channels utilized for sending beacons or acknowledge packets.

2. A responder is fixed to a tripod at the height of 1 meter. As indicated in [58] and [59], because an antenna power is lost if a device is close to the ground, the height of tags is maintained.

3. A pinger is attached to the front side of an experimenter's waist with a height of 1 meter.

4. From a point where the distance to the tripod is 40 meters, the experimenter approaches to the tripod, and stops when the buzzer sounds for the first time.

5. A relative distance between the fixed warning node and the point that the experimenter stopped, which is called a detection distance, is measured.

6. Procedures 4 and 5 are repeated for 30 times, for each combination of proposed methods.

The experiment was conducted at 5 different locations as shown in Figure3.7 and 3000 samples of detection distance are collected. Kemigawa football field is an ideal evaluation field where there is no obstacles. The University of Tokyo Hongo campus and the University of Electro-Communication are a location with a low ambient noise affecting 429 MHz frequency band although pedestrian traffic is busy at both places. In both the Gotanda business district and the Ginza shopping district, ambient noise levels affecting 429 MHz frequency band are high and pedestrian traffic is extremely busy.

(a) Kemigawa football field.

(b) University of Tokyo Hongo campus.

(c) UEC campus.


(d) Gotanda business district.

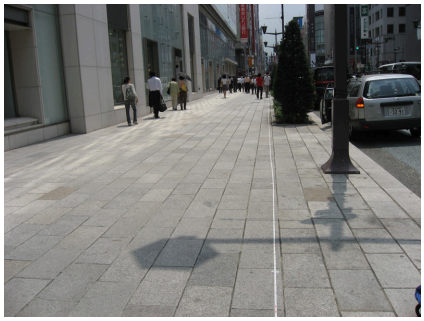

(e) Ginza shopping district.

Figure 3.7: Five locations for the experiment.

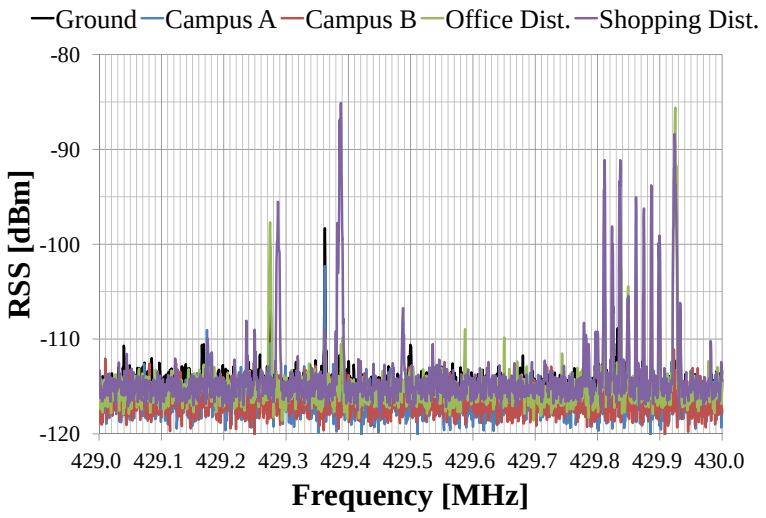


Figure 3.8: Ambient noise level for 429 MHz observed at experimental sites.

A responder node is stationary during the experiment. If an evaluated combination is found to be even useless in the stationary setting, that combination can be omitted for further evaluations for the proposed system.

## 3.6 Results and Analysis

### 3.6.1 Ambient Noise Levels

At each experimental field, an ambient noise level over five different frequency bands are measured by utilizing a spectrum analyzer. Figure3.8 shows the ambient noise level for 429 MHz band, and Figure3.9 shows the ambient noise level for 858 MHz. Here only the base band and the frequency band that is twice of the base band are shown since other frequency bands did not show a significant ambient noise levels compared to these frequency bands. Brief notes of field characteristics and ambient noise levels at five experimental fields are given in following small sections.

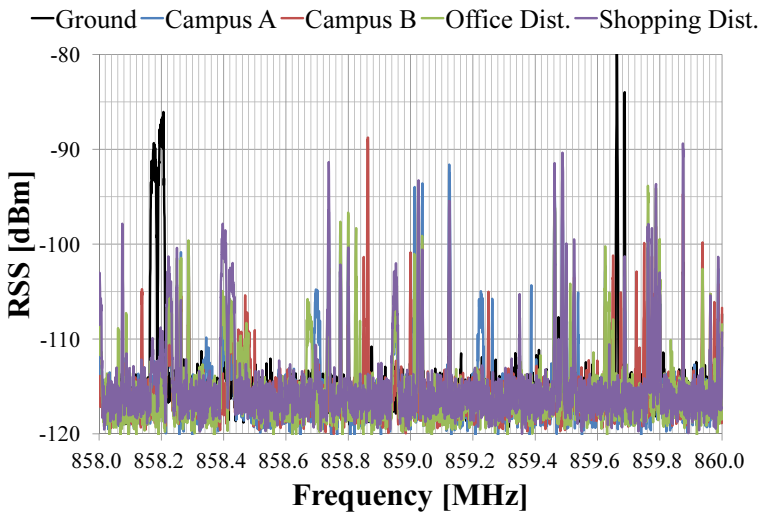


Figure 3.9: Ambient noise level for 859 MHz observed at experimental sites.

### Kemigawa football field

The dimension of the Kemigawa football field is 150 meters by 70 meters. It is a flat field without obstructions. Thus it is close to an ideal radio environment. In addition, no significant ambient noise is found through out all frequency bands, except that an activity of the Multi-Channel Access (MCA) radio is observed at the 858 MHz band.

### Hongo campus near the Tatsuokamon

This is the most busiest street in the Hongo campus of the University of Tokyo, since there are a lot of cars and buses visiting the University of Tokyo Hospital. However, no significant ambient noise is found through out all frequency bands except the MCA radio.

**UEC campus near the building W-7**

This is a quiet campus district in the University of Electro-Communications where many students utilize a bicycle for a transportation. The experiment is conducted on a sidewalk. No significant noise is found through out all frequency bands except the MCA radio.

**Gotanda business district**

This is a busy sidewalk that runs parallel with National Route 1, the biggest highway in Japan. The location was chosen so that it is possible to extend a tape measure for 40 meters and that does not obstruct any businesses or shops. Noises that spans for 50 KHz are observed at 429.25 MHz and at 429.90 MHz, and the MCA radio activities in the 858 MHz band are observed.

**Ginza shopping district**

This is the most crowded place among five experimental locations. There are many cars and people coming and going the street all the time. Noises that spans for 50 KHz are observed at several frequencies in the 429 MHz band. In addition an activities of the MCA radio in the 858 MHz band are observed.

It is important to measure an ambient noise level of an experimental field, especially for evaluating a system that exploits a signal strength to acquire a higher context such as a proximity or a link quality information. RF channels utilized during a transmission of beacons and packets are determined from empirical ambient noise levels over the 429 MHz band.

### 3.6.2 Proximity Detection

As a measure of $var_{det}$, 95 % confidence interval is employed, assuming that collected data is normally distributed. The variation measure is compared for each evaluated combination at 5 experimental fields. Figure3.10 shows the variation of combinations with 0 exchange protocol, and Figure3.11 shows that with 1 exchange protocol. Figure3.12 shows the difference between the median of observed detection distance and $d_{thd}$ when the experiment is conducted at the shopping district.

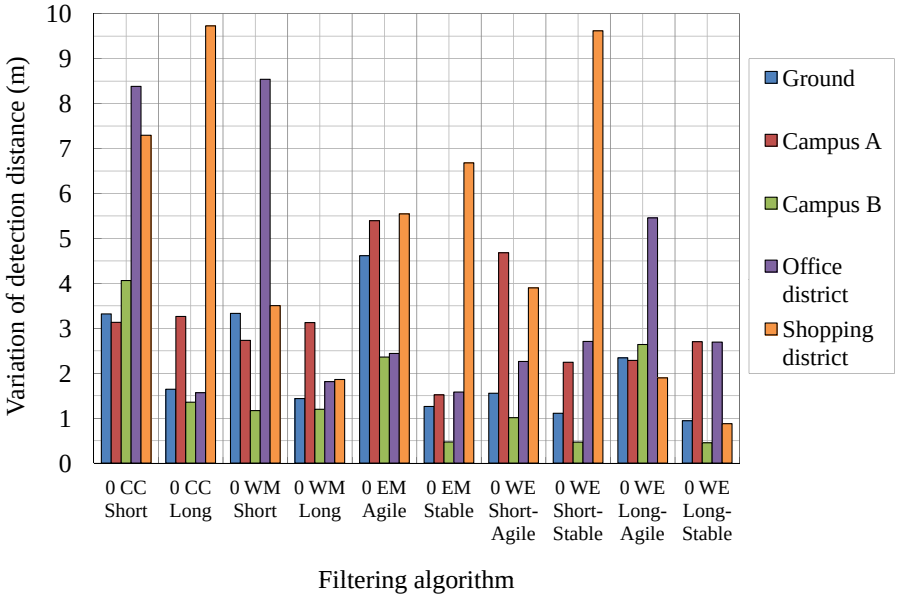


Figure 3.10: Variation of detection distance for the 0 exchange protocol.

By comparing Figure3.10 and Figure3.11, it is observable that the 1 exchange protocol successfully suppresses the variation of detection distance. However, at the business district and the shopping district where pedestrian and automobile traffic is busy and surrounded by tall buildings, there are several filtering methods that the variation remains large although the 1 exchange protocol is used together. This indicates that these filtering methods are not capable of suppressing the variation of detection distance and will not be further evaluated for a future experiment. These are CC, WM, EM with the *Agile* configuration, and WE with the *Short-Agile* configuration. Notice that the WM filtering method with the 1 exchange protocol seems that it has successfully reduced $var_{det}$, whereas Figure3.12 shows that the median of observed detection distance of the WM filtering method is much greater than the $d_{thd}$. It is suspected that the reflected radio signal is strong at the point where the median of observed detection distance collected with the WM filtering method, so that its variation is small but the difference from the $d_{thd}$ is large. The WM filtering method is considered to be affected by the small-scale

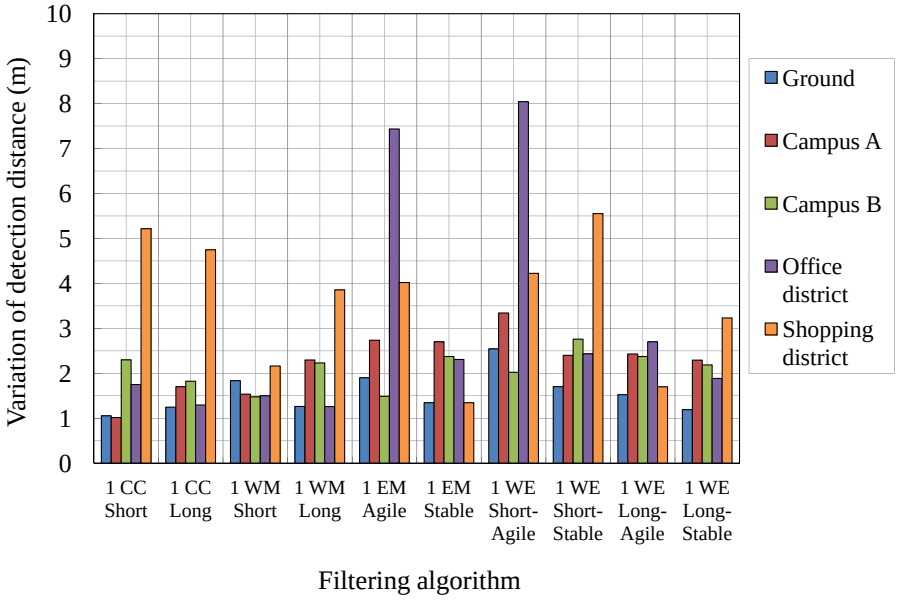


Figure 3.11: Variation of detection distance for the 1 exchange protocol.

fading effect, and thus it is excluded as a candidate for a future evaluation.

There are 4 combinations which successfully suppressed the $var_{det}$ up to 5 meter across different experimental fields. These are EM with the *Stable* configuration, WE with the *Short-Stable* configuration, WE with the *Long-Agile* configuration, and WE with the *Long-Stable* configuration. The performance of these filtering methods is improved by employing the 1 exchange protocol. The variation of observed detection distance with the WE filtering method with the *Long-Agile* configuration is less than 4 meters across 5 locations. This is a large improvement in the infrastructure-less and ad-hoc communication setting, compared to other combinations.

It is observable from Figure3.12 that these filtering methods detect a proximity at the point closer than the target distance $d_{thd}$. This phenomenon is observed because the beacon sending time used in the experiment is much less than the sampling time required by these filtering methods. Table 3.2 shows the minimum number of samples required for the filtered RSSI value to be greater than or equal

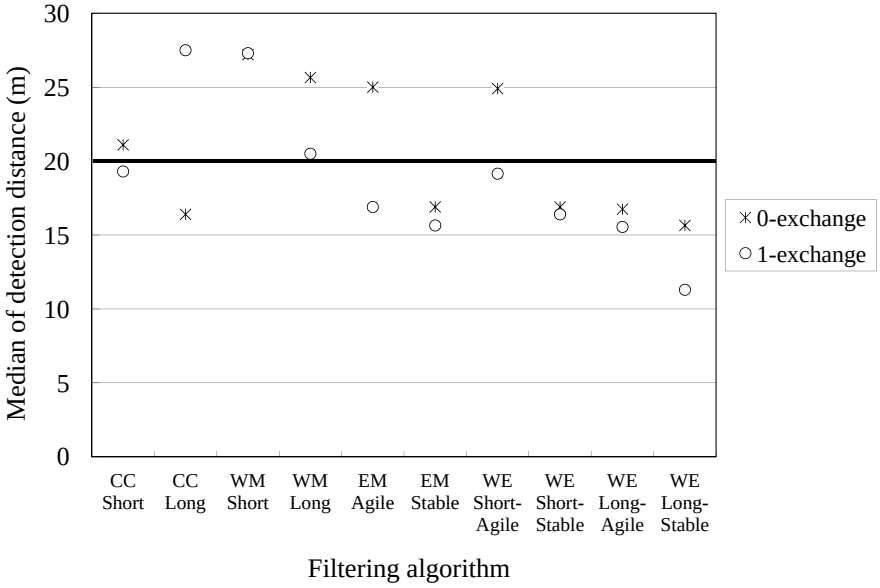


Figure 3.12: Difference of the median of observed detection distance and $d_{thd}$ at the shopping district.

to the RSSI threshold value at $d_{thd}$. These numbers are calculated assuming that the RSSI threshold value is 23, which corresponds to the register value at $d_{thd}$ used in CC1020, and obtained RSSI values at $d_{thd}$ are all equal to 23. The hundredth place of the filtered RSSI value is rounded up and compared with the threshold. In addition, initial values for WM, EM, and WE filtering methods are 15, which corresponds to the carrier sensing level obtained when the RF channel is not utilized. Since the carrier sensing time is 4 ms on the active radio tag and the beacon sending time is 44 ms, the maximum number of times that a node is able to sample RSSI from a single beacon is 11. So, it is not possible to sample the ideal number of RSSI from a single beacon at $d_{thd}$, if one of EM *Stable*, WE *Short-Stable*, and WE *Long-Stable* filtering methods is used. There exists a variation of actual RSSI values obtained at $d_{thd}$, and the sampling time for exceeding the threshold value is usually longer than the ideal sampling time. As a result, the difference $dif_{det}$ for the WE *Long-Agile* filtering method is observed although its ideal sampling time is

Table 3.2: Number of samples required to exceed the RSSI threshold value at $d_{thd}$.

| Filtering method | Parameters | Num. sample req'd |
|---|---|---|
| CC | Short | 3 |
| CC | Long | 6 |
| WM | Short | 3 |
| WM | Long | 6 |
| EM | Agile | 6 |
| EM | Stable | 14 |
| WE | Short-Agile | 7 |
| WE | Short-Stable | 16 |
| WE | Long-Agile | 10 |
| WE | Long-Stable | 17 |

40 ms. It is possible to reduce the difference from the $d_{thd}$ by making the beacon sending time longer than the value used in the experiment.

## 3.7 Discussions

There is a trade-off between the communication protocol without a packet exchange and the $N$ packet exchange protocol. In the $N$ packet exchange protocol, a packet exchange is executed between nodes for $N$ times, which increases a proximity detection latency. With the active RF tags exploited for the evaluations, single packet exchange costs almost 100 ms, since the propagation time of the 10 byte packet is 44 ms and a carrier sensing time is 4 ms. From the result shown above, it is expected that the ranging accuracy increases as the number of packet exchange is increased. However it requires an additional time cost, which is a crucial factor for the proximity detection system since a real-time detection is expected.

In addition, when there are many users in proximity, the overhead of waiting time

caused by a medium access control protocol becomes critical. In the worst case, a node needs to wait for $t_{dly} \cdot O(n)$ where $t_{dly}$ is the time required for the proximity detection and $n$ is a number of nearby nodes. A property of the system that each node does not know their relative locations prohibits to utilize a scheduling based medium access control protocol. A node may yield the proximity detection if it knows that there is no approaching node, but that contradicts with the purpose of the system.

These problems may be overcome by employing an active RF tag with the higher communication rate. For example, the communication rate of 180 kbps reduces the single packet exchange cost to 1 ms and $t_{dly}$ is reduced to hundredth of the original delay time.

## 3.8 Summary

Designing a proximity detection system from low power radio devices without any supporting infrastructure is a challenging task, because the RSS measurement, which is the primary method for estimating the distance between two devices in this setting, is influenced by a lot of environmental factors and thus unstable. To overcome the small-scale fading influencing the on-line RSS measurements, statistical filtering methods were evaluated through extensive real-world experiments. It has been shown that an exponentially weighted moving average with a combination of the proposed packet exchange protocol successfully suppressed a distance variation of the proximity detection system to less than 3 meters in a busy shopping district.

# Chapter 4

# Relative and Partial Location Systems

In this chapter, relative location system and partial location system supported by the location information infrastructure are described. Definitions of these systems are provided first, then approaches and designs of these systems are presented.

## 4.1 Definitions

The primary purpose of the ubiquitous computing is to find out the relationships of objects and users from sensory devices. As long as the object relationships are revealed in some part, the information is useful for the context aware applications.

In this thesis, relative location systems and partial location systems are defined as follows.

**Relative Location System** The relative location system provides geometric notions such as distance and angle to indicate the position of the users relative to target objects and places of interest.

**Partial Location System** The partial location system provides incomplete or partial relative location information of the users.

As for the partial location system, it manages location information of target objects such as only degrees of latitude but not degrees of longitude on the geographic coordinate system.

## 4.2 Overview of Proposed Systems

This chapter introduces relative and partial location systems based on Time-of-flight (TOF) enabled active RFID tags. The ultra-wideband impulse radio (UWB-IR) transceiver introduced in [6] is utilized for evaluations in this chapter. The transceiver emits nanosecond-order width pulses which are spread to 700 MHz bandwidth with a center frequency of 4.1 GHz using the direct sequence-spectrum spreading (DSSS) system.

A relative positioning system that measures the lateral distance between two mobile objects is proposed using UWB-IR active RF tags. Specifically, a scenario assumed for the proposed relative positioning system is a collision detection system between a vehicle and a pedestrian. TOF based bilateration is exploited to localize relative positions of mobile entities in the proposed method. Geometric Dilution of Precision (GDOP) is a key evaluation factor for the TOF based location system, as it indicates accuracy degradation which depends on the geometric layout of distance measurement devices. An error mitigation technique for the lateral distance measurement system is proposed and evaluated by both simulations and real-world evaluations.

A partial positioning system that locates target objects in a direction parallel to infrastructural devices is proposed using UWB-IR tags. In areas filled with objects that obstruct RF signals, it is difficult for the target objects to maintain LOS conditions on all directions. However, common approaches for TOF-based localization system require infrastructural devices to surround the target areas for localizing target objects, to minimize error due to geometric layout of infrastructural devices. The proposed positioning system relaxes the LOS condition required for the target localization to only one direction, by sacrificing a localization accuracy perpendicular to infrastructural device arrays. The proposed positioning system is based on a user-centric architecture for scalability and on-time synchronization mechanism among UWB-IR tags is proposed for reducing deployment cost.

## 4.3 Lateral Distance Measurement System

### 4.3.1 TOF Measurement

Distance between two UWB-IR tags is estimated by measuring a round trip time of a packet exchanged between tags. This method has an advantage over a single packet TOF ranging method, because an accurate clock synchronization between a sender tag and a receiver tag is not required for the method that measures the round trip time. The distance between two UWB tags, $d_{node}$, is calculated as follows:

$$d_{node} = c \times t_{RTT}/2 \tag{4.1}$$

where c is the speed of light and $t_{RTT}$ is the round trip time. It is reported in [6] that a ranging accuracy of 30 cm is achieved with the UWB-IR tags.

### 4.3.2 Measuring Relative Position on a 2D Plane

The alignment of UWB-IR tags are shown in Figure4.1. A tracker node measures distances to base stations 1 and 2 by using the ranging capability of the UWB-IR active RF tags. Two base stations are separated by a known distance $d_{base}$ and mounted on a single mobile entity. In this system, a motor vehicle is assumed for the mobile entity so that $d_{base}$ is approximately 1 to 2 meters. These base stations are reference points for the tracker node to execute bilateration on a 2D plane to determine its position relative to a mobile object such that base stations are mounted. A pair of measured distance $d_1$ and $d_2$ is used for computing angles $\phi$ and $\omega$, which are formed by $d_{base}$ and $d_1$, and $d_{base}$ and $d_2$ respectively. These angles are computed by using the law of cosines as shown below:

$$\phi = \arccos\left(\frac{d_{base}^2 + d_1^2 - d_2^2}{2d_{base}d_1}\right), \tag{4.2}$$

$$\omega = \arccos\left(\frac{d_{base}^2 + d_2^2 - d_1^2}{2d_{base}d_2}\right). \tag{4.3}$$

A relative lateral distance, $d_{lat}$, between the tracker node and base stations when $\phi$ is greater than $\pi/2$ is shown in Figure4.2. While the relative longitudinal distance, $d_{long}$, indicates a distance between a vehicle with a pair of UWB-IR

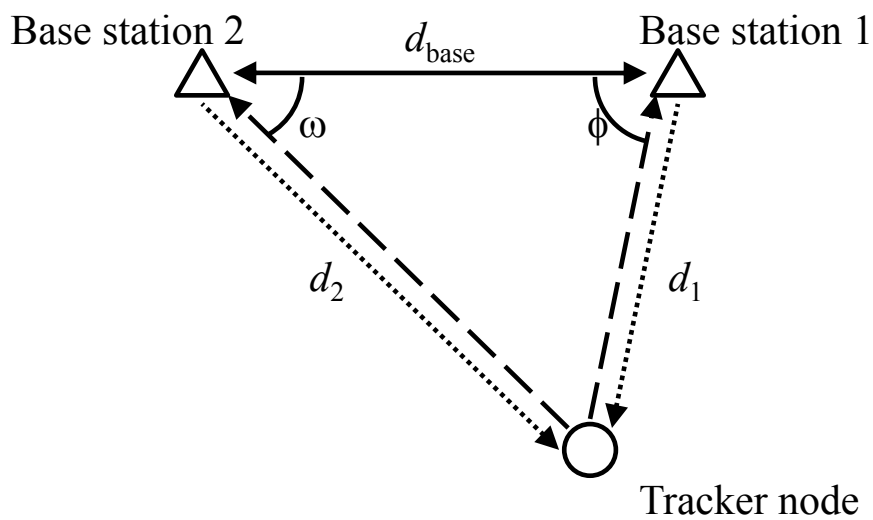


Figure 4.1: The alignment of UWB-IR tags for bilateration.

tags and a pedestrian carrying the UWB-IR tag, the relative lateral distance, $d_{lat}$, is a direct indicator for predicting whether the target vehicle will collide or not with the pedestrian carrying the tracker node if the target vehicle kept its velocity unchanged. Ranging measurements $d_1$ and $d_2$ are both utilized for the calculation of $d_{lat}$. When $\phi$ is greater than $\pi/2$ and $\omega$ is less than $\pi/2$, $d_{lat}$ can be calculated in following two equations:

$$d_{lat1} = d_1 sin(\alpha); \alpha = \phi - \pi/2, \tag{4.4}$$

$$d_{lat2} = d_2 sin(\beta) - d_{base}; \beta = \pi/2 - \omega. \tag{4.5}$$

In the case of $\omega$ is greater than $\pi/2$ and $\phi$ is less than $\pi/2$, $d_2$ and $\omega$ are substituted for $d_1$ and $\phi$ respectively in (4.4) and vice versa for (4.5). $d_{lat}$ is estimated from averaging $d_{lat1}$ and $d_{lat2}$ computed from (4.4) and (4.5) as follows:

$$d_{lat} = \frac{d_{lat1} + d_{lat2}}{2} \tag{4.6}$$

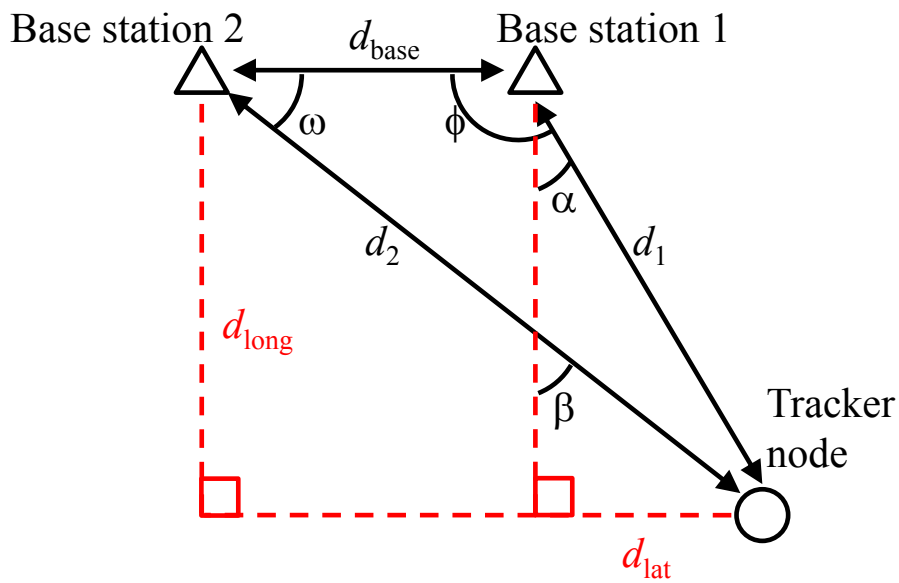


Figure 4.2: Relative lateral distance, $d_{lat}$, between the tracker node and base stations.

When $\phi$ and $\omega$ are both less than $\pi/2$, $d_{lat1}$ and $d_{lat2}$ are calculated from (4.4) and (4.5), although the resulting $d_{lat}$ is less than zero in this case. The absolute value of the calculated lateral distance represents the lateral distance to the base station 1 from the tracker node. A relative longitudinal distance, $d_{long}$, is calculated similarly as follows:

$$d_{long} = \frac{d_1 cos(\alpha) + d_2 cos(\beta)}{2} \tag{4.7}$$

The tracker node is able to find the relative position of the target vehicle either approaching to or departing from the tracker node. Bilateration gives two possible positions of the tracker node across the axis formed by two base stations. The ambiguity of the target vehicle position is resolved by placing base stations in front of headlights as shown in Figure4.3. UWB-IR uses relatively high frequency, thus the emitted signal propagates in a rectilinear path between a pair of UWB transceivers.

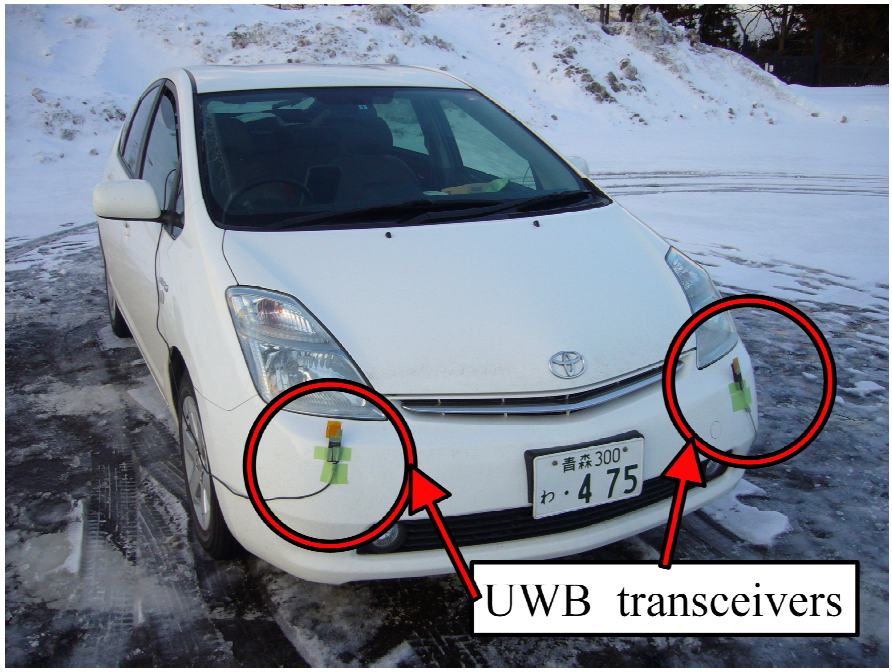


Figure 4.3: Placement of UWB base stations on a vehicle.

Communication between base stations and the target node is established only if there is a line-of-sight between UWB nodes. Since the radio signal does not penetrate through the vehicle's metal body, the tracker node communicates with the target vehicle in the case that the target vehicle approaches to the tracker node.

### 4.3.3 Ranging Error and Its Effect to Position Measurement

Ranging error of the UWB-IR tag causes an error to estimated angles $\phi$ and $\omega$, and estimated $d_{lat}$. Let $d^*_{lat}$ and $d^*_{long}$ denote the real relative lateral and longitudinal distance between the target vehicle and tracker node respectively. To quantitatively study a relationship between estimated $d_{lat}$ and $d^*_{long}$, a 95 % confidence interval of estimated $d_{lat}$ is calculated from 300 samples of randomly generated $d_1$ and $d_2$ for each $d^*_{long}$ from 1 m to 30 m. In the calculation, the ranging error of $d_1$ and $d_2$ is assumed to follow the normal distribution with 1.0 ns standard deviation [60]. The mean value of randomly generated $d_1$ and $d_2$ is the ideal distance $d^*_1$ and $d^*_2$ at each $d^*_{long}$ when $d_{base}$ is 1.2 m and $d^*_{lat}$ is fixed to 4.4 m. $d^*_1$ and $d^*_2$ are

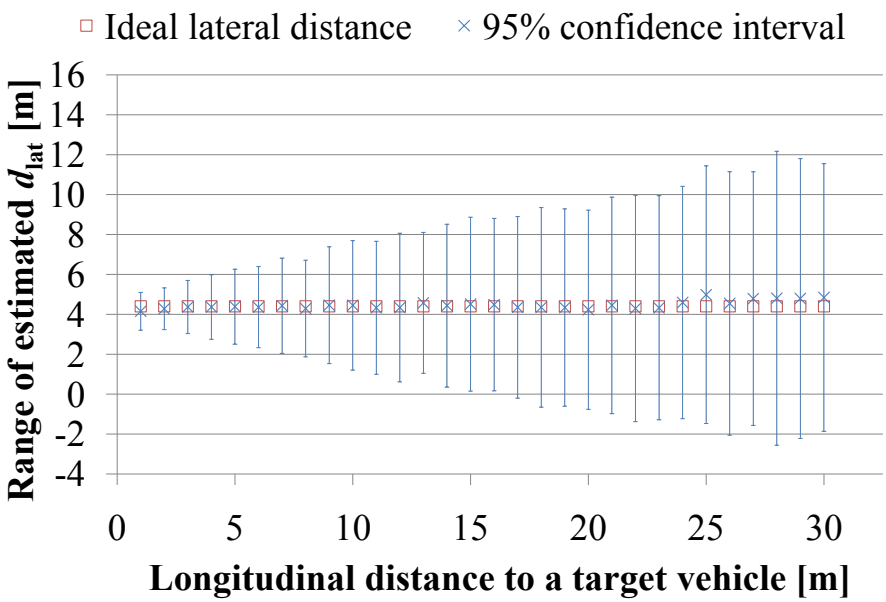


Figure 4.4: A relationship between 95 % confidence interval of observable $d_{lat}$ and $d_{long}$ with 30 cm ranging error of the UWB-IR system.

calculated as follows:

$$d_1^* = \sqrt{{d_{lat}^*}^2 + {d_{long}^*}^2}, \tag{4.8}$$

$$d_2^* = \sqrt{(d_{lat}^* + d_{base})^2 + {d_{long}^*}^2}. \tag{4.9}$$

The chosen value of $d_{base}$ corresponds to a typical car width. This resembles a scenario such that the target vehicle approaches the tracker node on a pedestrian walk and the vehicle drives away without colliding into the tracker node. Figure4.4 shows the relationship between the 95 % confidence interval and $d_{long}^*$.

95 % confidence intervals drawn in Figure4.4 show that an accuracy of estimated $d_{lat}$ is degraded as the increase of $d_{long}^*$. This occurs because the error range of $\phi$ and $\omega$ decreases non-linearly with $d_{long}^*$ and their standard deviation saturates to approximately 8 degrees as shown in Figure4.5 and Table 4.1. Thus the estimation error of $d_{lat}$ calculated by (4.6) increases as the increase of $d_{long}^*$.

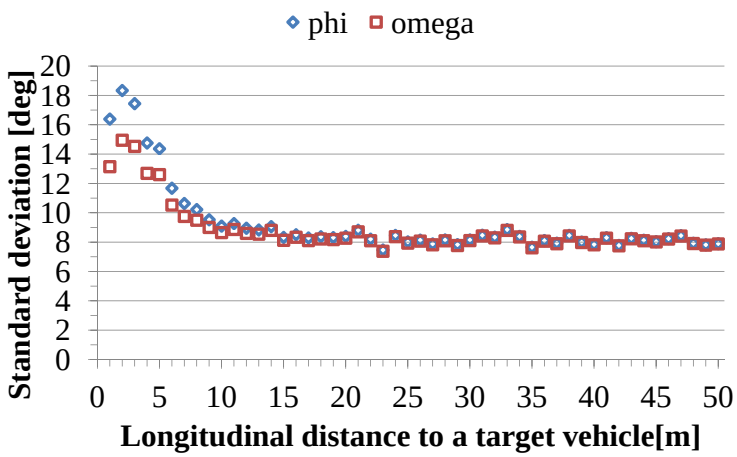


Figure 4.5: Standard deviation of estimated angles $\phi$ and $\omega$ vs. the longitudinal distance between the target vehicle and the tracker node.

Table 4.1: Standard deviations of angles and $d_{lat}$ for selected $d_{long}$

| | **Standard deviation** | | |
|---|---|---|---|
| $d_{long}$ [m] | $\phi$ [deg] | $\omega$ [deg] | $d_{lat}$ [m] |
| 5 | 12.97 | 11.41 | 0.965 |
| 15 | 8.641 | 8.437 | 2.209 |
| 30 | 8.027 | 7.979 | 3.384 |

### 4.3.4 Data filtering method

It is necessary to reduce the error range of estimated lateral distance. The user of the tracker node receives benefit from determining a possibility of collision with a nearby target vehicle at the farthest possible distance. As discussed in the previous subsection, the error in estimating lateral distance is largely affected by the error

in estimating angles $\phi$ and $\omega$ when $d^*_{long}$ is large. Applying a time-series filter on angles $\phi$ and $\omega$ is proposed to reduce the estimation error of the relative lateral distance. An applicability of the exponentially weighted moving average (EWMA) filter for estimating lateral distance is studied by simulations and field experiments.

The EWMA filter is a simple time-series filtering method that its transfer function is identical to the first-order low pass filter. The filtered time-series, $y_t$, using the EWMA filter is calculated as follows:

$$y_t = y_{t-1}(1-\alpha) + \alpha x_t, 0 \leq \alpha < 1 \tag{4.10}$$

where $x_t$ represents the unfiltered time-series and $\alpha$ represents the filter constant. The computation requires $O(1)$ bytes of memory and $y_t$ can be calculated by a single multiplication, so that it can be easily implemented and used on low power mobile computers.

### 4.3.5 Simulation

An optimal filtering parameter for the proposed filtering method is explored by simulations. The optimal filtering parameter reduces the estimation error of the relative lateral distance between the target vehicle and the tracker node while retaining responsiveness to a change in the true lateral distance. The estimation error of the relative lateral distance $\varepsilon(d_{lat})$ is defined as follows:

$$\varepsilon(d_{lat}) = d_{lat\_measured} - d^*_{lat} \tag{4.11}$$

where $d_{lat\_measured}$ is the lateral distance calculated by measured $d_1$ and $d_2$ using (4.6), and $d^*_{lat}$ is the ideal lateral distance which is calculated from the true position of the vehicle relative to the tracker node at a given timing.

#### Evaluation by scenarios

Three scenarios are considered for evaluating performance of the EWMA filter with a varied filter constant. It is reported in [61] that accidents between pedestrians and battery-operated vehicles are expected in following situations due to quietness of moving battery operated vehicles at slow speed less than 5.56 m/s. In

all scenarios, the position of the tracker node is defined as the origin and the tracker node is assumed to be stationary for simplification. The target vehicle moves along a pass determined for each scenario and the width of the target vehicle is 1.2 m.

1. **Collision** A target vehicle approaches toward a tracker node from the initial relative longitudinal distance of 30 m. They collide after some time period, which is determined by the relative velocity between the target vehicle and the tracker node. $d^*_{lat}$ is zero in this scenario.

2. **Pedestrian walk** The target vehicle approaches toward the tracker node from the initial longitudinal distance of 30 m, but their relative lateral distance is maintained at 4.4 m. The relative position of a pedestrian carrying the tracker node and the target vehicle is depicted in Figure4.6. This scenario represents a case that the pedestrian is located on a pedestrian walk and the target vehicle runs a road next to the pedestrian walk. A collision between the target vehicle and the pedestrian will not occur if the pedestrian maintains walking on the pedestrian walk and the vehicle runs on the vehicle road.

3. **Intersection** The target vehicle turns left on a T-shaped intersection when the tracker node attempts to cross the intersection as shown in Figure4.7. The vehicle starts to turn left when its relative position to the tracker node $(d_{lat}, d_{long})$ becomes (5 m, 5 m). Its turning curve radius is 5 m. The initial relative position of the target vehicle is (5 m, 25 m).

In this simulation experiment, simulated distances $d_1$ and $d_2$ are generated randomly from a normally distributed random value with the mean $d_k(t)$ and the standard deviation 0.117 m. $d_k(t)$ represents the ideal distance between the tracker node and the base station $k$ at time $t$. $d_1(t)$ and $d_2(t)$ are calculated by (4.8) and (4.9) respectively. $d^*_{lat}(t)$ and $d^*_{long}(t)$ are calculated for each scenario, from the target vehicle speed of 2.78 m/s. The standard deviation of ranging accuracy is approximated as 0.117 m by assuming that 99 % of measured distance retains 30 cm ranging accuracy. $d_1$ and $d_2$ are generated every 8 Hz until the longitudinal distance between the target vehicle and the pedestrian becomes zero. Packet loss between the tracker node and base stations is not considered in the simulation

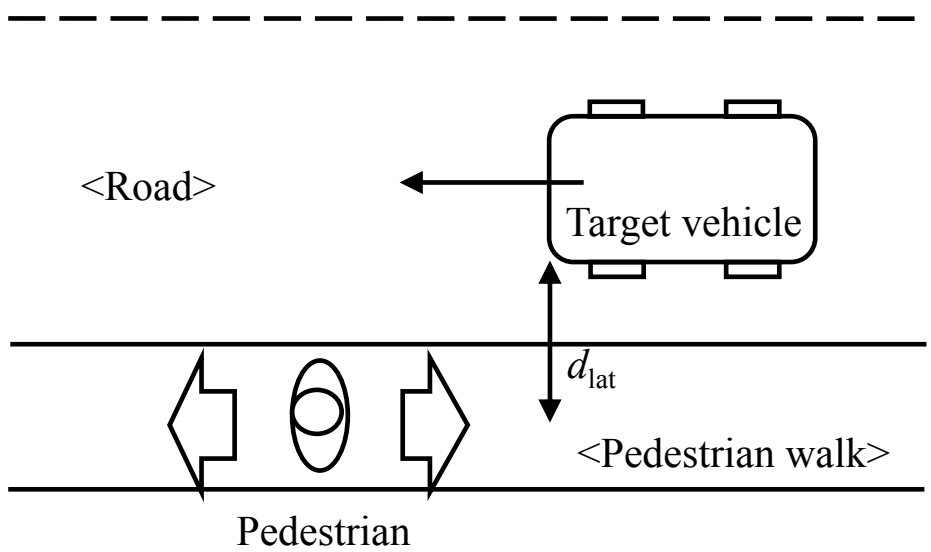


Figure 4.6: "Pedestrian walk" scenario. $d^*_{lat}$ is maintained while the target vehicle approaches the pedestrian.

model. In addition, $d_1$ and $d_2$ have the same time-stamp, by assuming that ranging between the tracker node and two base stations on the target vehicle are completed at the same timing.

A set of $d_1$ and $d_2$ for each scenario is generated 300 times. While the target vehicle approaches the pedestrian, $\varepsilon(d_{lat})$ is recorded at the same timing as the simulated measurement of $d_1$ and $d_2$ for 9 variations of the EWMA filter constant. The filter constant is varied from 0.1 to 0.9. The standard deviation of recorded $\varepsilon(d_{lat})$ is calculated for each simulation trial, and averaged over 300 trials for each scenario. The average of the standard deviation of $\varepsilon(d_{lat})$ for each scenario and the filter constant is plotted in Figure4.8. The filter constant value of 1 indicates that angle data is not processed by the EWMA filter.

Notice from Figure4.8 that the estimation error can be reduced the most when the filter constant equals to 0.2. For scenarios 1 and 2, the relative lateral distance

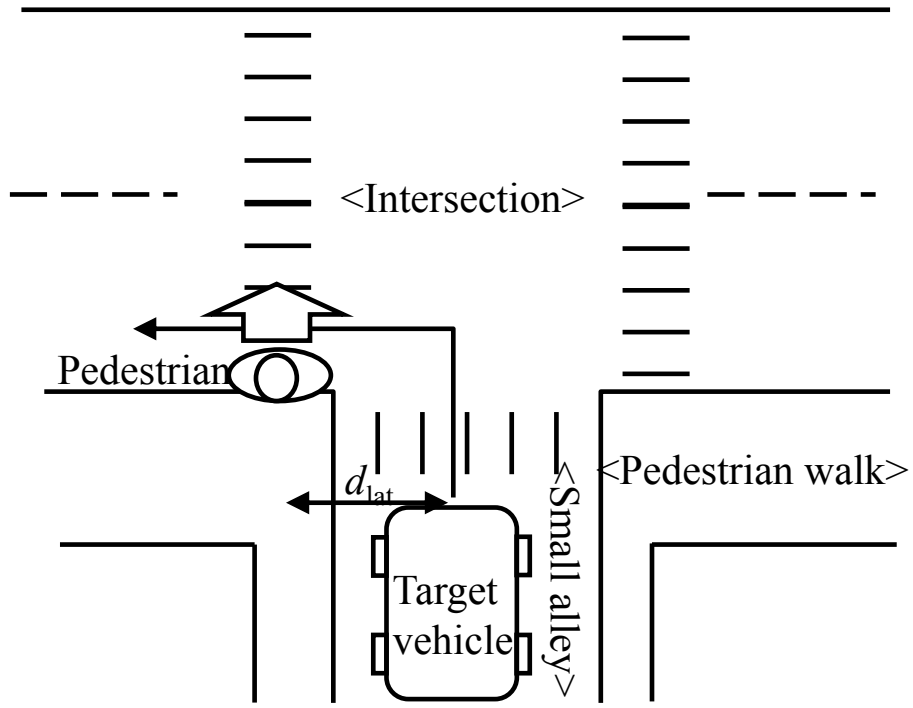


Figure 4.7: "Intersection" scenario. The target vehicle turns left at the intersection and approaches the pedestrian.

between the target vehicle and the tracker node does not change while the target vehicle approaches the tracker node, so that it is a natural choice to select the filter constant of the EWMA as small as possible. However, as in the scenario 3 such that the target vehicle makes a turn, the filter constant of 0.1 causes the tracker node to lose an ability to properly locate the relative position of the target vehicle. Figure4.9 shows one of simulation trials for the scenario 3. It shows that the EWMA with $\alpha = 0.2$ retains a responsiveness to the change in the lateral distance while minimizing the estimation error. The estimation error of the relative lateral distance is kept under 2 m when the distance between the target vehicle and the tracker node is less than 20 m. In addition, the tracker node is successful in tracking the change in the relative lateral distance when the target vehicle reaches the intersection and starts turning to left.

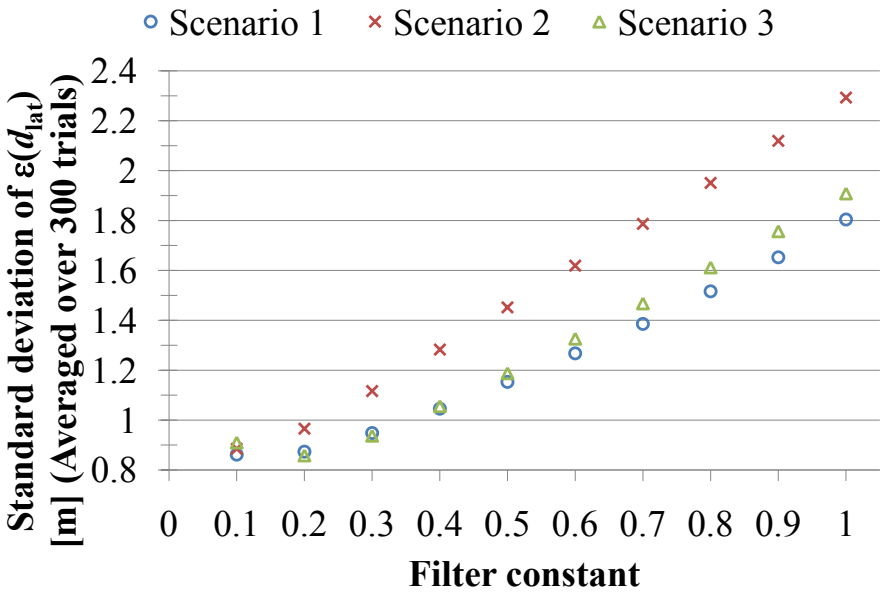


Figure 4.8: The relationship between the averaged standard deviation of $\epsilon(d_{lat})$ and the filter constant for each scenario.

### Evaluation by relative vehicle speeds

In this simulation, the relationship between the relative speed of the target vehicle and the estimation error of the relative lateral distance is evaluated. Three relative speeds, 2.78 m/s, 5.56 m/s, and 8.33 m/s, are evaluated in the simulation. "Pedestrian walk" scenario described above is used in the simulation. For each vehicle speed, a set of $d_1$ and $d_2$ is generated 300 times in the same manner as the previous simulation. From generated data set, angles $\phi$ and $\omega$ are calculated and filtered using 9 variations of the EWMA filter constant. Figure4.10 shows the relationship between the average standard deviation of $\varepsilon(d_{lat})$ and 9 filter constants for each relative speed. The average standard deviation of $\varepsilon(d_{lat})$ is calculated from 300 simulation trials.

Although the filter constant value of 0.1 effectively reduces $\varepsilon(d_{lat})$ when the relative speed is 2.78 m/s and 5.56 m/s, the value of 0.2 gives the best result when

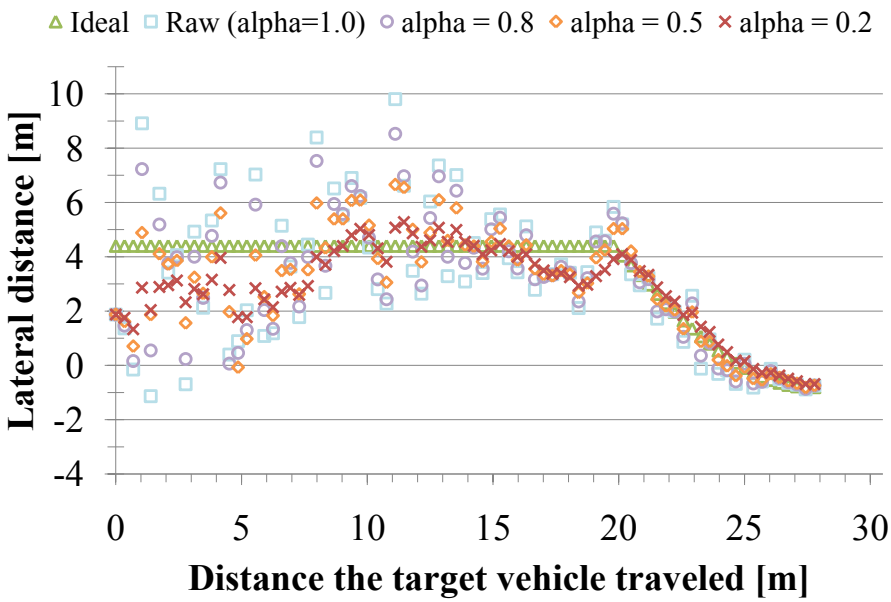


Figure 4.9: A simulation trial of "Intersection" scenario. The relationship between lateral distance and the distance that the target vehicle traveled is plotted.

the relative speed is 8.33 m/s. The filter constant value of 0.1 increases the overall error in the estimation of the relative lateral distance when the relative speed is large. Since the frequency of ranging requests to base stations is fixed among these three relative speeds, the number of obtainable samples $d_1$ and $d_2$ is not enough for conducting the correct estimation of the relative lateral distance using the filter constant value of 0.1 when the relative speed is 8.33 m/s.

Since it is important to retain responsiveness to the change in the relative lateral distance as well as minimizing $\varepsilon(d_{lat})$, the filter constant value of 0.2 is a preferred choice for this system.

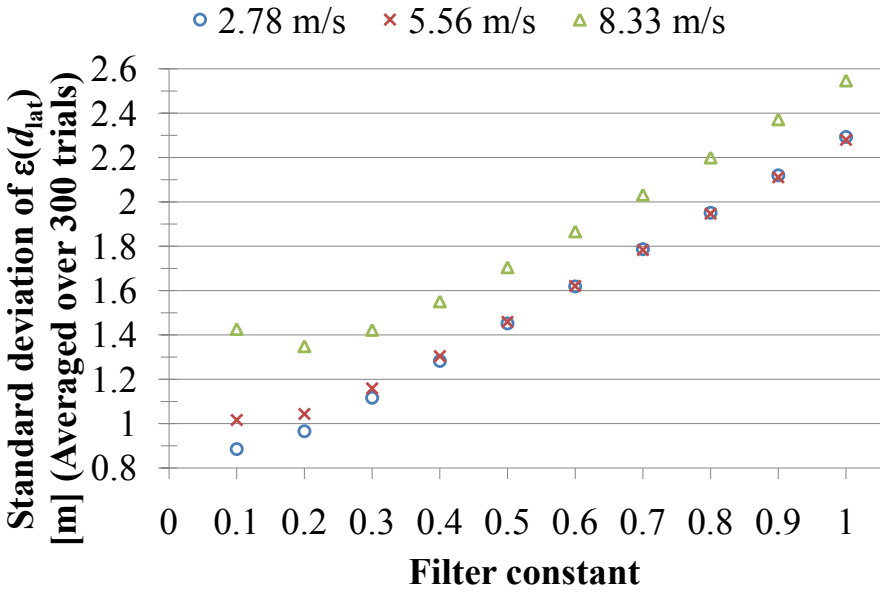


Figure 4.10: The relationship between the averaged standard deviation of $\epsilon(d_{lat})$ and the filter constant for each experimented relative speed.

### 4.3.6 Field Experiments

#### UWB hardware

Field experiments have been conducted for evaluating the performance of the EWMA filter applied to real-time data from the UWB transceiver device. The UWB transceiver device for the tracker node is shown in Figure4.11. The UWB LSI developed by YRP UNL is attached to a Bluetooth communication module and connected to an omni-directional UWB monopole antenna. Ranging data collected by the UWB LSI is sent to a mobile terminal via Bluetooth and the relative lateral distance is calculated and recorded in real-time by the mobile terminal. The picture of the mobile terminal is shown in Figure4.12. A pair of the UWB LSI for base stations is attached in front of the vehicle as shown in Figure4.3. Base stations 1 and 2 are attached on the left door side and the right door side of the vehicle

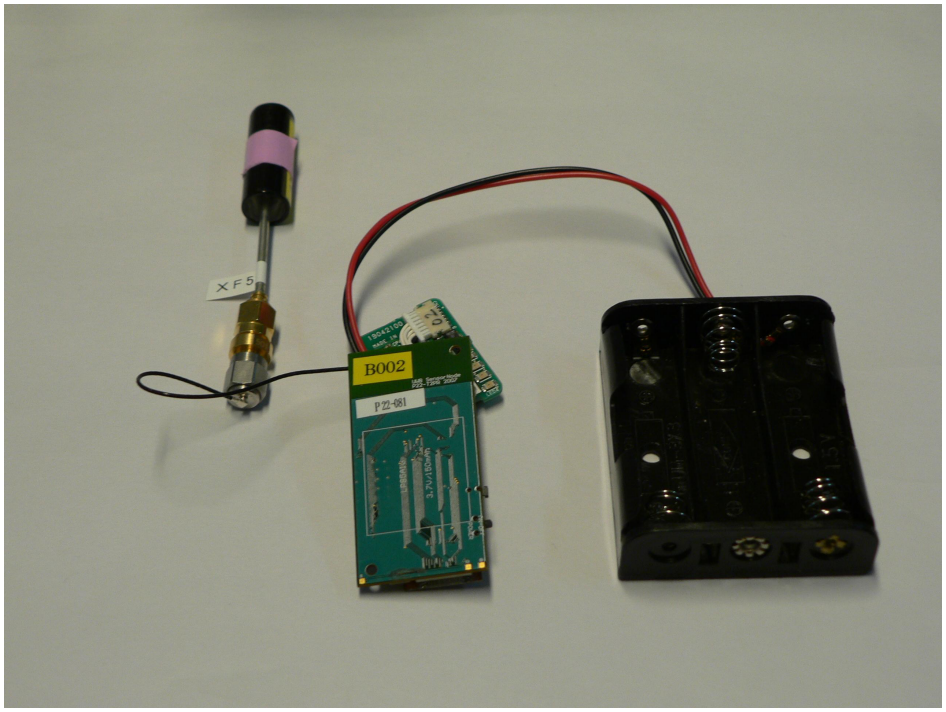


Figure 4.11: The UWB-IR active RF tag for the tracker node.

respectively.

There are two significant differences in the real UWB device from assumptions made in simulations, which affect the estimation error of the relative lateral distance. In simulations, packet loss is assumed to not occur between two UWB transceivers, whereas the packet loss rate of the UWB LSI in a RF anechoic chamber is less than 2 %, which is empirically confirmed when the distance between UWB transceivers is 1 m and their height is maintained at 1 m. It is expected that the packet loss rate increases when UWB transceivers are used outdoor due to the multi-path effect caused by surrounding buildings.

The second difference is the timing difference in obtaining $d_1$ and $d_2$. With the current implementation of the UWB LSI, one-to-one communication is assumed for obtaining a distance between UWB transceivers. Thus the tracker node needs to send two independent ranging requests to each base station for executing bilateration. The timing difference is expected to increase the estimation error of the

Figure 4.12: The mobile terminal for on-line calculation of its relative position to the vehicle.

relative lateral distance as the moving speed of the target vehicle increases. The highest frequency that the UWB LSI is capable of sending a ranging packet is 16 Hz. If the UWB LSI sends a ranging packet at the rate of 16 Hz, the distance that the vehicle moves before sending the second ranging request is 17 cm, 35 cm, and 52 cm for the relative velocity of 2.78 m/s, 5.56 m/s, and 8.33 m/s respectively. Since the expected ranging accuracy of the UWB LSI is 30 cm, it is expected that the increase of the estimation error in the relative lateral distance is observed in the case that the vehicle moves in 8.33 m/s.

### 4.3.7 Results and Discussions

The "pedestrian walk" scenario was chosen for evaluating the EWMA filter in field experiments. The picture of the experimental site is shown in Figure4.13. The "pedestrian walk" scenario was repeated three times for three variations of target

Figure 4.13: Experimental site for "pedestrian walk" scenario.

vehicle speed. Variations of the aimed vehicle speed were 2.78 m/s, 5.56 m/s, and 8.33 m/s. To make sure that the vehicle moves in a constant speed during an experimental trial, a wait line for the vehicle was marked on the road, which was 20 m away from a start line of the experimental zone. For each trial, the vehicle accelerated to the aimed speed before the start line. The tracker node was placed on the pedestrian walk along an end line of the experimental zone. The height of the tracker node was fixed to 1 m using cardboard boxes. Distance between the start line and the end line was 30 m. To measure the actual speed of the vehicle for the trial, absolute time that the vehicle crossed the start line and the end line was recorded for each trial.

Table 4.2 summarizes results of field experiments. For each recorded $d_{lat}$ at sampling time $t$, $\varepsilon(d_{lat}(t))$ is calculated from $d^*_{lat}(t)$ of the "pedestrian-walk" scenario. $d^*_{lat}(t)$ is constant over sampling time $t$ and it is 4.4 m for the scenario. The standard deviation of $\varepsilon(d_{lat})$, $s(\varepsilon(d_{lat}))$, while the vehicle approaches the tracker node

Table 4.2: Vehicle speed and the standard deviation of $\varepsilon(d_{lat})$.[1]

| **Aimed speed [m/s]** | **Measured speed [m/s]** | $s(\varepsilon(d_{lat}))$ **[m]** $d_{long} \leq 30$ **m** | | $s(\varepsilon(d_{lat}))$ **[m]** $d_{long} \leq 15$ **m** | |
|---|---|---|---|---|---|
| | | **Raw data** | **EWMA** ($\alpha = 0.2$) | **Raw data** | **EWMA** ($\alpha = 0.2$) |
| 2.78 | 2.78 | 3.650 | 1.667 | 1.943 | 0.945 |
| 5.56 | 5.22 | 5.229 | 2.588 | 2.913 | 1.012 |
| 8.33 | 7.11 | 6.837 | 2.779 | 3.864 | 1.624 |

[1] Measured vehicle speeds and standard deviations are averaged over 3 experimental trials.

is computed for each experimental trial. In addition, $s(\varepsilon(d_{lat}))$ is computed again for the case that $d_{long}$ is less than 15 m. $d_{long}$ corresponds to the distance that the vehicle traveled during the experimental trial. Table 4.2 shows averaged $s(\varepsilon(d_{lat}))$ over three experimental trials for each aimed vehicle speed.

The EWMA filter successfully reduces $\varepsilon(d_{lat})$, especially when $d_{long}$ is less than 15 m as shown in Table 4.2. Measured values of standard deviation of $\varepsilon(d_{lat})$ for each vehicle speed when $d_{long}$ is less than 15 m conform with the simulated result as depicted in Figure4.10, although it is slightly higher than the simulated result for the case of the aimed vehicle speed at 8.33 m/s. The value of the standard deviation of $\varepsilon(d_{lat})$ in the simulated result is 1.349 for 8.33 m/s. Figure4.14 and Figure4.15 plot the relationship between the estimated $d_{lat}$ with and without the EWMA filter applied and the distance that the target vehicle traveled when the aimed vehicle speed is 2.78 m/s and 8.33 m/s respectively. From these plot, it is observable that the error of estimated $d_{lat}$ is less than 3 m when the EWMA filter is exploited, whereas it is greater than 8 m without filtering at $d_{long}$ equals 15 m.

Larger estimation error of $d_{lat}$ than simulation results is observable when $d_{long}$ is greater than 15 m. Packet loss is one of two reasons that caused this result. Figure4.14 shows that the value of the estimated $d_{lat}$ is suddenly decreased to 0 m when the distance that the vehicle traveled is 10 m. This result is caused by the loss

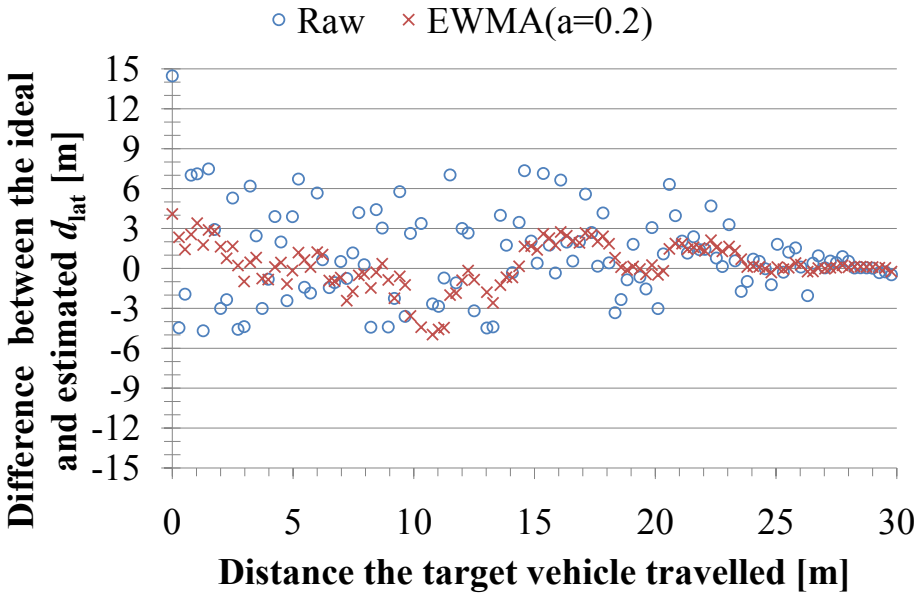


Figure 4.14: A field experimental trial for the aimed vehicle speed of 2.78 m/s. The relationship between the estimated $d_{lat}$ and the distance the target vehicle traveled is plotted.

of ranging packet to the base station 1 while $d_2$ is updated at the constant rate. The current implementation of the relative lateral distance estimation updates the value at the rate of 8 Hz. If new ranging data for $d_1$ or $d_2$ is not received in the update cycle, a previously measured distance is utilized for the relative lateral distance calculation. In the case of Figure4.14, the value of $d_1$ used for the relative lateral distance calculation is maintained while the value of $d_2$ is updated. The updated value of $d_2$ is less than its previous value since the target vehicle approaches the tracker node. Thus the estimated lateral distance decreases as if the tracker node is in front of the target vehicle.

Another reason for the observed estimation error is the timing difference in measuring $d_1$ and $d_2$, which is observable especially in the case that the aimed target vehicle speed is 8.33 m/s. Notice from Figure4.15 that the estimated relative lateral

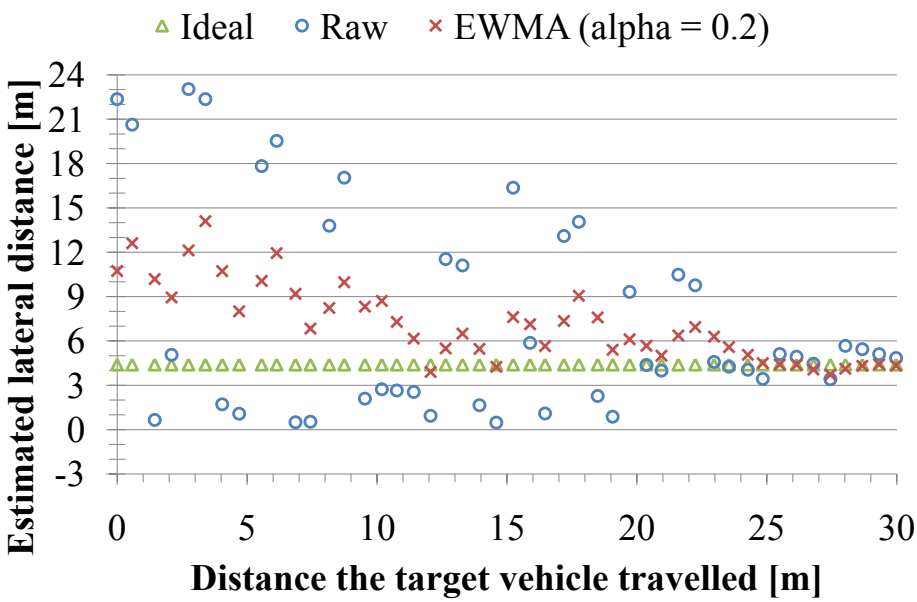


Figure 4.15: A field experimental trial for the aimed vehicle speed of 8.33 m/s. The relationship between the estimated $d_{lat}$ and the distance the target vehicle traveled is plotted.

distance is much larger than the ideal lateral distance when the target vehicle is away from the tracker node. This phenomenon occurs in the case that the relative lateral distance is calculated from $d_1$ and $d_2$ such that $d_2$ is measured first and the vehicle moves while the measurement of $d_1$ is completed. In this case, measured $d_1$ is smaller than $d_1$ at the time when $d_2$ is measured. Since ranging error has greater effect on the estimation of $d_{lat}$ when $d_{long}$ is large than when $d_{long}$ is small, the timing difference in ranging to base stations causes estimated $d_{lat}$ to increase when the distance between the tracker node and the target vehicle is large.

## 4.4 Active Sonar System

There are three requirements imposed on the TOF-based positioning system for areas filled with obstacles.

1. Relaxed LOS conditions. It is difficult for the target objects to maintain LOS conditions to infrastructural devices in all directions.

2. Scalability. User-centric architecture needs to be maintained for the localization system to operate when there are many target objects.

3. On-time synchronous operation. To reduce the cost of synchronization among infrastructural devices, a communication mechanism that does not require synchronization among infrastructural devices is necessary.

To satisfy above requirements, the positioning method exploited in the proposed system utilizes a multiple hyperbola-hyperbola intersection method, which allows three anchor nodes aligned on a line to find the position of the target node. In addition, in the proposed positioning method, the task of the target node is limited to measure TDOA information of anchor node triples and anchor nodes can operate asynchronously from each other thus it is not necessary to physically wire anchor nodes. Thus the scalability of the system in terms of obtaining timing information for the localization procedure is maintained, even when the number of target node increases. Also, the positioning system is easily expandable by adding an anchor node triple to the target site because each anchor node triple can independently provide location information to the target node.

### 4.4.1 Positioning Algorithm

An anchor node triple aligned on a line forms a single positioning system. The positioning procedure is initiated by one of anchor nodes, called an initiator node which transmits a beacon. The beacon sent from the initiator node is received by other anchor nodes and a target node. Anchor nodes listening for the beacon sent from the initiator node are referred as the reflector node. When reflector nodes receive the beacon from the initiator node, they immediately send beacons to the

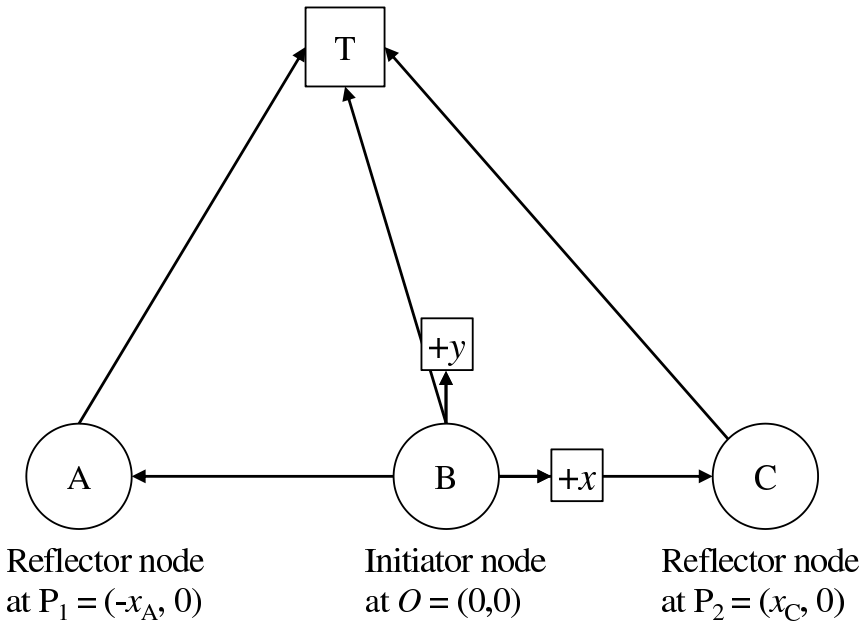


Figure 4.16: Illustration of the hyperbola-hyperbola positioning. Anchor nodes are aligned on a line. The node B operates as the initiator node and the node A and C work as the reflector node.

target node. The target node receives beacons from reflector nodes, so that it can measure the time difference of arrival of the beacon sent by the initiator node and the beacon sent by the reflector node. Given the initiator node's position $O$ and positions of reflector nodes $P_1$ and $P_2$, a single transmission of the initiator node's beacon allows the target node to obtain two hyperbolas with foci at $(O, P_1)$ and $(O, P_2)$. Figure4.16 illustrates the proposed positioning method such that the node B operates as the initiator node and the node A and C work as the reflector node. The semi-major axis of the hyperbola with foci at $(O, P_1)$ is given by $a_{AB} = t_{B-A} - d_{AB}$, where $t_{B-A}$ is the measured time difference of arrival of the beacon sent by the node B and the beacon sent by the node A, and $d_{AB} = x_A$ is the distance between the node A and B.

Intersection of two hyperbolas is calculated by solving a quadratic equation.

For example, to find the intersection of hyperbolas $(O, P_1)$ and $(O, P_2)$, following quadratic equations are utilized:

$$y^2 = L_{BC}x^2 + M_{BC}x + N_{BC}, \tag{4.12}$$

$$y^2 = L_{AB}x^2 + M_{AB}x + N_{AB}, \tag{4.13}$$

where $(x, y)$ is the coordinate of the target,

$$L_{BC} = \frac{x_C^2}{4a_{BC}^2} - 1, \tag{4.14}$$

$$M_{BC} = -\frac{(x_C - 2a_{BC})(x_C + 2a_{BC})x_C}{4a_{BC}^2}, \tag{4.15}$$

$$N_{BC} = \frac{(x_C - 2a_{BC})^2(x_C + 2a_{BC})^2}{16a_{BC}^2}, \tag{4.16}$$

and similarly for $L_{AB}$, $M_{AB}$, and $N_{AB}$.

Intersection of two hyperbolas gives four candidate positions of the target node. Among them, two positions are obtained from changing the sign of the y-coordinate of other two because anchor nodes are aligned on a line. By limiting the answer positions to quadrants I and II of the coordinate system defined by the anchor node triple, two candidate positions are obtained for the target node. To determine the position of the target node from candidate positions, one way is to bound the region of interest and test whether candidate positions lie inside of the bounded region. If only one of candidate positions lie inside of the bounded region, the target node position is uniquely determined. If both candidate positions or neither of them lie inside of the bounded region, the target node position is undefined with this trial of TDOA measurements.

Another way to uniquely determine the target node position from candidate positions is to conduct the TDOA measurements again with a different initiator node. One of reflector nodes now operates as the initiator node and the previous initiator node work as the reflector node, to let the target node to obtain another pair of hyperbolas. For example, when the node A from Figure4.16 operates as the initiator node and the node B and C work as the reflector node, the target node can obtain a hyperbola with foci at $(P_1, P_2)$ and the semi-major axis of $a_{AC} = t_{C-A} - d_{AC}$, where $t_{C-A}$ is the TDOA of beacons sent from the reflector node C and

the initiator node A and $d_{AC} = x_A + x_C$ is the distance between the node A and the node C. With two pairs of hyperbolas, $\{(O, P_1), (O, P_2)\}$ and $\{(O, P_1), (P_1, P_2)\}$, the receiver node obtains four candidate positions $\{p_1 = (x_1, y_1), p_2 = (x_2, y_2), p_3 = (x_3, y_3), p_4 = (x_4, y_4)\}$. The distances along the x-axis between candidate positions $p_i, p_j$ are calculated as $x_{ij} = |x_i - x_j|$ where $i \neq j$, then the target position is determined by averaged position of $p_i$ and $p_j$ such that $x_{ij} < \epsilon$, where $\epsilon$ is a small constant determined from the time resolution of the UWB transceiver. The x-coordinates of candidate positions are compared for choosing the target position because the accuracy in the direction of the y-axis is degraded as anchor nodes are aligned on a line.

With real hardware, a reflector node $R$ requires a time to process the beacon received from the initiator node and to prepare sending its beacon, introducing the time delay at the reflector node $T_d^R$ to the TDOA measured by the target node. So, as for the aforementioned hyperbola with foci at $(O, P_1)$, its semi-major axis becomes $a_{AB} = t_{B-A} - d_{AB} - T_d^A$, where $T_d^A$ is the time delay of the node A when it operated as the reflector node. The time delay can be measured by the conventional loop-back tests, and the measured value is stored to the ROM for each UWB transceiver before the system deployment. To allow the target node to subtract the time delay at the reflector node, the reflector node always send its processing time along with the beacon.

### 4.4.2 Initiation Procedure

As discussed in the previous subsection, multiple anchor nodes among the anchor node triple are expected to execute the role of the initiator node, to let the target node to obtain multiple pairs of hyperbolas for uniquely determining its position. In order to execute the initiator role, each anchor node of the anchor node triple tries to transmit the initiation beacon in a random period with a simple CSMA/CA media access control protocol for avoiding the collision. Anchor nodes operate as a reflector node while it awaits for the next transmission time and while it is in the back-off status. Figure4.17 shows the state diagram of the anchor node.

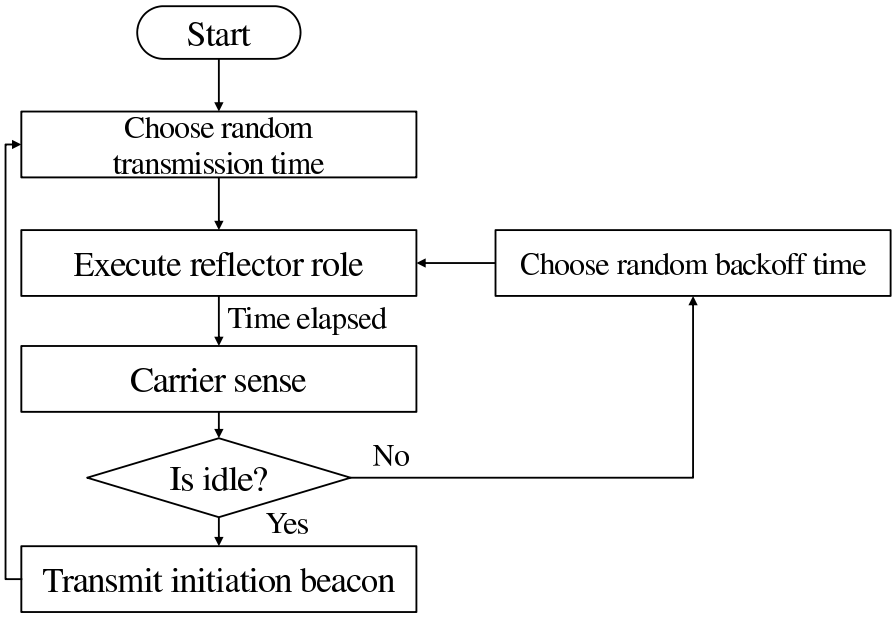


Figure 4.17: The state diagram of anchor nodes.

### 4.4.3 Implementation

Anchor nodes and a target node are prepared from UWB-IR devices. The UWB module transmits 2 nano-second pulses with a center frequency of 4.1 GHz a using the direct sequence spectrum spreading (DSSS) system. The pulse repetition rate is 32 MHz and the 3 dB frequency bandwidth is 700 MHz. The UWB module complies with the Federal Communications Commission (FCC) spectrum mask. It achieves a pulse sampling resolution of 0.5 nanoseconds and its communication distance is 30 meters. Its data rate is 258 kbps and the duration of a single packet is less than 5 ms when its operates at 258 kbps.

Anchor nodes are implemented with the UWB module introduced above. It uses a UWB omni-directional antenna equipped to obtain a receiver gain of 2.6 dBi. The module is programmed to normally work as the reflector node, then it operates as the initiator node when the randomly selected transmission time is elapsed. The transmission time is selected between 300 ms to 1000 ms, so that

each anchor node does not exceed the low duty cycle requirement regulated by the European Commission (EC) [62].

### 4.4.4 Experimental Results and Discussions

A field experiment has been conducted at an indoor parking space of a shopping mall with the courtesy of Mitsui Shopping Park LaLaport Kashiwanoha[1], to evaluate the robustness of the proposed positioning method in an area crowded with vehicles that obstruct RF signals. The positioning accuracy and the successful rate of the target localization are evaluated from the experiment and compared between the passive location system and the proposed method. The passive location system requires anchor nodes to be placed so that they surround the target area. UWB anchor nodes were attached to structural columns surrounding a single section of the parking space, due to the limitations imposed on the experiments in the parking area of the shopping mall. Experiments were conducted while visitors park their vehicles to the experimented section of the parking area, to evaluate the effects of RF obstructing objects in the target area. Results of the experiment provide insight of effects of parked vehicles on UWB timing signals and the positioning results.

#### Vehicle Localization at Indoor Parking Space

Figure4.18 shows the picture of the experimented section of the parking space while it is empty, and Figure4.19 shows the brief layout of the experimented section depicting parking slot numbers and the anchor node deployment. Table 4.3 lists coordinates of anchor nodes in the relative coordinate system defined by the origin anchor S/B and the x-axis defined by anchors 3/A and 4/C. The dimension of the section is 26.4 m x 15.3 m x 2.3 m, and it contains 20 parking slots that each have a dimension of 2.5 m x 3.8 m.

Anchor nodes were attached to the designated columns and their antennas were placed at the height of 1.8 m, a half-meter below the ceiling. The vehicle equipped with the UWB receiver was parked at the parking slot 6 for two hours. In order

[1] http://www.lalaport.jp/

Figure 4.18: The indoor parking section of the shopping mall.

Table 4.3: Coordinates of anchor nodes.

| Anchor node | x [m] | y [m] |
|---|---|---|
| 1 | -10.8 | 15.2 |
| 2 | 15.77 | 15.2 |
| 3/A | -10.8 | 0.0 |
| S/B | 0.0 | 0.0 |
| 4/C | 15.8 | 0.0 |

to conduct timing signal measurements for both the passive location system and the proposed positioning system at the same time, two anchor nodes were placed to positions 3/A, S/B, and 4/C, so that the total of eight anchor nodes were deployed in the space. The passive location system was formed by anchor nodes 1, 2, 3, 4, S, and the transmitter node mounted on the vehicle. On the other

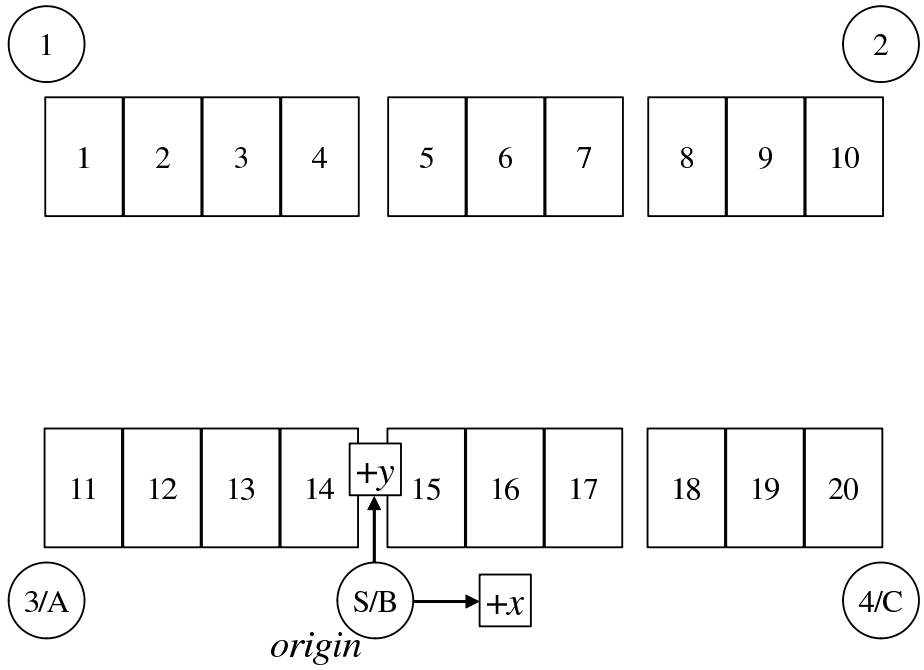


Figure 4.19: The layout of the parking section and anchor node placement.

hand, the proposed positioning system was formed by anchor nodes A, B, C, and the receiver node mounted on the vehicle. The rate of emitting a timing signal for the passive location system was fixed to 0.5 second. The proposed system conducted the initiation procedure with the transmission period randomly chosen from 0.3 to 0.7 second. The passive location system was built from five anchor nodes to create an asynchronous positioning system as introduced in [60] and to keep geographical dilution of precision (GDOP) low inside the surrounded region [27]. During the experiment, time is recorded when a parking slot was occupied by a visitor's vehicle and when the visitor's vehicle left the slot, to identify a time interval that the line-of-sight between the target vehicle and an anchor node was maintained or obstructed by other vehicles. The experimented section of the parking space was empty between 13:00 and 13:38, and all parking slots were full between 14:52 to 14:57.

Figure4.20 shows the parking slot occupancy status during the two hour exper-

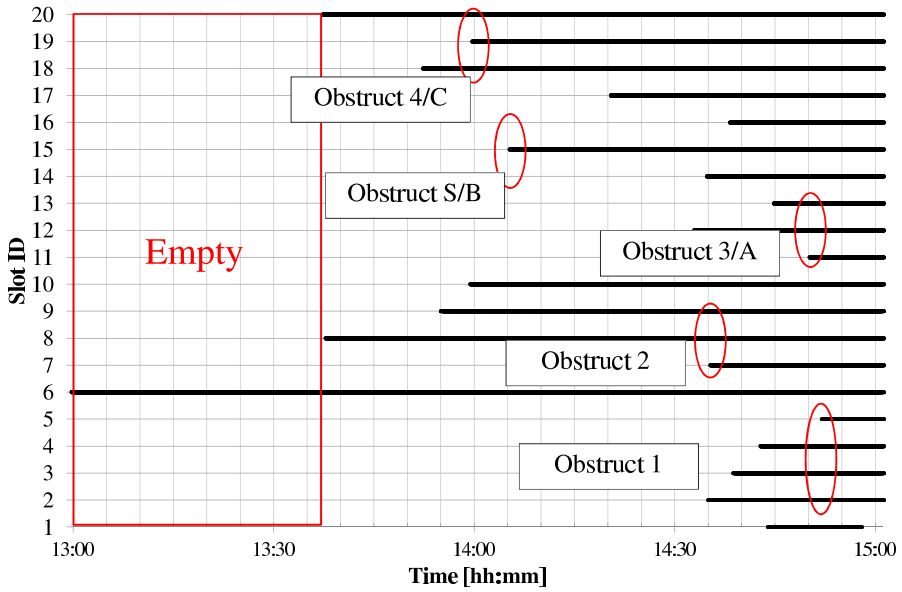


Figure 4.20: Slot occupancy data from 13:00 to 15:00. A solid line indicates that the slot is occupied.

iment. Circles are depicted on the graph to indicate timings that visitor vehicles are parked to specific parking slots, so that the line-of-sight between the target vehicle and anchor nodes are obstructed. The possible obstruction of the LOS is determined from the occupancy status of parking slots on a line connecting the target vehicle and the anchor node. Table 4.4 summarizes time intervals during the possible obstruction of the LOS between the target vehicle and each anchor node.

Table 4.5 shows statistics of positioning errors of both positioning systems. Both the passive location system and the proposed positioning system have shown that they achieve the positioning accuracy that allows them to distinguish vehicle's position at a granularity of a single parking slot. Especially in the direction of x-axis formed by the line connecting anchors A, B, and C, the observed error is less than a meter.

Table 4.4: Parking area status and the time interval that the possible LOS obstruction occurred.

| Status | From [hh:mm:ss] | To[hh:mm:ss] |
|---|---|---|
| Empty | 13:00:00 | 13:38:00 |
| Obstructed Anchor 1 (Slots 2, 3, 4, 5) | 14:52:16 | 15:00:00 |
| Obstructed Anchor 2 (Slots 7, 8, 9) | 14:35:34 | 15:00:00 |
| Obstructed Anchor 3/A (Slots 11, 12, 13) | 14:50:24 | 15:00:00 |
| Obstructed Anchor S/B (Slots 15) | 14:05:32 | 15:00:00 |
| Obstructed Anchor 4/C (Slots 18, 19, 20) | 13:59:57 | 15:00:00 |
| Full occupied | 14:52:16 | 14:57:41 |

Table 4.5: Statistics of positioning error

| System | | Mean [m] | Median [m] | $90^{th}$ perc. [m] | Std.Dev.[m] |
|---|---|---|---|---|---|
| Passive location | | 1.49 | 1.45 | 2.23 | 0.94 |
| | x-direction | 0.26 | 0.20 | 0.48 | 0.33 |
| | y-direction | 1.43 | 1.44 | 2.19 | 0.93 |
| Proposed system | | 0.74 | 0.45 | 1.75 | 1.47 |
| | x-direction | 0.24 | 0.23 | 0.37 | 0.14 |
| | y-direction | 0.66 | 0.38 | 1.71 | 1.48 |

Figure4.21 shows the success rate of the position estimation by both the passive location system and the proposed positioning system for each parking occupancy state of the experimented section. Figure4.22 shows the success rate calculated over 1 minute observation window during the experiment. The success rate is calculated by dividing the number of the successful position estimation by the number of expected position estimation during time intervals of possible anchor obstructions. The number of expected position estimations is counted from the interval of a

timing signal transmission by the target node for the passive location system or the initiator anchor node for the proposed positioning system, which is 1 second. From Figure4.21, it is observable that both system can achieve the estimation success rate of 75 to 78 % when the experimented section is empty. On the other hand, when the experimented section is filled with vehicles, the passive location system could not estimate the position of the target vehicle while the proposed positioning system maintained the success rate of 65 %. Specifically, the LOS obstruction to anchor nodes 1 and 2, when visitor's vehicles parked the parking slot number 2 and 7 at 14:35, caused the passive location system to unable to locate the target vehicle as can be seen by comparing Figure4.20 and Figure4.22. The difference in the estimation success rate among positioning systems is obtained because the passive location system requires all anchor nodes surrounding the target area to successfully receive the timing signal transmitted by the target node on the vehicle, whereas the proposed positioning system requires anchor nodes deployed in front of the target vehicle.

## 4.5 Summary

TOF based positioning systems for measuring a relative positional relation of two mobile objects and for determining partial coordinates of a mobile object are proposed in this chapter.

The proposed method exploits TOF based bilateration to determine relative positions The EWMA filter for estimated angles is proposed and thoroughly evaluated by simulations and field experiments, in order to reduce estimation error of the relative lateral distance calculated by TOA based bilateration. The results obtained from field experiments have shown that the estimation error of the lateral distance between two mobile objects is reduced from 8 meters to 3 meters, when their longitudinal distance is less than 15 meters.

In addition to the relative positioning system, a partial positioning system locates multiple target objects with a user-centric communication architecture while infrastructural devices are not synchronized. The proposed partial positioning system relaxes the LOS condition required for the target object, so that the positioning

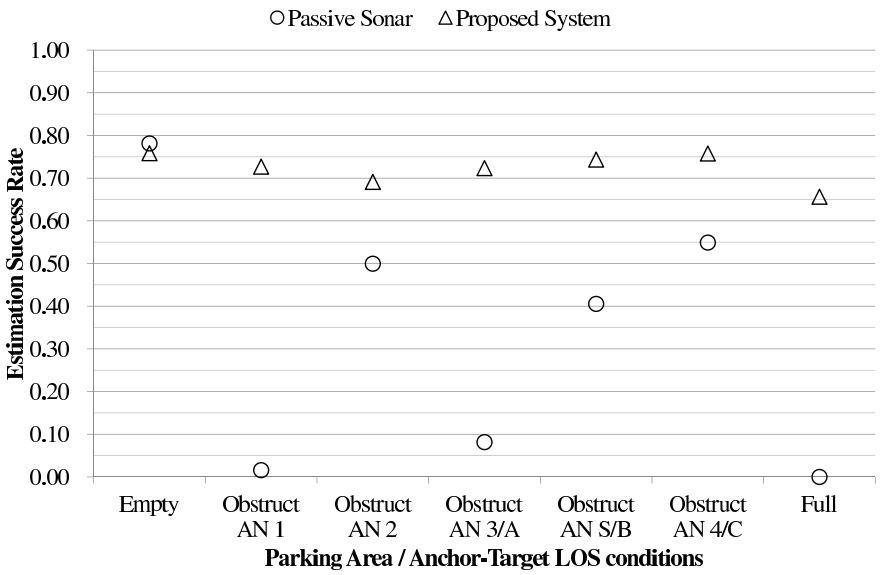


Figure 4.21: Success rate of the position estimation for the passive location system and the proposed positioning system.

system is able to provide the position information to the user when target areas are filled with metallic objects obstructing RF signals. The results have shown that the target localization accuracy of 50 cm is achieved and a successful localization rate of 70 % while the ordinary TDOA location system have completely lost the localization capability due to obstacles in the target areas.

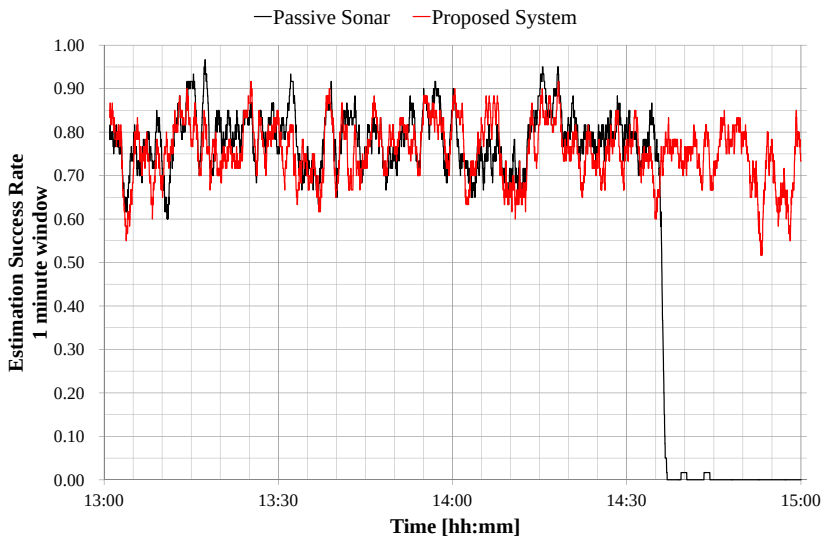


Figure 4.22: Success rate over 1 minute window during the experiment.

# Chapter 5

# Absolute Location Systems

In this chapter, absolute location systems targeted for a large area deployment and ad-hoc deployment are considered. The proposed methods are implemented on active RFID tags and evaluated in real-world environments. Results and analyses of the experiments are discussed. Summaries are presented in the end of the chapter.

## 5.1 RF Model Generation

### 5.1.1 System Overview

For the location information infrastructure based on active RFID tags, locations of deployed tags are managed since tags are newly attached to the places of interest by a service provider. Thus, instead of taking approaches based on zero-calibration or RF map generation as reviewed in Chapter 2, the proposed method tries to construct RF models for each deployed tag from training data collected by conducting a pre-survey.

RSS samples collected from deployed tags are associated with distance information estimated from recorded velocities of a data collector. Previous approaches have exploited an odometer to record true distance information between the data collector and deployed devices. The proposed method does not use an odometer for that purpose; it estimates distance information between the data collector and deployed devices by walking a pre-defined route and several checkpoints to linear-interpolate the distance walked by the data collector.

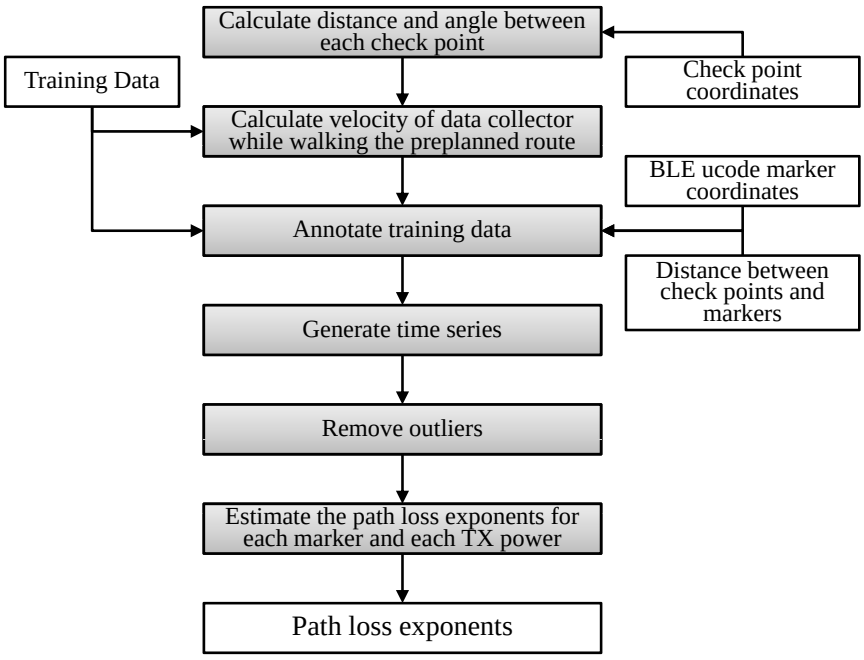


Figure 5.1: Flowchart for estimating the path loss coefficient for each marker and each transmission power.

Estimated distance information is associated with a sampled RSS obtained by receiving a periodic beacon transmitted by deployed tags. RSS samples are annotated with the distance information between the data collector and tags, then the coefficient of the log-distance path loss model for each tag is estimated using these information. The proposed method also classifies RSS samples by a transmission power, to increase the distance estimation accuracy provided by the generated log-distance path loss model. In addition, a novel outlier filtering method is also incorporated for generating the log distance path loss model for each active RFID tag and for processing RSS samples on-line.

### 5.1.2 Procedures to Obtain Path Loss Exponents

A complete flowchart for estimating the path loss coefficient for each tag and each transmission power is shown in Figure5.1. Each task of the flowchart is explained in details.

### Determining the Training Route

Given a placement plan of active RFID tags, a route for obtaining training data is determined. The training route is chosen so that it covers an area surrounded by active RFID tags and outside of the area. Geographical Information System (GIS) software is utilized for planning the training route. After the training route is determined, checkpoints are added to the route. Check points are the positions for a data collector to temporary stop and record current time while walking the training route. Check points are chosen so that any path between two checkpoints is straight in order to estimate the velocity of the data collector by recorded timestamps and linear-interpolation technique.

### Calculating the Velocity

The data collector uses a mobile device to collect RSS samples obtained from beacons transmitted by deployed tags. In addition to collecting RSS samples, the mobile device enables the data collector to record timestamps when he stopped at a checkpoint. This procedure allows a data analyzer to later estimate the velocity of the data collector between any two checkpoints.

### Annotating RSS Samples

Once the data collector has aggregated RSS samples from deployed tags, Each RSS sample of a beacon is annotated with a distance information between the data collector and the tag that is responsible for sending the beacon. This is possible since the data collector has moved along the pre-defined training route and his walking velocities between any two checkpoints are estimated. In addition, a RSS sample of a beacon is converted to a path loss by checking the transmission power of the tag when it sent the corresponding beacon. The path loss $PL$ is calculated as follows:

$$PL = P_{TX} - RSS, \tag{5.1}$$

where $P_{TX}$ is the transmission power of the tag when it send the corresponding beacon and $RSS$ is the observed RSS when the data collector received the beacon.

### Generating a Time Series

A time series data is generated by scanning the annotated records of received beacons. The time series data provides information on how many beacons are received from each tag between fixed time intervals. In addition, this procedure is executed in order to apply a time series filter for removing outlier from annotated path loss data.

### Removing Outliers

In order to remove outliers from annotated path loss data, the distance based local outlier detection algorithm is exploited [63]. Empirical observations on sampled RSS data obtained in an anechoic chamber suggest that outliers occur randomly and do not depend on the distance between the receiver and tags. The main idea of the distance based outlier detection algorithm is to calculate a statistic of *distances* between $N$ recently accepted values and the newly received value, which is compared with another statistics of $N$ accepted values. The *distance* indicates the absolute value of the difference between the accepted value and the newly received value. To apply the algorithm for the time series of path loss data, the mean value of calculated *distance* and the standard deviation of $N$ accepted values. The newly received value is accepted if it is less than 1.96 times the standard deviation of accepted values.

In addition to the filtering procedure, the acceptance range adjusting algorithm is incorporated to the outlier filtering algorithm. In a case such that the next received value is not accepted by the outlier filter, a normal random value calculated from the mean and the 1.03 times the standard deviation of $N$ accepted values is inserted to the window, to gradually increase the acceptance range of the outlier filtering algorithm.

Figure5.2 shows the plot of raw data of observed path loss against distance between the data collector and tags, whereas Figure5.3 shows the plot of filtered data of observed path loss against distance between the data collector and tags. By comparing these plots, it is evident that the proposed outlier filtering algorithm effectively removed outliers from observed path loss data.

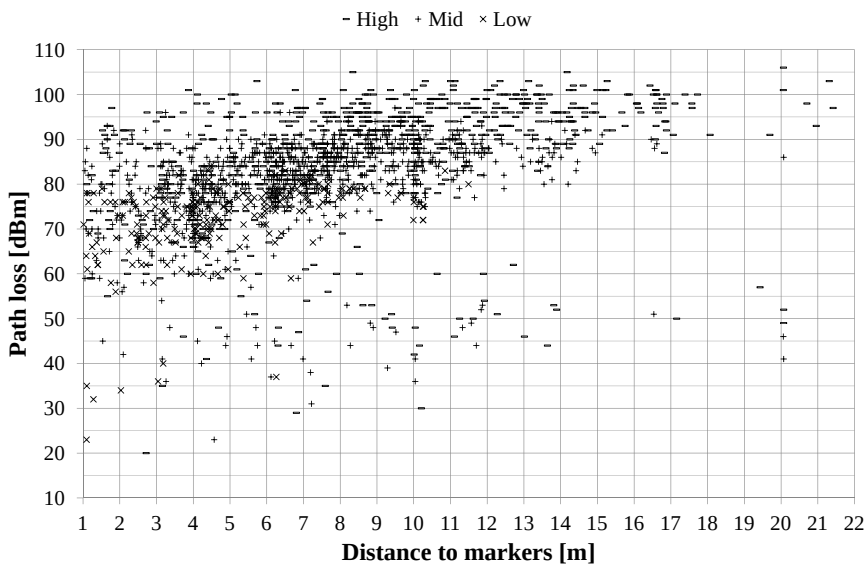


Figure 5.2: Plot of observed path loss against distance between the data collector and markers.

#### Estimating the Path Loss Coefficients

The path loss coefficients for each marker and each transmission power is calculated from the filtered time series, using the log-distance path loss model without the normal random variable representing fading effects: $P = P_1 + 10nlog_{10}d$, where $P$ is the path loss, $P_1$ is the path loss when the distance between a receiver and a transmitter is one meter, $n$ is the path loss coefficient, and $d$ is the distance between the receiver and the transmitter.

### 5.1.3 Positioning Using Multiple Path Loss Exponents

For the on-line phase when the actual positioning procedure is conducted, the outlier detection algorithm is executed for each measured sample and the low pass filter is applied to smoothen the measured path loss level for each tag and each transmission power level. Using the path loss coefficients for each tag and each

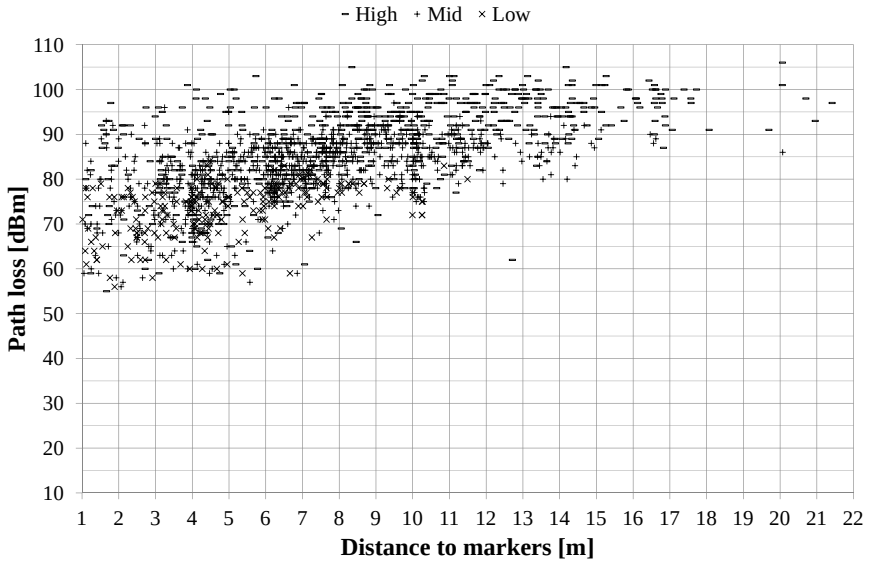


Figure 5.3: Plot of observed path loss against distance between the data collector and markers after the outlier filter is applied to the time series.

transmission power level, the multiple distances to a single tag are obtained in case that the receiver received beacons with different transmission power levels from an active RFID tag. When multiple distances are estimated for a single tag, the distance estimated from the low transmission power signal is chosen since the standard deviation of observed path loss is the smallest among others as shown in Figure5.4.

Figure5.4 shows the standard deviation cumulative distributed functions (CDFs) of path losses observed at the receiver for high, mid, and low transmission power signals in indoor environment. Path losses have been measured for each transmission power when the distance between the receiver and the transmitter was varied from 1 to 30 meters while maintaining the line-of-sight (LOS) condition and while obstructing the LOS condition. This shows that the receiver has more chance of receiving the indirect path signals when the transmission power is high compared to when the transmission power is low, since the power loss of the signal occurred

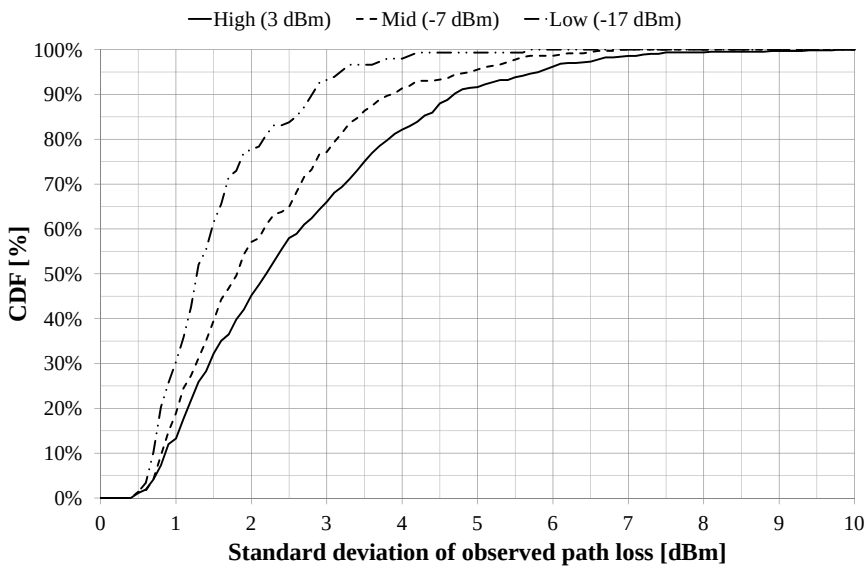


Figure 5.4: Standard deviation CDFs of observed path losses for each transmission power.

by hitting obstacles is not sufficient for the receiver to drop or ignore the signal when the transmission power is high. Thus it is reasonable to choose the estimated distance with a low power signal to obtain accurate result on the distance estimation.

The estimated distance between the receiver and the tag is compared with the proximity threshold level of the tag to determine the proximity status with the tag. For estimating the current position of the mobile device, the trilateration is executed using estimated distances between the mobile device and surrounding tags, if the receiver knows distances to at least three active RFID tags. The gradient descent method is implemented for solving the maximum likelihood estimator of the lateration based positioning [64], which can be expressed as:

$$\theta_{ML} = \arg\min_{[xy]^T} \sum_{i=1}^{N} \frac{(d_{mea_i} - d_{est_i}(x,y))^2}{\sigma_i^2}, \tag{5.2}$$

where $N$ represents the number of tags involved in the lateration, $d_{mea_i}$ represents

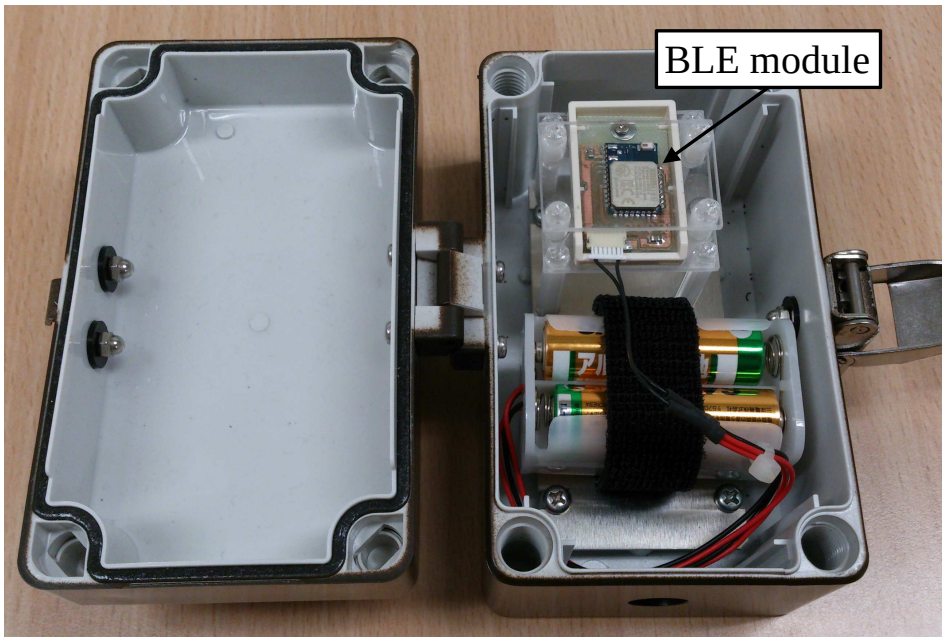


Figure 5.5: BLE active RFID tag.

the measured distance between the $i$th tag and the receiver, $d_{est_i}$ represents the estimated distance between the $i$th tag and the estimated position of the receiver, and $\sigma_i^2$ represents the variance of the measured distance between the $i$th tag and and the receiver.

### 5.1.4 Implementation

Figure5.5 shows the picture of the active RFID tag based on Bluetooth Low Energy (BLE) module. The BLE active tag periodically transmits an advertising packet for every 300 milli-seconds, and it continuously operates for a year with four AAA batteries which have 4000 mAh for the battery capacity. In a single advertising packet, 128 bits unique ID that follows the ucode format [65] is contained for identifying the place of the deployment. The ucode is a world-wide unique identifier certified by ITU-T [66], which can be issued to individual objects, places, and even concepts in the real world for the identification purpose.

In addition to the ucode, the advertising packet contains the transmission power

level using the AD format of the BLE specification [67], so that a receiver device can compute the path loss level from the RSS and the transmission power level. The BLE active tag is programmed to change its transmission power level after a single transmission of an advertising packet. It utilizes three transmission power levels: high = 3 dBm, mid = -7 dBm, and low = -17 dBm, and it changes the transmission power level according to the following sequence: 3 dBm → -17 dBm → -7 dBm → -17 dBm. So the high power advertising packet is transmitted for every 1200 milli-seconds, and the low power advertising packet is transmitted for every 600 milli-seconds. Low power advertising packets are transmitted two times more than the high and mid power packet. This allows the receiver device to estimate the distance to the BLE active tag using more low power advertising packets than high and mid power packets, resulting in sampling less varied RSS values.

### 5.1.5 Evaluations

An experiment was conducted to evaluate the accuracy of distance and position estimation using the BLE active tag and the proposed positioning procedures. 6 BLE active tags were placed in the office environment, which has a dimension of 30 meter x 20 meter. Advertising packets from active tags were collected using an iPhone at 173 evaluation points covering the entire office. Evaluation points can be classified into line-of-sight (LOS) or non-line-of-sight (NLOS) relative to each tag. The classification is done by evaluating the existence of metallic objects that lie between the evaluation point and the tag. For this experiment, the receiver was stationary at each evaluation point for one minute, to evaluate the accuracy achievable with the proposed multi-power transmission levels and compare it with the ordinary RSS lateration method. Figure5.6 shows the layout of the office, tags, and metallic objects.

Prior to the experiment, a training data was collected by the data collector who walked the office while holding the iPhone on his hand. Checkpoints were chosen from evaluation points where the collector needed to change the direction to continue walking the office. The data collector walked the predefined route for three times to obtain the training data. Figure5.7 shows the training route for the


Figure 5.6: The layout of the office. Positions of tags are marked with alphabets. Black lines represent metallic objects in the office.

office, which basically covers entire office where a person can walk.

The collected training data was processed to obtain a total of four different sets of path loss coefficients:

1. path loss coefficient generated by mixing measured path loss data from all tags and all transmission power levels,

2. path loss coefficients generated for 6 BLE active tags but mixed measured path loss data from different transmission power levels,

3. path loss coefficients generated for three different transmission power levels but mixed measured path loss data from different tags, and

4. path loss coefficients generated for each tag and each transmission power level.

These different methods for generating path loss coefficients are applied to raw


Figure 5.7: The training route for the office.

Table 5.1: Statistics of estimated distance error.

| Data | Mean [m] | Med. [m] | $90^{th}$ %. [m] | SD. [m] |
|---|---|---|---|---|
| Raw | 6.55 | 2.60 | 13.13 | 12.01 |
| Filtered | 3.74 | 2.52 | 7.48 | 4.49 |

path loss data and filtered path loss data using the outlier detection algorithm, to evaluate the effects of removing outliers.

### Effects of the Outlier Filtering Algorithm

First, for a case that transmission power levels are ignored, the effect of the outlier filtering algorithm is evaluated. Table 5.1 shows the statistics of estimated distance errors obtained from all tags and all evaluation points, namely, mean, median, $90^{th}$ percentile, and standard deviation. As expected, distance estimation using the path loss coefficients generated by the filtered training data gives lower standard deviation than the one generated by the raw training data.

Table 5.2: Statistics of estimated distance error using path loss coefficients calculated from filtered data.

| Method | | Mean [m] | Med. [m] | $90^{th}$ %. [m] | SD. [m] |
|---|---|---|---|---|---|
| 1 | ALL | 4.55 | 3.36 | 10.22 | 3.89 |
| | LOS | 3.16 | 2.68 | 6.00 | 2.23 |
| | NLOS | 5.48 | 4.45 | 12.00 | 4.46 |
| 2 | ALL | 3.74 | 2.52 | 7.48 | 4.49 |
| | LOS | 2.02 | 1.64 | 4.23 | 1.51 |
| | NLOS | 4.90 | 3.04 | 11.95 | 5.37 |
| 3 | ALL | 3.09 | 2.51 | 6.80 | 2.44 |
| | LOS | 2.72 | 2.31 | 5.39 | 1.92 |
| | NLOS | 3.34 | 2.66 | 7.51 | 2.71 |
| 4 | ALL | 2.80 | 2.38 | 5.73 | 2.13 |
| | LOS | 2.24 | 1.81 | 4.67 | 1.76 |
| | NLOS | 3.18 | 2.75 | 6.17 | 2.27 |

**Effects of Multi-Power RF Models**

Table 5.2 shows the statistics of estimated distance errors using path loss coefficients calculated from filtered training data, for four different methods described above. For each method, statistics are calculated from all data, data obtained from evaluation points where the LOS condition to tags is maintained, and data obtained from evaluation points where the LOS condition to tags is not maintained. The mean distance error is improved from 3.74 m to 2.80 m by utilizing the transmission power information and by preparing path loss coefficients for each marker and each transmission power. Also, the $90^{th}$ percentile value of the method 4 is improved from 7.48 meter obtained from the method 2 to 5.73 meter, providing 23 % improvement to the estimation accuracy. By focusing on the distance estimation accuracy in the LOS area, the method 2 gave a slightly better results than the method 4. However the method 4 significantly produced better results than other methods when the LOS condition is not achievable between a tag and an evaluation point.

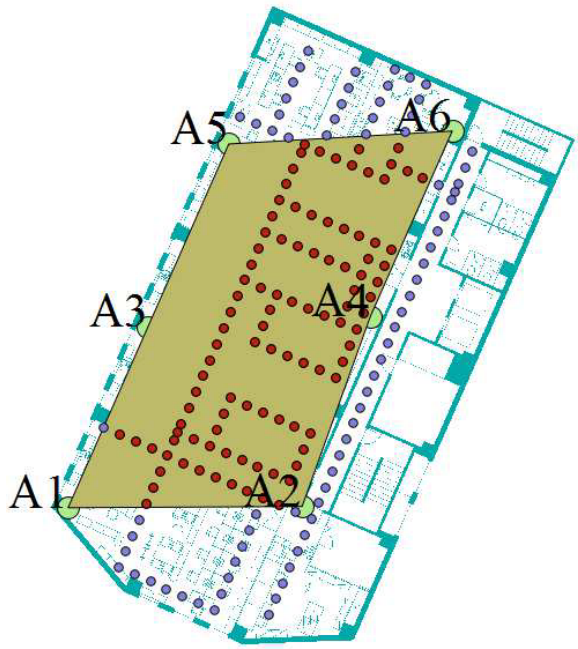


Figure 5.8: The layout of the office, marker positions, and evaluation points. The region formed by connecting tags is drawn on top of the layout of the office.

### Discussions on Degrees of Error by Location Points

For the estimated positioning errors, statistics are compared among four methods for the path loss coefficients calculation and the location of evaluation points. Evaluation points can be classified into two groups: IN group represents evaluation points inside of the region formed by connecting deployed markers, and OUT group represents evaluation points outside of the region. Figure 5.8 shows the region formed by connecting markers.

Table 5.3 shows the statistics of estimated position errors using path loss coefficients calculated from filtered training data, for the method 2 and the method 4. It is observable that the method 4 that considers the transmission power level produces better results in positioning accuracy compared to the method 2 that does not utilize the transmission power level differences for calculating the path loss coefficients. In particular, 46 % improvement is obtained for the the $90^{th}$

Table 5.3: Statistics of estimated position error using path loss coefficients calculated from filtered data.

| Method | | Mean [m] | Med. [m] | $90^{th}$ %. [m] | SD. [m] |
|---|---|---|---|---|---|
| 2 | ALL | 5.56 | 4.34 | 11.02 | 3.92 |
| | IN | 5.86 | 4.42 | 11.14 | 4.08 |
| | OUT | 4.86 | 3.88 | 10.47 | 3.48 |
| 4 | ALL | 3.47 | 3.04 | 6.21 | 2.24 |
| | IN | 3.25 | 2.94 | 5.98 | 1.95 |
| | OUT | 3.97 | 3.30 | 7.83 | 2.76 |

percentile of the positioning error by utilizing the method 4 for evaluation points inside of the region. On the other hand, the $90^{th}$ percentile of the positioning error is 7.83 meter for evaluation points outside the region defined by markers. This was observed since the geographical dilution of precision (GDOP) outside of the region is greater than the inside, when the lateration technique is employed for determining the position of the receiver [27].

## 5.2 Self Anchor Calibration

To implement the self-localization mechanism of anchor nodes on a UWB-IR localization system, there are three engineering problems to solve:

1. designing a ranging protocol;
2. designing a neighbor set search algorithm;
3. designing a self-localization algorithm.

In addition, a method to construct a data path from an anchor node to a location calculation server is necessary, especially for a system involving a large number of anchor nodes, but this topic is out of scope of this paper.

### 5.2.1 Ranging protocol

With a UWB-IR module, a distance between anchor nodes is estimated by measuring a time-of-flight (TOF) of a packet. Estimating a distance between two

anchor nodes using a single packet TOF requires anchor nodes to be synchronized in sub-nanosecond order. Thus, two-way time-of-arrival-based (TW-TOA) ranging protocol [68] is implemented for the proposed system, which does not require anchor nodes to be synchronized.

A practical issue of exploiting the TW-TOA ranging protocol is to estimate the packet processing time of the receiver node. The packet processing time at the receiver node is the time elapsed between the moment that the ranging packet is received and the moment that the response packet is sent. For the proposed system, the packet processing time of every anchor nodes is estimated before the deployment by conducting test measurements that collect TOF samples when a distance between anchor nodes is fixed.

### 5.2.2 Neighbor set searching algorithm

Since it is costly to execute the TW-TOA ranging protocol for every possible combinations of anchor node pairs, the proposed system runs a neighbor set searching algorithm as described in Figure5.9, to determine anchor nodes that are reachable from a target anchor node. A target anchor node broadcasts a packet for $N_{broadcast}$ times, for allowing the control server to inspect the packet error rates (PER) between the target anchor node to other anchor nodes. Each receiver anchor node reports the number of times it successfully received broadcast packets to the control server. The control server then adds receiver nodes with a low PER to a neighbor set of the target node.

Besides reducing the number of TW-TOA ranging, neighbor set lists are utilized for obtaining sub-graphs with a bilateration ordering such that vertices are deployed anchor nodes and edges correspond to the reachability between anchor nodes. A graph has a bilateration ordering if its vertices are ordered as $v_1, v_2, \ldots, v_n$ such that $v_1$ and $v_2$ are connected, and each $v_i$ with $i > 2$ has at least two vertices $v_j$, where $j < i$, are connected. Bilateration graphs are utilized to localize anchor nodes as described in the next subsection.

```
for all anchor nodes, a_i do
  for n = 0 to N_broadcast do
    a_i broadcasts a packet
  end for
  for anchor node a_j s.t. j ≠ i do
    if a_j received packets from a_i more than T_broadcast times then
      add a_j to set NB_i
    end if
  end for
end for
```

Figure 5.9: Procedures of the ranging pair selection algorithm.

### 5.2.3 Self-localization algorithm

Anchor nodes are localized successively using distance information obtained from TW-TOA ranging and the bilateration algorithm introduced in [69]. Localization by bilateration means finding coordinates of a target node given its distances to point $A$ and point $B$, and coordinates of those points. Thus bilateration gives two possible positions of the target node coordinates, and the bilateration algorithm finitely localizes anchor node positions. To uniquely localize anchor nodes by distance information, it is necessary to find a fully-connected quadrilateral [70] from the bilateration sub-graph.

The proposed system finds and utilizes the smallest fully-connected quadrilateral from the bilateration graph, which does not include an anchor node inside the quadrilateral, as seed anchor nodes. This allows the bilateration algorithm to select unambiguously determine the position of the fifth anchor node and subsequent anchor nodes when they are reachable to at least three vertices of the quadrilateral.

### 5.2.4 Implementations

The UWB-IR localization system estimates the position of a target node by TDOA measurements obtained from signal exchange among the target node and anchor nodes. Figure5.10 depicts the overview of the proposed localization system.

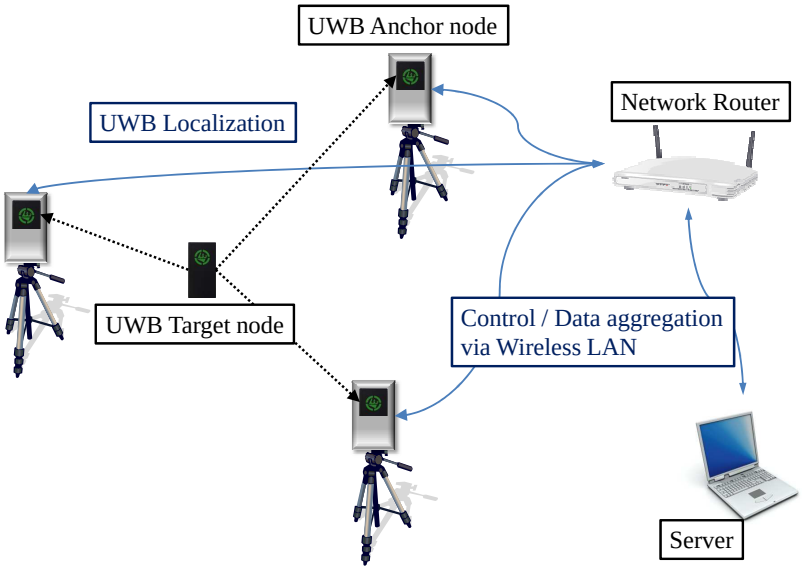


Figure 5.10: The UWB positioning system overview.

TDOA measurements are conducted using UWB-IR communication among target and anchor nodes, and measured TDOA results are uploaded to a calculation server via the wireless LAN. The WLAN communication is exploited for controlling the anchor node behavior as well. This section describes hardware and software design of a portable UWB anchor node for implementing the localization system.

### UWB-IR Module

The anchor node is equipped with a UWB-IR module, which is pre-produced by YRP UNL using a practical UWB-IR transceiver chip introduced in [6]. Figure5.11 shows the picture of the module. The transceiver emits 2 ns width pulses over 3.4 to 4.8 GHz frequency band, with the pulse repetition frequency of 32 MHz. Impulses are modulated with differential BPSK.

The pre-produced UWB-IR module conforms the spectrum mask specified by ARIB STD-T91 [71], but it does not satisfy the transmission data rate restriction since the maximum transmission data rate achievable with the UWB-IR transceiver


Figure 5.11: The UWB-IR module.

is 32 MHz. For UWB-IR modules utilized for the experiments presented in this paper, all modules received experimental radio station licenses.

### Anchor Node Architecture

In addition to the UWB-IR module, a low power wireless LAN module and a GPS module are mounted on the anchor node. Figure5.12 shows the block diagram of the anchor node. The WLAN module and the GPS module are connected to the microcontroller unit (MCU) mounted on the UWB-IR module via SCIF. As the WLAN module accepts AT modem commands for the control, the firmware for the MCU implements an AT command analyzer and issuer. The firmware also implements GPS data analyzer. Figure5.13 shows the software components implemented on the MCU of the UWB-IR module.

As stated above, the WLAN is the main medium for communicating with the calculation server. The AT command analyzer extracts the server command and the server command analyzer executes control commands for the UWB-IR transceiver.

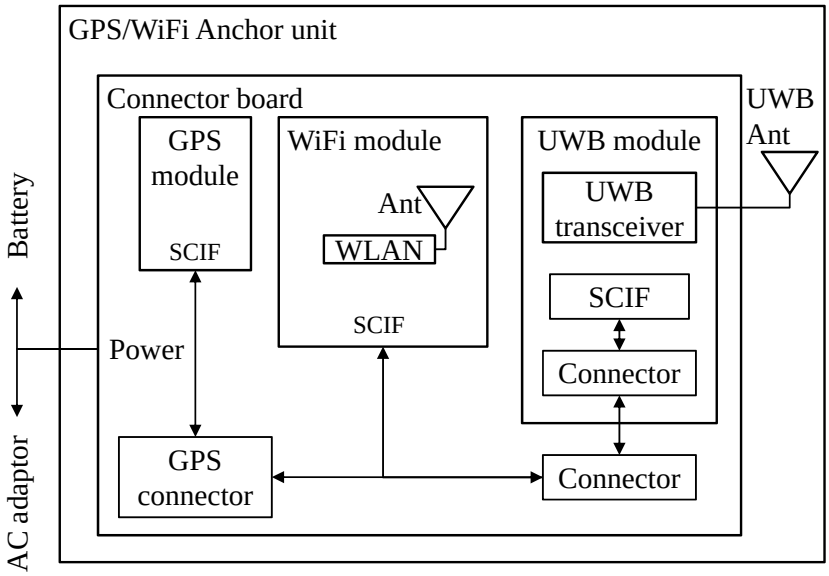


Figure 5.12: Block diagram of the UWB anchor node.

For each command received from the server, the UWB-IR module sends an acknowledgement, thus the AT command is issued after executing control commands. When measurement data such as TDOA related parameters is ready, the AT command is asynchronously issued by the UWB-IR module for transmitting data to the server. GPS data retrieved by the GPS data analyzer is also asynchronously sent to the server via the WLAN module.

Although the current radio law in Japan does not allow the usage of UWB radio for outdoor, the GPS module enables the anchor node to obtain its absolute coordinate. Integrating the absolute coordinate and the relative position estimated by the self-localization algorithm is useful for determining the absolute position of anchor nodes deployed both indoor and outdoor. By using relative position information of anchor nodes, the absolute position of indoor anchor nodes is estimated from the absolute position of outdoor anchor nodes.

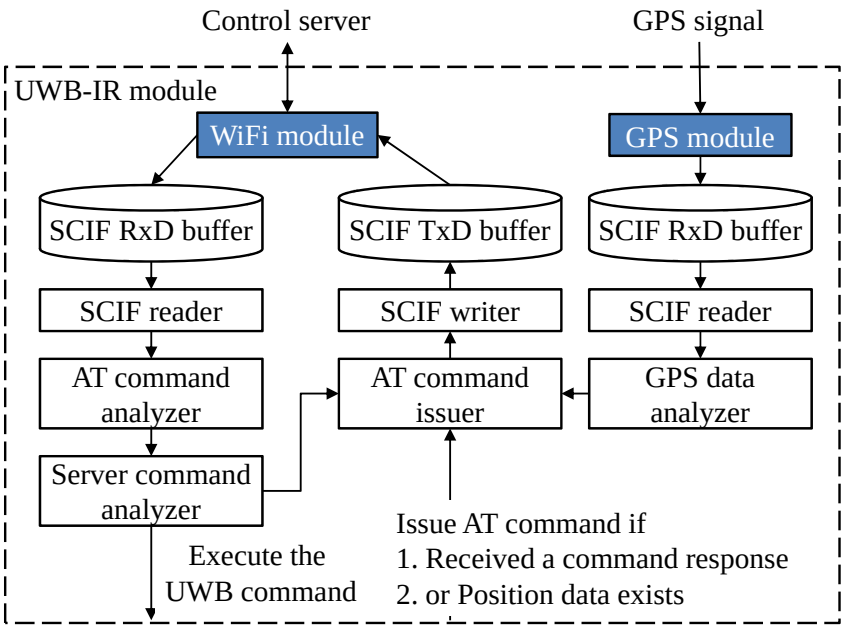


Figure 5.13: Software components of the UWB anchor node.

**Portable Anchor Node**

Figure5.14 shows the picture of the anchor node and Table 5.4 summarizes hardware specifications of the anchor node. The portability of the anchor node is achieved by operating hardware using batteries. The GPS/WiFi anchor unit is connected to a battery box which contains 4 D-size batteries. With the battery box, the anchor node is able to continuously operate for 40 hours. For the indoor usage where AC power supplies are available, the anchor unit can be connected to an AC adaptor to build a prolonged location monitoring system. The anchor unit and the battery box are supported by a tripod to heighten the UWB antenna and to make the anchor unit portable.

### 5.2.5 Evaluation

This section presents experimental results of the proposed self-localization mechanism and localization of a target node using the TDOA algorithm with self-localized anchor nodes. To conduct experiments using real hardware, 8 anchor

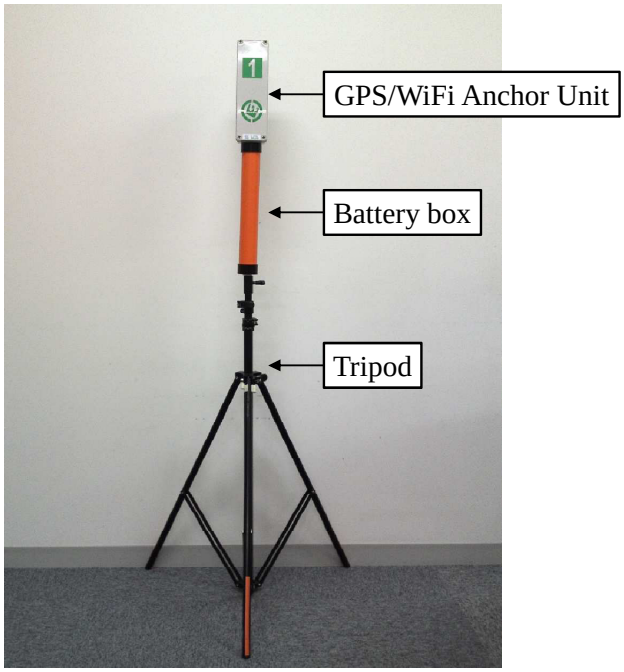


Figure 5.14: UWB anchor node.

units and 1 target node are prepared. In experiments, each anchor node is connected to the calculation server via WLAN, so that ranging and TDOA results are sent directly to the server. The server calculates the position of anchor nodes and target nodes from aggregated TDOA related parameters from each anchor node.

Experiments on self-localization accuracy are conducted in a 20 meter x 20 meter indoor room, where 8 anchor nodes are placed to surround the room. The distance between anchor nodes is estimated by obtaining 5 TOF measurements and taking their median. Figure5.15 shows the cumulative probabilities of positioning errors of anchor nodes from 300 executions of the self-localization procedure, which includes re-measurement of distance. This shows that 90th percentile localization error of 80 cm is achieved for the proposed self-localization system.

An example scenario is considered and evaluated. Four anchor nodes are deployed to surround a small room, for locating the position of a target node in the room. Table 5.5 shows estimated relative coordinates of anchor nodes and a target node and Figure5.16 shows a plot of the results. Localization error of 85 cm is

Table 5.4: Hardware specifications of the portable anchor node.

| | | |
|---|---|---|
| UWB type | | Impulse-based direct sequence UWB |
| Frequency band | | 3.4 GHz to 4.8 GHz |
| Positioning accuracy | | ± 30 cm |
| Communication distance | | 30 meters |
| Communication rate | | 258 kbps |
| Dimension | | W81 x H274 x D72 mm<br>(Excluding a tripod and a batterycase) |
| Environmental conditions | | 0 to 50 degree Celsius<br>30 to 80 % RH |
| Send interval | | 50 ms to 200 minutes |
| Power | AC adaptor | DC: 5 V / 1.0 A |
| | Battery | DC: 6 V (4 D-size batteries) 12000 mAh |
| Continuous operation time | | 40 hours |
| Wireless LAN | | IEEE802.11b/g<br>(WPA/WPA2-AES/TKIP,WEP) |
| Positioning | | Assisted GPS and UWB self-localizer |

obtained for the anchor node localization using the proposed method, and that of 47 cm is obtained for the target node localization using the TDOA algorithm. Estimated anchor node and target node positions achieves the localization error less than 1 meter.

## 5.3 Summary

This chapter explored issues on the infrastructural device deployment for the localization system.

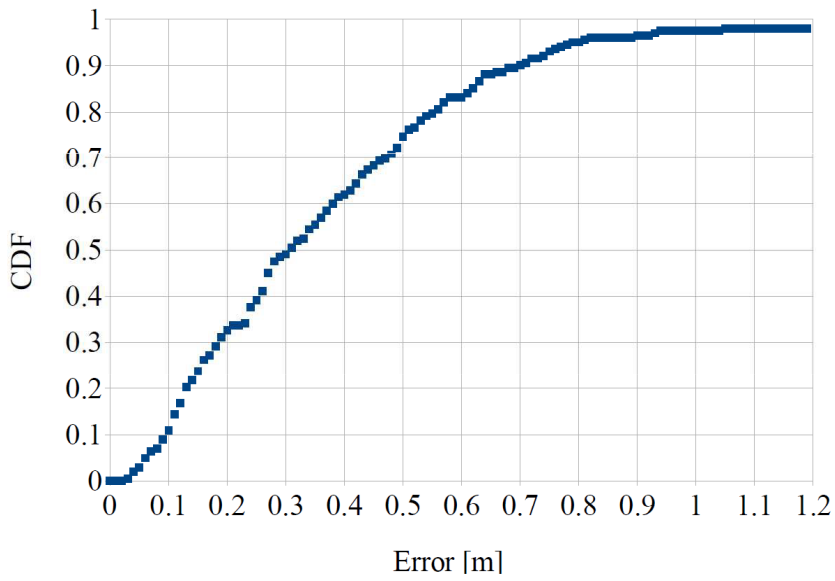


Figure 5.15: The CDF of positioning errors of anchor nodes.

Table 5.5: True and calculated coordinates of anchor/target nodes.

| Node | x [m] | y [m] | $\hat{x}$ [m] | $\hat{y}$ [m] |
|---|---|---|---|---|
| Anchor1 (origin) | 0 | 0 | 0 | 0 |
| Anchor2 (2nd) | 2.31 | 0 | 2.61 | 0 |
| Anchor3 | -0.14 | 4.46 | 0.63 | 4.82 |
| Anchor4 | 2.23 | 4.53 | 2.25 | 4.69 |
| Target1 | 1.40 | 2.84 | 1.51 | 3.30 |

For the RSS based location system, surveying RF signal map of the target areas is the common method to increase the localization accuracy, but this requires extensive efforts for the pre-survey procedures and it is not acceptable to apply for the large area deployment. The proposed approach has shown a systematic procedure to estimate a propagation constant of the log distance path loss model

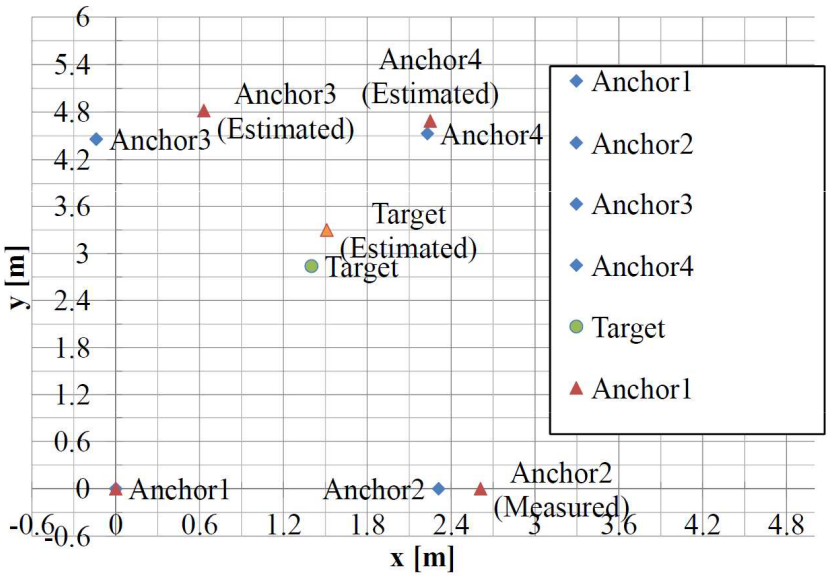


Figure 5.16: Plot of true and calculated coordinates of anchor/target nodes.

for each active RFID tag. The proposed approach has incorporated multiple transmission power levels for the estimation of the propagation constant. In addition, a novel outlier filtering algorithm has been proposed in order to remove outliers from training data and from on-line RSS samples. The experimental results have shown that the proposed method has successfully reduced localization error of 2 meters on average.

To reduce the cost of deployment of infrastructural devices, it is preferable for active RFID tags to locate their positions automatically when they are deployed to the target field. In addition to the reduction of the deployment cost, this function is useful for deploying the localization system in an ad-hoc manner, for example, to deploy the localization system to a disaster site for securing safety. The proposed system exploits TOF enabled active RFID tags to execute a self-calibration algorithm based on rigid quadrilaterals. The experimental results have shown that infrastructural devices can locate their positions with the proposed algorithm and the localization accuracy of 1 meter is achieved.

# Chapter 6

# Application of Location System

This chapter explores applications of position and distance measurement systems. The application of intelligent transportation systems (ITS) is considered by using the partial location system. Implementation details and discussions on the ITS system is provided.

## 6.1 Indoor Vehicle Positioning

One of interesting applications of location technology is to locate a parked vehicle, for aiding the owner of the vehicle to locate his car and providing navigation services. There are many mobile apps available online, which realize the vehicle locator system for outdoor environment using Global Positioning System (GPS). However it remains to be difficult to locate or track a vehicle in indoor environment where satellites signals are unreachable to positioning targets. Exploiting RF fingerprints of WLAN signals for developing the positioning system is one of approaches to design the vehicle locator system for indoor environment as studied in [72] [73]. In a real indoor parking space, the best achievable positioning accuracy using the WLAN RF fingerprinting is reported to be around two to four meters [73]. Thus it is not applicable to obtain information on which individual parking slots are filled at the moment, useful for parking space management and guiding the users to unfilled parking slots.

## 6.2 Application of Partial Location System

The TOF based partial location system based on UWB-IR active tags satisfies technical requirements imposed on the indoor vehicle locator system: scalability, low deployment cost, and a relaxed LOS conditions for the localization.

### 6.2.1 Scalability

With the proposed active sonar system introduced in Chapter 4, the vehicle locator device mounted on a target vehicle is required to execute receiving process only for the localization, which brings scalability to the positioning system, compared to other methods that require the vehicle's device to transmit or return timing signals.

### 6.2.2 Deployment Cost

The proposed system does not require infrastructural devices to be connected each other. The passive location system [74] also utilizes TDOA information for localizing target objects, but the main difference compared to the proposed location system is that it follows an infrastructure-centric approach. Thus the passive location system requires infrastructural devices to be connected via a network for aggregating TDOA information collected by infrastructural devices. On the other hand, the proposed active location system follows the user-centric approach thus infrastructural devices work independently from each other using a on-time synchronization procedure as introduced in Chapter 4. In addition, the proposed system does not require a roaming system for expanding the target areas. The passive location system requires a roaming system to expand the target area as the localization is conducted by a unit of *cell* formed by infrastructural device triples. On the other hand, the proposed system is easily expandable by adding the anchor node triples to desired target areas since the target node locates its position relative to the anchor node triples.

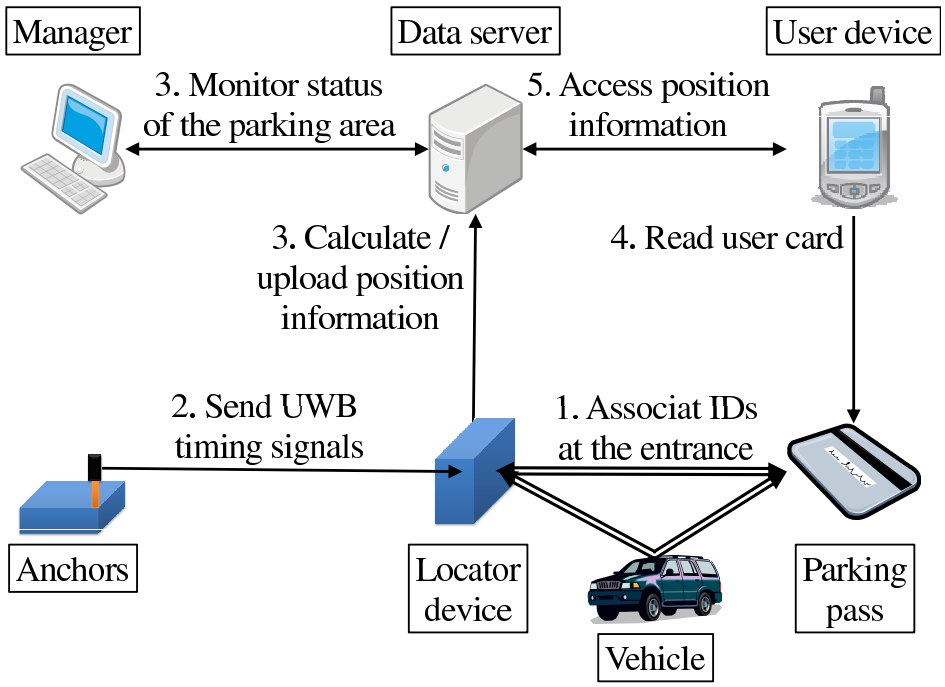


Figure 6.1: Components of the vehicle locator system and the action flowchart.

### 6.2.3 Relaxed LOS Condition

The proposed method allows anchor nodes to be deployed on a line for localizing the target device. As the parking area is filled with vehicles, it becomes difficult to maintain the line-of-sight (LOS) conditions between the vehicle locator and anchor nodes on the direction of sides and the back of the vehicle. Since localization accuracy of a time based location system is sensitive to the LOS conditions between anchor nodes and the receiver, the approach can localize the target position by utilizing anchor nodes placed in front of the vehicle.

## 6.3 Vehicle Locator System Architecture

Figure6.1 shows the components of the vehicle locator system and action flowchart. The vehicle locator system is built from a license plate recognition system, a parking ticket system, and the positioning system.

### 6.3.1 Registration of the Vehicle

The license plate recognition system is utilized to associate the user's vehicle and the ID of the vehicle locator. The vehicle locator that associated with the license plate of the user's vehicle is provided to the user along with a parking pass issued by the parking ticket system. The issued parking pass is also associated with the ID of the vehicle locator and the license plate number, to allow the user to access his vehicle information online by using the ID of the parking pass. The vehicle locator device contains a passive RFID tag, which stores the ucode. By reading the ucode of the vehicle locator device and associating with the license plate number of the target vehicle, the registration of the vehicle to the system is completed.

### 6.3.2 Localization

Anchors periodically execute roles of the initiator node and the reflector node according to the initiation procedure among the anchor node triple. Their relative positions and the pre-measured delay time are sent along with the timing signal, so that the vehicle locator can calculate the position of the receiver relative to anchor nodes by using the proposed positioning method. Anchor node triples are given a group ID in order to reject initiator's beacon from other anchor node triples, so that reflector nodes respond to the beacon sent by the initiator node that belongs to the group. The group ID is also utilized by the data server for locating the anchor node triple positions in the parking space.

After the ID association procedure among the vehicle locator, the vehicle, and the parking pass, the vehicle locator is provided to the user at the entrance. The vehicle locator is supposed to be left in the vehicle for locating its position in the parking space. The vehicle locator listens for UWB signals from anchor node triples deployed in the parking space intermittently. Once TDOA information of the anchor node triple is collected, it executes the positioning procedure described in the previous section. The vehicle locator uploads the position information relative to the anchor node triple that involved in the positioning along with its ID to the data server.

### 6.3.3 Aggregation of Location Information

A data server collects relative position information from vehicle locators. From the relative position of the vehicle locator, the data server determines a parking slot number by comparing with the parking area map. The data server provides monitoring information to managers of the parking space, such as the time of entry of a specific vehicle and the position of each vehicle at a granularity of a parking slot. Also the users receive benefits by accessing to the data server such as finding a nearest exit of the parking space or locating his vehicle when leaving the parking area. The users can access his vehicle information by using the ID of the parking apss as an access code.

IDs of a vehicle, a vehicle locator, and a parking pass are associated and managed by the data server for assuring that the vehicle checked-in at the entrance leaves the parking area with a proper owner of the vehicle. If there is an association between the vehicle locator and the vehicle but no link to the parking pass, then the system allows the vehicle to exit the parking area without the parking pass, allowing a car thief to easily steal the target vehicle. Although users can access the location information of the vehicle by using the ID of the vehicle locator as the access code, the vehicle locator system without the identification of users contains security issues. In addition, in the case that there is no link between the vehicle locator and the vehicle, the positioning system can falsely detect the position of the vehicle, for example, when the vehicle locator is removed from the vehicle.

## 6.4 Implementations

A prototype system is created by preparing UWB anchor nodes, a vehicle locator device, a data server, and a digital signage. The digital signage is utilized for displaying the position of the requested vehicle. The vehicle locator consists of a UWB module, a Bluetooth Low Energy (BLE) module, a circularly polarised (CP) antenna for ultra-wideband radio, a passive RFID tag, and batteries. The target node operates with three AAA batteries, which can supply 2000 mAh to the device. The device operates for 1 year when it requested TDOA measurements at the rate of 0.1 Hz, or it can operate for 1100 hours when its TDOA sampling rate

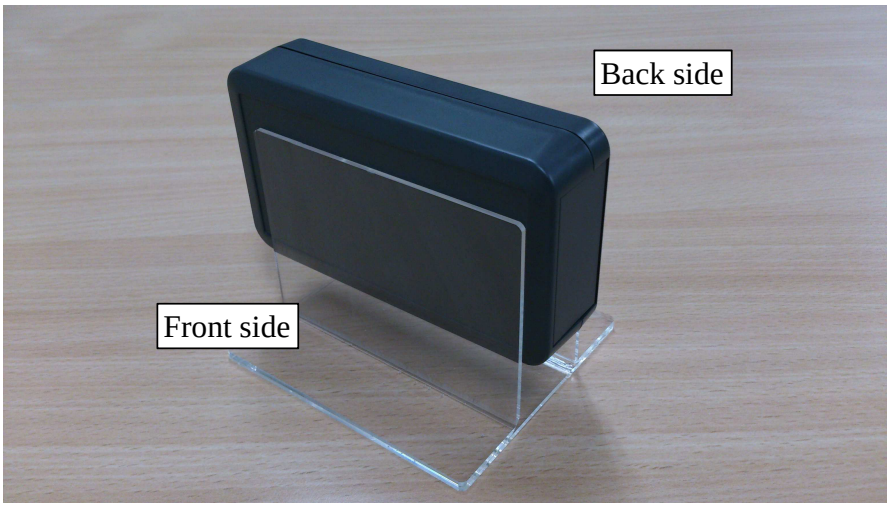


Figure 6.2: Exterior of the prototype device.

is 1 second. Figure6.2 and Figure6.3 are pictures of the target node, showing the exterior and the interior of the device.

The UWB module is connected to the BLE module via UART. TDOA data received by the UWB module is transferred to the BLE module and the BLE module sends data to the data server equipped with a BLE dongle. The current implementation of the BLE module utilizes BLE advertisements for sending relative position information using the manufacture specific command field. The packet format of the advertise packet containing relative position information is shown in Figure6.4. The ID of a target device and a group ID of an anchor node triple has a length of 4 bytes. The field length of distances to reflector nodes are 2 bytes and expressed in centimeters. The position of the target node is expressed with 4 bytes: signed 2 bytes each for x-coordinate and y-coordinate in centimeters.

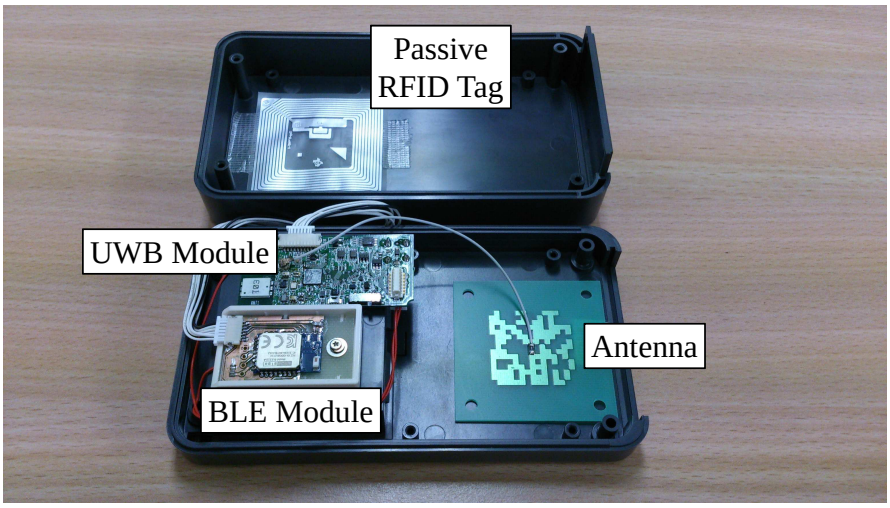


Figure 6.3: Details of the prototyped device.

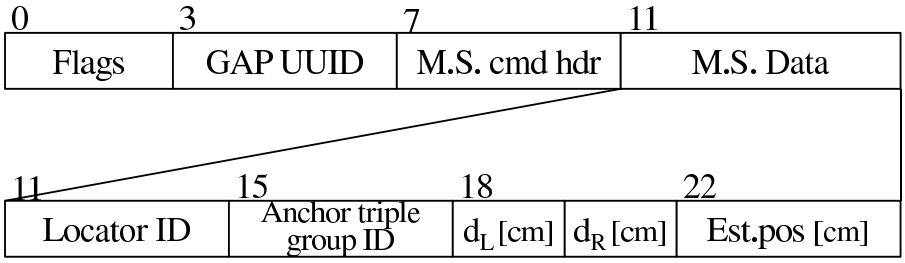


Figure 6.4: The format of the advertising packet.

## 6.5 Experiments

A vehicle attached with the locator device is parked in the monitored area where UWB anchor triples are deployed. The test user issued a query of his vehicle by accessing the location information via the digital signage using his parking ticket card. The parking ticket card contains the passive RFID tag which is readable by


Figure 6.5: Digital signage shows the position of the vehicle when the user entered the ID of the parking pass to the signage unit.

the RFID reader embedded to the digital signage. Figure6.5 shows the result of the query using the digital signage showing the position of the requested vehicle correctly.

## 6.6 Discussions

The advantage of using the UWB positioning system for the vehicle locator system is not only limited to the positioning accuracy achieved. Compared to the video camera based system, the privacy issue that arises when users vehicle is pictured anywhere in the parking area for locating vehicles is minimized since the proposed system takes a picture of the vehicle at the entrance only. In addition, although the parking-slot management is realizable by placing bumpers or low-frequency sensors, a renovation of the existing infrastructure is necessary for these approaches. Compared to sensor-based approaches for the slot management, the

proposed vehicle locator system based on UWB positioning technology can be installed to the existing parking area without large renovations.

The vehicle locator system can be more sophisticated than the current architecture by embedding the UWB transceiver to the parking pass, so that the parking pass works as a smart vehicle locator while it is placed inside of the vehicle. Since introducing a smart parking pass to the system still requires the user identification information, the user can use his RFID card or a smartphone that implements Near Field Communication (NFC) card as an identifier used at the entrance for associating IDs. With this scenario, the RFID read at the entrance gate becomes the accessor to obtain the vehicle status from the system.

## 6.7 Summary

This chapter introduced an application of the proposed location system, focusing on the application of partial location system for the indoor vehicle locator system. System requirements of the vehicle locator system are discussed, then the overall system architecture is depicted. Implementation details based on TOF enabled tags are introduced, and discussions on advantages of exploiting TOF enabled tags are provided.

# Chapter 7

# Conclusions

This research explored three location information classes to be supported by the location information infrastructure, namely, proximity status, relative and/or partial location, and absolute location. For each location information scheme, associated issues are clarified and discussed through proposed algorithms and real world evaluations. The effectiveness of the proposed approach has been shown by exploiting proposed methods to ubiquitous computing applications that sensory devices recognize target objects based on a user-centric communication architecture.

## 7.1 Overview of Chapters

This section summarizes each chapter of the thesis.

### 7.1.1 Related Work

In Chapter 2, related work on proximity detection localization systems is presented with a classification of previous studies based on hardware technologies employed. Advantages and disadvantages of each technology and method are summarized. Then problems that arise from realizing three location scheme: proximity, relative and/or partial, and absolute, are discussed with an introduction of previous work on the discussed issues.

### 7.1.2 Proximity Detection System

In Chapter 3, a proximity detection system based on RSS enabled active RFID tags is introduced. System requirements on the proximity detection system are discussed first. Technical details on proposed communication protocols and statistical RSS filtering methods are presented. Then implementation details and procedures taken for the field experiment are explained. The experimental results have shown that 1-exchange exponentially weighted moving average filtering method successfully reduced the distance variation of the proximity detection system to less than 3 meters, while other approach produced a variation of 10 meters.

### 7.1.3 Relative and Partial Location Systems

In Chapter 4, relative and partial location systems are introduced. Definitions of these location schemes are explained first.

After the overview of proposed systems is provided, lateral distance measurement system is introduced. The lateral distance measurement system consists of three parts: TOF measurement, relative localization, and ranging error reduction. By focusing on the variation of angles formed by active tags due to geometric layout of tags, the proposed method has shown that applying a low pass filter on angles is effective to reduce the error of the lateral distance between mobile objects. The results were confirmed by both simulations and field experiments. The estimation error was reduced from 8 meters to 3 meters when the relative distance between mobile objects is less than 15 meters.

In section 4 of the chapter, the active sonar system is introduced. The active sonar system partially localize the target objects using an anchor node triple aligned in a line. The problems associated with TOF based location systems are summarized first, then the positioning algorithm solving these problems is proposed. The proposed system is implemented using TOF enabled tags, and experiments were conducted in an indoor parking space where there are many metallic objects that obstruct LOS conditions between TOF enabled tags. In the experiment, the proposed method was compared with the normal TDOA localization system to show its advantage on robustness. Since the proposed method relaxes the LOS condi-

tion between infrastructural devices and the target devices, the proposed method successfully maintained localization capability while the other method failed to do so when the space was filled with vehicles.

### 7.1.4 Absolute Location Systems

In Chapter 5, two important topics for the location systems are discussed. First topic is the method to capture RF characteristics of the target areas. Previous studies have utilized a fingerprinting technique, which basically generates a RF map of the target areas by conducting extensive and lengthy surveys. This is prohibited for the system to be deployed to large areas. Thus the systematic procedures for generating RF models for each deployed active RFID tag are proposed. The proposed procedures generate RF models for each tag and differentiating the model by variable transmission powers. The proposed procedures also incorporate an outlier filtering algorithm to remove unnecessary RSS samples for accurately estimating the RF models. Evaluations were conducted using Bluetooth Low Energy device as active RFID tag, which allows a commercial mobile device to collect training data and process RSS samples to locate its position on-line. Results obtained from experiments have shown that the considering transmission power difference increases the ranging and positioning accuracy. In addition the results have shown an effectiveness of the outlier filtering algorithm for generating the RF models.

Second topic of the chapter is to automatically calculate positions of the deployed devices. The self-localization algorithm based on rigid quadrilateral search is proposed, and have shown that the self-localization accuracy of sub-meter is achieved using TOF enabled tags.

### 7.1.5 Applications

The partial location system, introduced as the active sonar system, is applied for the vehicle locator system targeted for the indoor parking space. Since there is a demand to obtain parked vehicles in an accuracy of a parking slot, the TOF based active sonar system was chosen. In addition, in the parking area, many vehicles visit and leave the area, thus producing a lossy environment for the RF

based location system. The architecture of the vehicle locator system is depicted, and a prototype system is evaluated using the parking area of a shopping mall. Obtained results have shown that the vehicle locator system successfully locate the target vehicle.

## 7.2 Conclusions

This research explored a user-centric location information system based on active RFID tags. Technical challenges to realize a low cost and scalable location information system based on active RFID tags are identified by considering requirements imposed on three types of location information. For each location information type, proposals to solve challenges are made and evaluated through extensive field experiments using real hardware implementations. Evaluation results have shown that proposed methods improve accuracy of location information provided to the users while achieving low deployment cost, high robustness, and maintaining the scalability of the location system by following the user-centric communication approach.

# References


[1] K. Sakamura. The Objectives of the TRON Project. In *TRON Project 1987 Open-Architecture Computer Systems*, pages 3–16. Springer Japan, 1987.

[2] M. Weiser. Some Computer Science Issues in Ubiquitous Computing. *Commun. ACM*, 36(7):75–84, July 1993.

[3] J. Hightower and G. Borriello. Location systems for ubiquitous computing. *Computer*, 34(8):57–66, 2001.

[4] M. McCarthy, P. Duff, H.L. Muller, and C. Randell. Accessible Ultrasonic Positioning. *Pervasive Computing, IEEE*, 5(4):86–93, 2006.

[5] T. Rappaport. *Wireless Communications: Principles and Practice.* Prentice Hall PTR, Upper Saddle River, NJ, USA, 2nd edition, 2001.

[6] T. Nakagawa, G. Ono, R. Fujiwara, T. Norimatsu, T. Terada, M. Miyazaki, K. Suzuki, K. Yano, Y. Ogata, A. Maeki, S. Kobayashi, N. Koshizuka, and K. Sakamura. 1-cc Computer: Cross-Layer Integration With UWB-IR Communication and Locationing. *Solid-State Circuits, IEEE Journal of*, 43(4):964–973, 2008.

[7] N.R. Yousef, A.H. Sayed, and L.M.A. Jalloul. Robust wireless location over fading channels. *Vehicular Technology, IEEE Transactions on*, 52(1):117–126, 2003.

[8] P. Bahl and V.N. Padmanabhan. RADAR: an in-building RF-based user location and tracking system. In *INFOCOM 2000. Nineteenth Annual Joint*

*Conference of the IEEE Computer and Communications Societies. Proceedings. IEEE*, volume 2, pages 775–784 vol.2, 2000.

[9] T. Roos, P. Myllymäki, H. Tirri, P. Misikangas, and J. Sievänen. A probabilistic approach to WLAN user location estimation. *International Journal of Wireless Information Networks*, 9(3):155–164, 2002.

[10] P. Bahl, J. Padhye, L. Ravindranath, M. Singh, A. Wolman, and B. Zill. DAIR: A framework for managing enterprise wireless networks using desktop infrastructure. In *HotNets IV*, 2005.

[11] M. Youssef and A. Agrawala. The Horus WLAN Location Determination System. In *Proceedings of the 3rd International Conference on Mobile Systems, Applications, and Services*, MobiSys '05, pages 205–218, New York, NY, USA, 2005. ACM.

[12] V. Otsason, A. Varshavsky, A. LaMarca, and E. de Lara. Accurate GSM Indoor Localization. In *Proceedings of the 7th International Conference on Ubiquitous Computing*, UbiComp'05, pages 141–158, Berlin, Heidelberg, 2005. Springer-Verlag.

[13] A. Haeberlen, E. Flannery, A.M. Ladd, A. Rudys, D.S. Wallach, and L.E. Kavraki. Practical Robust Localization over Large-scale 802.11 Wireless Networks. In *Proceedings of the 10th Annual International Conference on Mobile Computing and Networking*, MobiCom '04, pages 70–84, New York, NY, USA, 2004. ACM.

[14] M. Azizyan, I. Constandache, and R.R. Choudhury. SurroundSense: Mobile Phone Localization via Ambience Fingerprinting. In *Proceedings of the 15th Annual International Conference on Mobile Computing and Networking*, MobiCom '09, pages 261–272, New York, NY, USA, 2009. ACM.

[15] S. Capkun, M. Hamdi, and J-P Hubaux. GPS-free positioning in mobile ad-hoc networks. In *System Sciences, 2001. Proceedings of the 34th Annual Hawaii International Conference on*, pages 10 pp.–, 2001.

[16] A. Savvides, C.C. Han, and M.B. Strivastava. Dynamic Fine-grained Localization in Ad-Hoc Networks of Sensors. In *Proceedings of the 7th Annual International Conference on Mobile Computing and Networking*, MobiCom '01, pages 166–179, New York, NY, USA, 2001. ACM.

[17] Y. Gwon and R. Jain. Error Characteristics and Calibration-free Techniques for Wireless LAN-based Location Estimation. In *Proceedings of the Second International Workshop on Mobility Management &Amp; Wireless Access Protocols*, MobiWac '04, pages 2–9, New York, NY, USA, 2004. ACM.

[18] N.B. Priyantha, H. Balakrishnan, E.D. Demaine, and S. Teller. Mobile-assisted localization in wireless sensor networks. In *INFOCOM 2005. 24th Annual Joint Conference of the IEEE Computer and Communications Societies. Proceedings IEEE*, volume 1, pages 172–183 vol. 1, 2005.

[19] D. Madigan, E. Einahrawy, R Martin, W. Ju, P. Krishnan, and A. Krishnakumar. Bayesian indoor positioning systems. In *INFOCOM 2005. 24th Annual Joint Conference of the IEEE Computer and Communications Societies. Proceedings IEEE*, volume 2, pages 1217–1227. IEEE, 2005.

[20] H. Lim, L. Kung, J.C. Hou, and H. Luo. Zero-Configuration, Robust Indoor Localization: Theory and Experimentation. In *INFOCOM 2006. 25th IEEE International Conference on Computer Communications. Proceedings*, pages 1–12, 2006.

[21] Y. Ji, S. Biaz, S. Pandey, and P. Agrawal. ARIADNE: A Dynamic Indoor Signal Map Construction and Localization System. In *Proceedings of the 4th International Conference on Mobile Systems, Applications and Services*, MobiSys '06, pages 151–164, New York, NY, USA, 2006. ACM.

[22] K. Chintalapudi, A. Iyer, and V. Padmanabhan. Indoor Localization Without the Pain. In *Proceedings of the Sixteenth Annual International Conference on Mobile Computing and Networking*, MobiCom '10, pages 173–184, New York, NY, USA, 2010. ACM.

[23] N. Patwari, J.N. Ash, S. Kyperountas, A.O. Hero, R.L. Moses, and N.S. Correal. Locating the nodes: cooperative localization in wireless sensor networks. *Signal Processing Magazine, IEEE*, 22(4):54–69, 2005.

[24] H. Wymeersch, J. Lien, and M.Z. Win. Cooperative Localization in Wireless Networks. *Proceedings of the IEEE*, 97(2):427–450, 2009.

[25] D.J. Torrieri. Statistical Theory of Passive Location Systems. *Aerospace and Electronic Systems, IEEE Transactions on*, AES-20(2):183–198, 1984.

[26] H.B. Lee. A Novel Procedure for Assessing the Accuracy of Hyperbolic Multilateration Systems. *Aerospace and Electronic Systems, IEEE Transactions on*, AES-11(1):2–15, 1975.

[27] N. Levanon. Lowest GDOP in 2-D scenarios. *Radar, Sonar and Navigation, IEE Proceedings* -, 147(3):149–155, 2000.

[28] P. Enge and P. Misra. Special Issue on Global Positioning System. *Proceedings of the IEEE*, 87(1):3–15, 1999.

[29] A. Varshavsky, E. de Lara, J. Hightower, A. LaMarca, and V. Otsason. GSM Indoor Localization. *Pervasive Mob. Comput.*, 3(6):698–720, December 2007.

[30] I. Constandache, R.R. Choudhury, and I. Rhee. Towards Mobile Phone Localization without War-Driving. In *INFOCOM, 2010 Proceedings IEEE*, pages 1–9, 2010.

[31] U. Birkel and M. Weber. Indoor localization with UMTS compared to WLAN. In *Indoor Positioning and Indoor Navigation (IPIN), 2012 International Conference on*, pages 1–6, 2012.

[32] P. Bahl, V.N. Padmanabhan, and A. Balachandran. Enhancements to the RADAR user location and tracking system. Technical report, technical report, Microsoft Research, 2000.

[33] M. Youssef and A. Agrawala. Handling samples correlation in the Horus system. In *INFOCOM 2004. Twenty-third AnnualJoint Conference of the*

*IEEE Computer and Communications Societies*, volume 2, pages 1023–1031 vol.2, 2004.

[34] A. LaMarca, Y. Chawathe, S. Consolvo, J. Hightower, I. Smith, J. Scott, T. Sohn, J. Howard, J. Hughes, F. Potter, J. Tabert, P. Powledge, G. Borriello, and B. Schilit. Place lab: Device positioning using radio beacons in the wild. In *Proceedings of the Third International Conference on Pervasive Computing*, PERVASIVE'05, pages 116–133, Berlin, Heidelberg, 2005. Springer-Verlag.

[35] J. Rekimoto, T. Miyaki, and T. Ishizawa. Lifetag: Wifi-based continuous location logging for life pattern analysis. In *Proceedings of the 3rd International Conference on Location-and Context-awareness*, LoCA'07, pages 35–49, Berlin, Heidelberg, 2007. Springer-Verlag.

[36] A. Rai, K.K. Chintalapudi, V.N. Padmanabhan, and R. Sen. Zee: Zero-effort Crowdsourcing for Indoor Localization. In *Proceedings of the 18th Annual International Conference on Mobile Computing and Networking*, Mobicom '12, pages 293–304, New York, NY, USA, 2012. ACM.

[37] K. Sakamura and C. Ishikawa. Internet of Things-From Ubiquitous Computing to Ubiquitous Intelligence Applications. *Internet of Things-Global Technological and Societal Trends From Smart Environments and Spaces to Green ICT*, page 115.

[38] S. Watanabe, S. Nishiyama, G. Hattori, C. Ono, N. Koshizuka, and K. Sakamura. Location detection method for ubiquitous environment using contactless ic cards. *The Special Interest Group Technical Reports of IPSJ. UBI, [Ubiquitous Computing System]*, 2003(39):73–78, apr 2003.

[39] Julian Randall, Oliver Amft, Jürgen Bohn, and Martin Burri. Luxtrace: Indoor positioning using building illumination. *Personal Ubiquitous Comput.*, 11(6):417–428, August 2007.

[40] R. Want, A. Hopper, V. Falcão, and J. Gibbons. The Active Badge Location System. *ACM Trans. Inf. Syst.*, 10(1):91–102, January 1992.

[41] R. Stoleru, P. Vicaire, T. He, and J.A. Stankovic. StarDust: A Flexible Architecture for Passive Localization in Wireless Sensor Networks. In *Proceedings of the 4th International Conference on Embedded Networked Sensor Systems*, SenSys '06, pages 57–70, New York, NY, USA, 2006. ACM.

[42] N. Tamiya, H. Mandai, and T. Fukae. Optical spread spectrum radar for lateral distance measurement (in japanese). *IEICE Technical Report. SST, Spread Spectrum*, 96(427):41–46, dec 1996.

[43] A. Ward, A. Jones, and A. Hopper. A new location technique for the active office. *Personal Communications, IEEE*, 4(5):42–47, 1997.

[44] N.B. Priyantha, A. Chakraborty, and H. Balakrishnan. The Cricket Location-support System. In *Proceedings of the 6th Annual International Conference on Mobile Computing and Networking*, MobiCom '00, pages 32–43, New York, NY, USA, 2000. ACM.

[45] Jeffrey Hightower, Roy Want, and Gaetano Borriello. SpotON: An indoor 3D location sensing technology based on RF signal strength. *UW CSE 00-02-02, University of Washington, Department of Computer Science and Engineering, Seattle, WA*, 1, 2000.

[46] Lionel M Ni, Yunhao Liu, Yiu Cho Lau, and Abhishek P Patil. LANDMARC: indoor location sensing using active RFID. *Wireless networks*, 10(6):701–710, 2004.

[47] A. Woo and D. Culler. Evaluation of Efficient Link Reliability estimators for Low-Power Wireless Networks. *Technical Report UCB//CSD-03-1270*, 2003.

[48] Paul Richardson and Dan Shan. Experimental Data Collection and Performance Analysis of Outdoor UWB Positioning System under Static and Mobile Conditions. *EURASIP Journal on Wireless Communications and Networking*, 2009. 13 pages, Article ID 618036, 2009.

[49] X. Li, B. Hua, Y. Shang, and Y. Xiong. A robust localization algorithm in

wireless sensor networks. *Frontiers of Computer Science in China*, 2:438–450, 2008. 10.1007/s11704-008-0018-7.

[50] R. Fujiwara, K. Mizugaki, T. Nakagawa, D. Maeda, and M. Miyazaki. TOA/TDOA hybrid relative positioning system using UWB-IR. In *Radio and Wireless Symposium, 2009. RWS '09. IEEE*, pages 679–682, 2009.

[51] Z. Sahinoglu and S. Gezici. Enhanced Position Estimation via Node Cooperation. In *Communications (ICC), 2010 IEEE International Conference on*, pages 1–6, 2010.

[52] Bruce Hendrickson. Conditions for unique graph realizations. *SIAM Journal on Computing*, 21(1):65–84, 1992.

[53] N. Patwari and A.O. Hero, III. Using Proximity and Quantized RSS for Sensor Localization in Wireless Networks. In *Proceedings of the 2Nd ACM International Conference on Wireless Sensor Networks and Applications*, WSNA '03, pages 20–29, New York, NY, USA, 2003. ACM.

[54] F. Cabrera-Mora and J. Xiao. Preprocessing technique to signal strength data of wireless sensor network for real-time distance estimation. In *Robotics and Automation, 2008. ICRA 2008. IEEE International Conference on*, pages 1537–1542, 2008.

[55] Chipcon. CC1020 Errata Notes.

[56] Chipcon. CC1020/1021 Received Signal Strength Indicator.

[57] American Association of State Highway and Transportation Officials. *Guide for the Development of Bicycle Facilities*. American Association of State Highway and Transportation Officials, Washington DC, 3rd edition, 1999.

[58] J.D. Parsons and J. David. *The Mobile Radio Propagation Channel*. Wiley Chichester, 2nd edition, 2000.

[59] G. Anastasi, A. Falchi, A. Passarella, M. Conti, and E. Gregori. Performance Measurements of Motes Sensor Networks. *Proceedings of the 7th ACM in-*

*ternational symposium on Modeling, analysis and simulation of wireless and mobile systems*, pages 174–181, 2004.

[60] K. Mizugaki, R. Fujiwara, T. Nakagawa, G. Ono, T. Norimatsu, T. Terada, M. Miyazaki, Y. Ogata, A. Maeki, S. Kobayashi, N. Koshizuka, and K. Sakamura. Accurate Wireless Location/Communication System With 22-cm Error Using UWB-IR. In *Radio and Wireless Symposium, 2007 IEEE*, pages 455–458, 2007.

[61] Committee of Reviewing Countermeasures to the Quietness of Hybrid Vehicles.

[62] The Commission of the European Communicties, Commission Decision of 21 February 2007 on allowing the use of the radio spectrum for equipment using ultra-wideband technology in a harmonised manner in the Community.

[63] N.H. Vu, V. Gopalkrishnan, and P. Namburi. Online Outlier Detection Based on Relative Neighbourhood Dissimilarity. In James Bailey, David Maier, Klaus-Dieter Schewe, Bernhard Thalheim, and XiaoyangSean Wang, editors, *Web Information Systems Engineering - WISE 2008*, volume 5175 of *Lecture Notes in Computer Science*, pages 50–61. Springer Berlin Heidelberg, 2008.

[64] J.J. Caffery. *Wireless Location in CDMA Cellular Radio Systems.* Kluwer Academic Publishers, Norwell, MA, USA, 1999.

[65] T-Engine Forum Ubiquitous ID Center Document 930-S101-1.A0.10/UID-00010-1.A0.10. Ubiquitous Code : ucode., July 28 2009.

[66] ITU-T H.642.1. Multimedia information access triggered by tag-based identification - Identification scheme., June 2009.

[67] Bluetooth SIG. Specification of the Bluetooth System. Version 4.0, December 2009.

[68] Z. Sahinoglu and S. Gezici. Ranging in the IEEE 802.15.4a Standard. In *Wireless and Microwave Technology Conference, 2006. WAMICON '06. IEEE Annual*, pages 1 –5, dec. 2006.

[69] David K. Goldenberg, Pascal Bihler, Ming Cao, Jia Fang, Brian D. O. Anderson, A. Stephen Morse, and Y. Richard Yang. Localization in sparse networks using sweeps. In *Proceedings of the 12th annual international conference on Mobile computing and networking*, MobiCom '06, pages 110–121, New York, NY, USA, 2006. ACM.

[70] David Moore, John Leonard, Daniela Rus, and Seth Teller. Robust distributed network localization with noisy range measurements. In *Proceedings of the 2nd international conference on Embedded networked sensor systems*, SenSys '04, pages 50–61, New York, NY, USA, 2004. ACM.

[71] ARIB STD-T91, UWB (Ultra-WideBand) Radio System, 2008.

[72] M. Di Mauro, G. Della Corte, A. L. Robustelli, P. Addesso, and M. Longo. A WLAN-based Location System for Indoor Parking Areas. In *Proceedings of the 17th International Conference on Software, Telecommunications and Computer Networks*, SoftCOM'09, pages 186–190, Piscataway, NJ, USA, 2009. IEEE Press.

[73] Gy. Gódor, Á. Huszák, and K. Farkas. Intelligent Indoor Parking. In *Proceedings of the 1st Global Virtual Conference (GV-CONF 2013)*, Stip, Macedonia, April 8. - 12., 2013.

[74] D.E. Manolakis. Efficient solution and performance analysis of 3-d position estimation by trilateration. *Aerospace and Electronic Systems, IEEE Transactions on*, 32(4):1239–1248, 1996.